Novel Approaches to Low Temperature Transient Liquid Phase Bonding in the In-Sn/Cu and In-Sn-Bi/Cu Systems

by

David S. Fischer

B.S. Materials Science and Engineering
Lehigh University, 2005

Submitted to the Department of Materials Science and Engineering
in Partial Fulfillment of the Requirements for the Degree of
Master of Science in Materials Science and Engineering

at the

Massachusetts Institute of Technology

February 2008

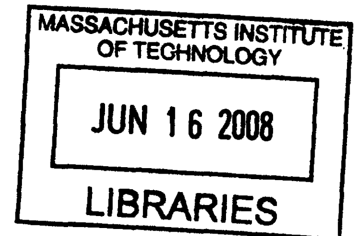

© 2008 Massachusetts Institute of Technology.
All rights reserved.

ARCHIVES

Signature of Author: __________________________
Department of Materials Science and Engineering
January 25, 2008

Certified by: __________________________
Thomas W. Eagar
Professor of Materials Engineering and Engineering Systems
Thesis Supervisor

Accepted by: __________________________
Samuel M. Allen
POSCO Professor of Physical Metallurgy
Chair, Department Committee on Graduate Students

Novel Approaches to Low Temperature Transient Liquid Phase Bonding in the In-Sn/Cu and In-Sn-Bi/Cu Systems

By

David S. Fischer

Submitted to the Department of Materials Science and Engineering on January 18, 2008
in partial fulfillment of the requirements for the Degree of Master of Science
in Materials Science and Engineering

Abstract

A fluxless low temperature transient liquid phase (LTTLP) bonding process was studied as a method of producing Cu/Cu joints below 125 °C and 75 °C using interlayer alloys from the In-Sn and In-Sn-Bi systems. Using thermodynamic models, three different compositions (wt. %) of base alloys were chosen to accomplish this task: 50In-43.6Sn-6.4Bi (T_m = 110 °C) and eutectic 50.9In-49.1Sn (T_m = 120 °C) alloys were used for bonding at 125 °C and a eutectic 48.3In-15.6Sn-36.1Bi (T_m = 60 °C) alloy was used for bonding at 75 °C. In addition, novel approaches to TLP bonding, including the addition of base material to the interlayer alloy and application of an electroless Ni diffusion barrier layer, were employed in an attempt to optimize this joining method.

The LTTLP processes were assessed based on their abilities to produce joints with minimal thickness, high reflow temperatures, and good mechanical properties at room/elevated temperatures. It was found that interlayer alloys containing higher Bi contents produced the thinnest joints, with the 48.3In-15.6Sn-36.1Bi alloy producing joints on the order of 10 μm. Increases in nominal Cu composition of the interlayer alloy tended to form larger joints. Application of the Ni layer was observed to decrease the growth rate of the eutectic In-Sn joints made with 5 wt % Cu additions. Shear tests were performed on the joints at room (25 °C) and operating (service) temperatures (100 °C). Most of the TLP joints had room temperature shear strengths around 13,000 – 17,000 psi (≈ 90 – 120 MPa), although increases in strength were observed for eutectic In-Sn joints with 2.5 and 5 wt% Cu additions. At operating temperature, TLP joints made within the In-Sn-Cu system were found to have strengths an order of magnitude higher than those made in the In-Sn-Bi-Cu system. Poor mechanical response of the Bi-containing joints was due to the presence of low melting In-Bi IPs present in the reaction zone. Eutectic In-Sn TLP joints made with 2.5 and 5 wt% Cu additions were found to have operational temperature shear strengths of 6,000 – 7,500 psi (≈ 40 – 50 MPa) and 7,500 – 9,500 psi (≈ 50 – 65 MPa), respectively.

Thesis Supervisor: Thomas Eagar
Title: Professor of Materials Engineering and Engineering Systems

Acknowledgements

There are many people whom I would like to thank since beginning my graduate studies at MIT. First, I must thank my thesis advisor, Thomas Eagar, for the guidance and mentorship he has given me since becoming a member of his research group.

I would like to thank the Intel Corporation ® for funding this project. In particular, I would like to thank Daewoong Suh and Jessica Weninger, my company liaisons, for their continued support throughout this project.

I must also acknowledge the contributions of Dr. Raymundo Arroyave at Texas A&M for his work on the thermodynamic modeling presented in this work. His computations greatly aided the experimental work performed in this study.

Much appreciation is given to Don Galler, Yin-Lin Xie, David Bono, and all of the other lab technicians who have assisted me during my research. I would also like to thank Harold Larson and Jeri Hill of the Welding and Joining Lab for their assistance over the past years. Special thanks to all of my UROPs, including Michele Dufalla, Sung Kim, and Naomi Coronel, for their endless efforts in the lab. Without all of these people, this work would not have been possible.

To all of my friends, both new and old, who have allowed me to enjoy my times spent outside of the lab. Particular thanks to my lab mate and good friend, Brian Hohmann, for showing me the ropes on surviving my first few years of grad school. His presence in the office has truly made my first few years at MIT an enjoyable experience. Thanks to my friends, and "personal trainers", Jay Trelewicz and Trey Holzwarth for keeping me physically (as well as mentally) fit. And, of course, much love goes out to my girlfriend Brooke who has made many long bus rides to visit me up in Boston.

Most importantly, I would like to dedicate this work to my family, whose encouragement and support have gotten me to where I am today. To Andrew, the best brother a guy could ever ask for. To my mom, who has always told me to stay positive and to never forget about health, happiness, and all of the more important things in life. And to my dad, whose early tutoring in math and science has inspired me to become an engineer in the first place. I love you all very much.

Table of Contents

Abstract 2
Acknowledgements 3
Table of Contents 4
List of Figures 6
List of Tables 10
Chapter 1: Introduction 11
1.1 Motivation for Thesis Work 11
1.2 Scope of Thesis 12
1.3 Overview of Thesis 13
Chapter 2: Background 13
2.1 Principles of TLP Bonding 13
2.2 Materials Selection for LTTLP Bonding 16
2.2.1 Practical Considerations 16
2.2.2 In-Sn-Cu and In-Sn-Bi-Cu Systems 18
2.3 Novel Approaches to TLP Bonding 20
2.3.1 Addition of Base Material to Interlayer Alloy 20
2.3.2 Diffusional Barrier Layers on Substrate 21
2.4 Summary of Target Goals 24
Chapter 3: Experimental Procedure 25
3.1 Sample Preparation 25
3.1.1 Alloy Production for TLP Interlayers 25
3.1.2 Differential Scanning Calorimetry 26
3.1.3 Production of TLP Joints 27
3.2 Microstructural and Phase Analysis 32
3.2.1 Metallographic Preparation 32
3.2.2 Scanning Electron Microscopy 32
3.2.3 Energy Dispersive Spectrometry 33
3.3 Mechanical Testing 35
3.3.1 Shear Tests 35
Chapter 4: Results and Discussion 37
4.1 Interlayer Alloy Melting Behavior 37
4.2 Determining Electroless Layer Thicknesses for Study 41
4.3 Effect of Cu Additions on Joint Thickness 45
4.4 Optimizing the LTTLP Process Design 48
4.4.1 Controlling Joint Thickness 49
i) In-Sn-Bi-Cu Systems 49
ii) In-Sn-Cu System 52
4.4.2 Compositional and Phase Analysis 57
i) In-Sn-Bi-Cu System 57
ii) In-Sn-Cu System 67
4.4.3 Mechanical Behavior and Failure Analysis 82
i) In-Sn-Bi-Cu Systems 82

ii) In-Sn-Cu System 86
Chapter 5: Concluding Remarks 95
5.1 Conclusions 95
5.1.1 Validation of Thermodynamic Database 95
5.1.2 Overall Evaluation of LTTLP Processes 97
i) Thickness of TLP Joints 97
ii) Microstructure of TLP Joints 100
iii) Mechanical Behavior of TLP Joints 101
iv) Final Recommendations 104
5.2 Future Work 105
Appendix A: Calculated Equilibrium Solidification Paths 107
References 112
About the Author 114

List of Figures

Figure 2.1: Stages of TLP bonding: (a) alloy heated slightly above its melting temperature (T_B); (b) dissolution of substrate; (c)-(d) isothermal solidification; (e) solid state homogenization; (f) final condition. (From Ref. [16]) ... 15
Figure 2.2: Calculated In-Sn-Bi ternary phase diagrams. The points 'A' and 'B' represent the eutectic and low-bismuth interlayer alloys, respectively. (From Ref. [6]) ... 19
Figure 2.3: Liquidus Calculations for 16Sn-6.4Bi-XCu (In-balance) alloys. For equilibrium solidification conditions, larger additions of Cu result in lower solidification temperatures. Scheil solidification calculations predict very similar solidification patterns for all alloys below 120 °C. ... 21
Figure 2.4: Solidification surface of a diffusion brazed Cu-Ag couple: (a) 125x; (b) 700x. A rough, cellular surface due to grain boundary grooving effects is observed on the Cu-Ag couple. (From Ref. [18]) ... 22
Figure 2.5: Cross-section of a Cu/In-48 at.%Sn/Cu sample diffusion soldered at 200 °C for 30 min. The η phase is formed with a duplex microstructure containing both coarse and fine grains. (From Ref. [42]) ... 23
Figure 3.1: Schematic of copper-to-copper sandwich bonds used to create TLP joints. ... 28
Figure 3.2: Experimental set-up for bonding procedure. Beads of interlayer alloys were spread on the heated surfaces of copper substrates using an ultrasonic lapper. The bonding procedure was done within a glove box containing an atmosphere of pure nitrogen and forming gas (95%N-5%H). ... 29
Figure 3.3: Pressing apparatus used to press the In-Sn-Bi-Cu TLP joints: (a) Dual-plate hot press used to press the Cu/Cu sandwich bonds to create TLP joints; (b) aluminum plates used to hold samples together during the pressing stage of the TLP process. ... 30
Figure 3.4: Pressing apparatus used to press the In-Sn-Cu TLP joints. ... 31
Figure 3.5: Two EDS diffusion profiling methods: (a) Typical line scan measurement; (b) Rectangular area scan technique used in the present work. Composition data obtained from each rectangular area was used to plot the diffusion profile of each elemental constituent across the TLP joint. ... 34
Figure 3.6: Shear testing experimental set-up: (a) Shear testing fixture (front view); (b) Shear testing fixture (side view); (c) Instron® machine; (d) Set-up for elevated temperature (100 °C) shear tests. ... 36
Figure 4.1: Melting behavior of 50In-43.6Sn-6.4Bi interlayer alloy: (a) DSC output of heat flow (mW) vs. temperature (°C); (b) Calculated equilibrium solidification path. Experimental determination (top graph) of the melting behavior of the interlayer alloy agrees very closely with that predicted through thermodynamic calculations (bottom graph). ... 38
Figure 4.2: Calculated solidification paths for (a) In-Sn-Bi-20Cu; and (b) In-Sn-5Cu interlayer alloys. Increasing amounts of Cu additions to the interlayer alloys decreases the fraction of liquid phase formed upon heating to the bonding temperature as a result of consumption of the MPDs by Cu-rich intermetallic phases. ... 40
Figure 4.3: Effect of Ni layer thickness on Cu diffusion during TLP bonding. As Ni layer thickness was increased, the degree of Cu diffusion into the joint during TLP bonding was decreased. Joints were produced using 50In-43.6Sn-6.4Bi interlayer with the following processing parameters: 450 psi pressure at 125 °C for 2 hrs. ... 43

Figure 4.4: Effect of Ni diffusion barrier layer on TLP process. Half-TLP joints produced with In-Sn eutectic interlayer alloy at 125 °C for 10 min: (a) no Ni layer; (b) 3min Ni plating. In the absence of a diffusion barrier layer, reactions between the solid Cu and liquid interlayer lead to formation of η phase at the S/L interface. No η phase is present when the Ni barrier layer is used. 44
Figure 4.5: Effect of Cu additions on resulting joint thickness in the In-Sn-Cu and In-Sn-Bi-Cu LTTLP systems. All TLP joints were made using the In-Sn-Bi-XCu interlayer alloy (constant 50In-43.6Sn-6.4Bi ratio) using 200 psi pressure at 125 °C for 2 hrs. Above 5 wt%Cu, increasing amounts of Cu additions drastically increase resulting joint thickness. The trend of increasing joint thickness with greater Cu additions seems to plateau at very high concentrations of copper (around 15 wt%Cu). 45
Figure 4.6: Effect of plating time on resulting joint thickness of In-Sn-Bi-XCu joints. The use of a Ni diffusion barrier layer is shown to potentially decrease the thickness of joints made using copper additions. Greater concentrations of base material to the interlayer require longer plating times to reduce the joint thickness to that of the standard In-Sn-Bi joint made with no copper additions. All joints were bonded at 125 °C for 2 hr under 50 psi. 51
Figure 4.7: Effect of dwell time on TLP joints made with In-Sn-XCu interlayers without Ni plating. Joint thickness of TLP joints made with 0 and 2.5 wt% Cu additions do not significantly change with bond time. Larger concentration of Cu (5 wt%) lead to a drastic increase in growth rate of the joints due to rapid growth of η phase from the S/L interface. All joints were bonded at 125 °C under 100 psi. 53
Figure 4.8: Effect of Ni plating on growth rate of In-Sn-0Cu TLP joints. Use of a Ni diffusion barrier layer does not significantly effect the growth rate of joint made without Cu additions. The same observation was made for the In-Sn-2.5Cu joints. All joints were bonded at 125 °C under 100 psi. 55
Figure 4.9: Effect of Ni plating on growth rate of In-Sn-5Cu TLP joints. Use of a Ni diffusion barrier decreases growth rate of joint made 5 wt% Cu additions due the suppression of η phase growth into the joint region during bonding. The growth rate decreases with increasing Ni layer thicknesses because of longer dissolution times for the thicker Ni layers. All joints were bonded at 125°C under 100 psi. 56
Figure 4.10: Prediction of phase fractions in In-Sn-Bi-XCu TLP joints (a) during bonding (T=125 °C); and (b) at room temperature (T=25 °C) 59
Figure 4.11: (a) SEM micrograph of low-Bi TLP joint. Regions of EDS analysis are shown in (b). Joint was bonded at 125 °C for 2 hr under 50 psi. 60
Figure 4.12: SEM micrograph of In-Sn-Bi-5Cu joint. A similar microstructure was also seen for the In-Sn-Bi-10Cu joint. Joint was bonded at 125°C for 2 hr under 50psi. 62
Figure 4.13: SEM micrograph of (a) In-Sn-Bi-5Cu (2 min plate); and (b) In-Sn-Bi-10Cu (2 min plate) joints. Joints were bonded at 125 °C for 2 hr under 50 psi. 63
Figure 4.14: Diffusion profiles for In-Sn-Bi-0Cu TLP joints with (a) no Ni plating; and (b) 2 min Ni plating. The Ni diffusion barrier layer was observed to severely retard Cu diffusion into the joint necessary for isothermal solidification. Joints were bonded at 125 °C for 2 hr under 50 psi. 65
Figure 4.15: SEM micrograph of (a) eutectic In-Sn-Bi; and (b) eutectic In-Sn-Bi-10Cu TLP joints. Joints were bonded at 75 °C for 2 hr under 50 psi. 67
Figure 4.16: SEM micrograph of eutectic (a) In-Sn; and (b) In-Sn-5Cu TLP joints. Less In-rich, low-melting phases were present in the In-Sn joints (as compared to those bonded in the In-

Sn-Bi system) due to the elimination of In-Bi intermetallic formation during TLP bonding. Joints were bonded at 125 °C for 2 hr under 100 psi. 69
Figure 4.17: SEM micrograph of In-Sn-2.5Cu joint. Joint was bonded at 125 °C for 2 hr under 100 psi. 70
Figure 4.18: (a) SEM micrograph and (b) diffusion profile of eutectic In-Sn joint after 1 hr dwell time. Joint was bonded at 125 °C under 100 psi. 71
Figure 4.19: (a) SEM micrograph and (b) diffusion profile of eutectic In-Sn joint after 4 hr dwell time. Joint was bonded at 125 °C under 100 psi. 72
Figure 4.20: (a) SEM micrograph and (b) diffusion profile of In-Sn-2.5Cu joint after 1 hr dwell time. Additions of 2.5wt% Cu to eutectic In-Sn interlayer alloy was seen to decrease the bond time necessary to obtain a high temperature stable microstructure. Joint was bonded at 125 °C under 100 psi. 74
Figure 4.21: (a) SEM micrograph and (b) diffusion profile of In-Sn-2.5Cu joint after 4 hr dwell time. Joint was bonded at 125 °C under 100 psi. 75
Figure 4.22: (a) SEM micrograph and (b) diffusion profile of In-Sn-5Cu joint after 1 hr dwell time. Joint was bonded at 125 °C under 100 psi. 77
Figure 4.23: (a) SEM micrograph and (b) diffusion profile of In-Sn-5Cu joint after 4 hr dwell time. Joint was bonded at 125 °C under 100 psi. 78
Figure 4.24: (a) SEM micrograph and (b) diffusion profile of In-Sn-5Cu joint (2 min plate) after 1 hr dwell time. Joint was bonded at 125 °C under 100 psi. 81
Figure 4.25: (a) SEM micrograph and (b) diffusion profile of In-Sn-5Cu joint (2 min plate) after 4 hr dwell time. Joint was bonded at 125 °C under 100 psi. 82
Figure 4.26: Room temperature shear strengths for TLP joints made with eutectic In-Sn interlayer using various dwell times and plating times. 87
Figure 4.27: Room temperature shear strengths for TLP joints made with In-Sn-2.5Cu interlayer and using various dwell times and plating times. Similar results were observed for the In-Sn-5Cu joints. 88
Figure 4.28: Operation temperature shear strengths for TLP joints made with In-Sn-0Cu interlayer and using various dwell times and plating times. 90
Figure 4.29: Operation temperature shear strengths for TLP joints made with In-Sn-2.5Cu interlayer and using various dwell times and plating times. Increased plating times seem to degrade the overall high temperature mechanical behavior of the In-Sn-2.5Cu joints. 91
Figure 4.30: Operation temperature shear strengths for TLP joints made with In-Sn-5Cu interlayer and using various dwell times and plating times. In contrast to the In-Sn-2.5Cu joints, increased plating times seem to improve the overall high temperature mechanical behavior of the In-Sn-2.5Cu joints. 93
Figure 4.31: SEM micrograph showing fracture surface of non-plated In-Sn-5Cu TLP joint shear tested at 100 °C. The fracture surface revealed two regions: A (η phase) and B (InSn (γ+β) phases). Fracture occurred mainly in the low melting B regions. Joint was bonded for 2 hr under 100 psi. 94
Figure 5.1: Spreading behavior observed for eutectic In-Sn-Bi alloy on Cu substrate having (a) no Cu additions; and (b) 5 wt% Cu additions. Increasing the Cu content of the interlayer alloy made it much easier to wet the Cu substrate during processing of the TLP joints. 106
Figure A.1: Equilibrium solidification paths calculated for the 50In-43.6Sn-6.4 Bi (low-Bi) alloy with (a) no Cu additions; (b) 5 wt% Cu additions; (c) 10 wt% Cu additions; and (d) 20 wt% Cu additions 108

Figure A.2: Equilibrium solidification paths calculated for the eutectic 50.9In-49.1Sn-6.4 alloy with (a) no Cu additions; (b) 2.5 wt% Cu additions; and (c) 5 wt% Cu additions. 109
Figure A.3: Prediction of phase fractions in TLP joints made with the low-Bi based In-Sn-Bi-XCu interlayer at (a) room temperature; (b) 100 °C; (c) 125 °C; and (d) 150 °C. Equilibrium conditions are assumed. 110
Figure A.4: Prediction of phase fractions in TLP joints made with eutectic based In-Sn-XCu interlayers at (a) room temperature; (b) 100 °C; (c) 125 °C; and (d) 150 °C. Equilibrium conditions are assumed. 111

List of Tables

Table I: Effect of copper additions on TLP formation in the In-Sn-Bi and In-Sn systems 39
Table II: Shear strength values measured for the low-Bi In-Sn-Bi-XCu TLP joints.................. 85

Chapter 1: Introduction

1.1 Motivation for Thesis Work

Lead-containing alloys are extensively used as soldering materials for electronic interconnects. However, increasingly stringent environmental regulations on the use of lead solders in electronics manufacturing have motivated research efforts into developing joining processes which use lead-free alloys [1]. Although several promising lead-free alloys have been developed for electronic packaging, the current alternatives present several difficulties that compromise the integrity of the interconnects [2]. One serious limitation of these lead-free solders is the increase in residual thermal stresses experienced during joint formation due to the increase in required bonding temperatures – about 20 to 40 °C higher than those commonly used for typical Pb-Sn eutectic solders (T_m = 183 °C). In addition to increased thermal stresses, higher bonding temperatures can be damaging to heat sensitive components. Thus, there is still a need for a reliable low temperature, lead-free joining technology which can replace the conventional soldering methods used in the electronics industry.

One joining method, known as low temperature transient liquid phase (LTTLP) diffusion bonding, has the potential to not only be used as a suitable replacement for existing soldering processes[3], but to improve upon them as well. Transient liquid phase diffusion bonding is a diffusion driven process which uses a low melting liquid interlayer as the soldering material to join two solid substrates. During the TLP process, the liquid interlayer undergoes isothermal solidification by the diffusion of one or more melting point depressants (MPDs) away from the interlayer and into the substrates. Since isothermal solidification takes place *gradually* at

temperatures much lower than the melting temperature of the base materials to be joined, there is a great reduction in thermal stresses during TLP bonding.

During the past few years, research has been done on using TLP bonding for low temperature joining applications [3, 4]. However, there are still obstacles associated with the process which limit the use of TLP bonding for large-scale joining applications. Specifically, the long times and/or high pressures required to make thin, robust joints has made TLP bonding an economically infeasible joining process for use in electronic packaging. Additionally, many previous LTTLP systems that have been studied require the use of aggressive soldering fluxes which not only makes production more expensive, but also produce chemical residues that are environmentally toxic. In response to these existing complications, the present research focuses on developing a novel lead-free LTTLP process that will improve upon and enhance the current form of Pb-free joining technologies that have been developed for electronic packaging.

1.2 Scope of Thesis

As mentioned in the previous section, there are still many limitations to using TLP bonding for large scale processes, including that of advanced electronic packaging. Taking these complications into consideration, a specific goal of the current work is to develop a LTTLP joining method that can be used to produce joints at temperatures less than 125 °C without the need of a chemical flux. These joints should maintain mechanical integrity up to 200 °C. Furthermore, optimization of the process parameters (i.e. bonding time, pressure, temperature, etc.) will be performed in order to make LTTLP bonding a practical joining method for industrial production. Novel approaches to TLP bonding such as the addition of the base material to the interlayer alloy, as well as the use of diffusion barrier layers to control intermetallic compound (IMC) formation will be studied as a means to achieve the target goals.

1.3 Overview of Thesis

The thesis is divided up into five different chapters. This chapter describes the motivations for the present work on LTTLP bonding. The second chapter gives background information about the TLP process. In addition, previous research related to this study is discussed. Chapter 3 details the experimental procedures used in this research. Chapter 4 provides a thorough analysis of the results obtained from the experimental work. The final chapter concludes with a summary of the results and discusses the implications of the results on the abilities of this project to achieve the previously defined goals. Recommendations for future work are given based on scientific findings.

Chapter 2: Background

2.1 Principles of TLP Bonding

Transient liquid phase bonding is not a novel process in itself. In fact, diffusion based bonding has been used for more than two thousand years, the earliest documented cases being in the Etruscan civilization [5, 6]. The earliest modern research of the topic dates back to an article published in 1959 [7], which described some the fundamental concepts of what was later termed "Transient Liquid Phase" bonding by Duvall et al. [6, 8]. Today, TLP bonding is becoming a major focus of research not only in the electronics industry, but in other engineering applications as well. For instance, researchers have been investigating the use of TLP bonding with advanced materials in order to produce similar and dissimilar joints between intermetallics [9-11] and superalloys [12, 13] for high-temperature applications such as aerospace engineering. The process known as transient liquid phase bonding has been described in the literature using various terms such as Diffusion Brazing (DFB) or Diffusion Soldering [14], Transient Insert

Liquid-Metal Diffusion (TILM) bonding [15], Solid Liquid Interdiffusion (SLID) bonding, and TLP bonding. All of these processes refer to the same diffusion driven process which will be described here.

Figure [16] shows a schematic diagram which depicts the fundamental process of TLP bonding in a binary alloy system. During the beginning stages, the interlayer alloy is heated to a temperature slightly above its melting point (T_B) (Fig. 2.1a), where it begins to dissolve the substrate (component 'A') until an equilibrium point is reached where the joint composition is shifted to that of the liquidus (C_L) and the substrate composition to that of the solidus (C_s) (Fig. 2.1b). This stage of the TLP bonding process is known as the dissolution stage, and is characterized by the growth of the liquid interlayer to a maximum thickness [17]. During isothermal solidification (Fig. 2.1c), the interlayer decreases in thickness due to diffusion of the low melting constituent (component 'B') of the interlayer alloy away from the joint into the substrate. The process is allowed to occur until the entire composition of the joint is below the solidus composition, thus completing the isothermal solidification process (Fig. 2.1d). Additional time is given for the joint to homogenize in composition and microstructure (Fig. 2.1e) until it is practically indistinguishable from the parent materials (Fig. 2.1f). At this point the joint has a melting point much higher than the original bonding temperature, allowing it to be used at elevated service temperatures.

Three important processing parameters of TLP bonding are the bonding time, temperature, and pressure. The bonding time, also called dwell time, must be long enough in order to allow the transient liquid phase to form and to allow sufficient diffusion of the melting point depressant (MPD) out of the interlayer into the substrate so that isothermal solidification

can occur. Although hard to predict, the dwell time necessary to produce a TLP joint is strongly dependant on the initial thickness of the interlayer, the concentration of MPD, and the diffusivity

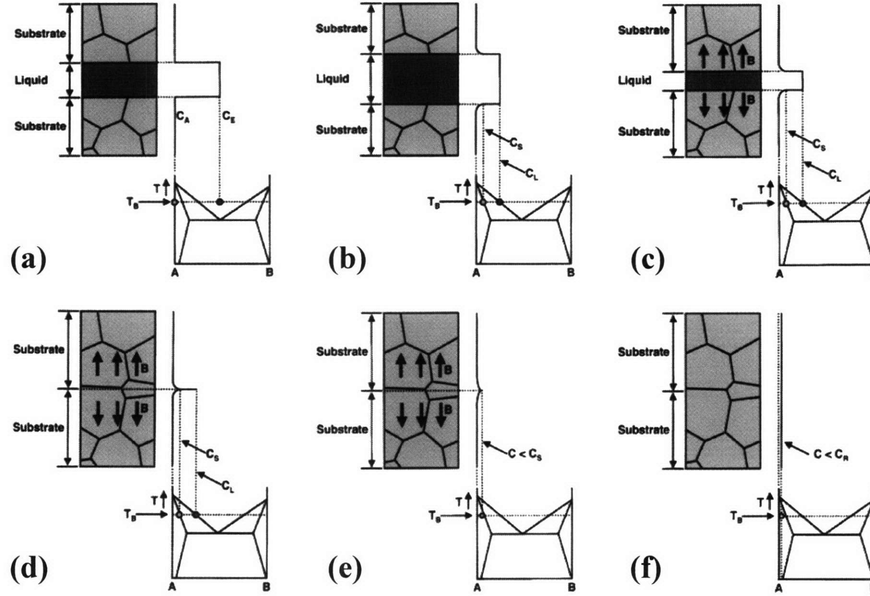

Figure 2.1: Stages of TLP bonding: (a) alloy heated slightly above its melting temperature (T_B); (b) dissolution of substrate; (c)-(d) isothermal solidification; (e) solid state homogenization; (f) final condition. (From Ref. [16])

of the MPD [9, 18]. Since the dwell time depends on the diffusion coefficient of the MPD, it is also related to the temperature. That is, a higher bonding temperature requires less dwell time, as expected from the Arrhenius relationship of the diffusion coefficient:

$$D = D_o \exp[-Q / RT] \qquad \text{(Eq. 1)}$$

where D_0 is the diffusion constant for the MPD, Q is the activation energy for diffusion of the MPD, R is the gas constant, and T is the bonding temperature. The bonding temperature used in a TLP bonding process should generally satisfy the following conditions: (1) it should be high enough so that the interlayer is fully or partially in the liquid state; (2) it should be in a range that prevents the formation of any intermetallic compounds (IMCs) that may impede the diffusion of MPD, and thus lengthen the time for isothermal solidification [9]. Finally, pressure is applied to

the joints during TLP bonding in order to expel excess liquid from the joint and thus reduce the time necessary for isothermal solidification. However, for large-scale industrial applications, the bonding pressure should be sufficiently low to minimize stresses on electronic package components during processing, as well as to reduce the amount of energy used during processing to minimize operation costs. Bonding pressure also plays an integral role in controlling interface diffusion during TLP bonding [9].

2.2 Materials Selection for LTTLP Bonding

2.2.1 Practical Considerations

Many of the lead-free soldering technologies that have been developed over the past decade to replace conventional Pb-Sn soldering methods have been geared toward reflow or wave soldering processes. The most popular lead-free alloy that is being used by the electronics industry is the ternary eutectic Sn-Ag-Cu (SAC) alloy (T_m = 217 °C), although tin-copper (Sn-Cu) alloys are also alternatively used due to their lower costs [19, 20]. Other lead-free solders that have been studied include Sn-Ag, Sn-Ag-Bi, and other ternary and quaternary alloys [19, 21, 22]. Extensive research has been done on predicting the thermodynamics [23-30] and kinetics [31-34] of such solders, as well as on assessing thermal [35, 36], mechanical [37, 38], electrical [39], and other properties associated with joint reliability. However, most of these solders have melting temperatures higher than that of the eutectic Pb-Sn solder (T_m = 183 °C). Therefore, many of the material systems studied are not well-suited for reduced temperature joining (i.e. below 183 °C), especially where thermal stresses and heat-sensitivity are of great concern. In the case of LTTLP bonding, there is still a need to develop a reliable materials system.

When choosing a materials system for a TLP process, there are certain considerations that must be taken into account. The most important is the temperature at which the parent metal or

interlayer alloy will form a liquid phase. For this work, this temperature was defined to be less than 125 °C. The low melting temperature phase must also have solubility for the MPD. In order to achieve complete isothermal solidification in reasonable times, the diffusivity of the MPD must be above 10^{-8} cm^2/sec [40]. Therefore, if a phase diagram is known for the materials system under consideration, it is advisable to avoid the formation of intermetallics that may limit the diffusivity of the MPD; or likewise, embrittle the joint. As mentioned in the previous section, this can be done by varying the bonding temperature [9]. Alternatively, the composition of interlayer alloy can be changed in such a fashion that does not favor the formation of these IMCs. Finally, for practical reasons, it is advisable to use a materials system in which the low melting phase does not greatly fluctuate with slight composition variations. This lessens the tolerance that has to be achieved during large-scale production of the joints, making the electronic packaging process more reliable.

Presently, the most complete and reliable phase equilibria information for TLP processes is for binary alloy systems such as the Cu-Sn or Cu-Ag systems. Binary phase diagrams for these types of systems have already been well developed, and so accurate prediction of equilibrium phases and resulting microstructures of TLP joints made with these materials is relatively straightforward. Unfortunately, most binary systems can not be used to bond at reduced temperatures. For instance, it has been shown that in order to make robust TLP joints using the Cu-Sn system, a joining temperature of at least 676 °C should be used in order to avoid the formation of brittle intermetallics such as Cu_3Sn (ε). For Cu-In, a bonding temperature above 631 °C must be used in order to prevent the formation of Cu_7In_3 (δ) [41]. Practical issues such as these, limits the use of binary alloys for low temperature TLP bonding in electronic packaging applications. In order to develop a successful TLP process, one must turn to ternary and

quaternary alloy systems; those of which are yet to have complete phase diagrams over the entire compositional and temperature ranges that are of soldering interest [24].

2.2.2 In-Sn-Cu and In-Sn-Bi-Cu Systems

The materials systems studied in this research for the LTTLP bonding of copper were the In-Sn-Cu and In-Sn-Bi-Cu systems. In the In-Sn-Cu system, the interlayer is a eutectic In-49.1Sn (wt.%)[1] alloy which has a melting temperature of 120 °C. Although there are no phase diagrams available for the In-Sn-Cu system at temperatures below 400 °C, characterization of diffusion soldered copper-to-copper joints made with an In-Sn eutectic alloy was performed by Sommadossi et al. [42]. Particularly, it was noted that at bonding temperatures below 200 °C, only the η intermetallic phase (IP) grows. The η phase [$Cu_2(In,Sn)$] is based on the Cu_2In binary IP which has the ability to dissolve a third element (Sn in this case) [42]. Since the melting point of the η phase is 500 °C, it can be used to stabilize the joint at elevated service temperatures. However, there are some complications which arise during the formation of the η phase which must be taken into account when using the In-Sn-Cu TLP system. These will be discussed in Section 2.3.2.

In order to depress the melting temperature of the In-49.1Sn alloy even further, bismuth additions can be added to the alloy, thus creating a In-Sn-Bi-Cu quaternary TLP system. Lowering the melting temperature has some advantages – one being that a lower melting interlayer allows the TLP joining process to be used at lower temperatures which further reduces thermal stresses during bonding. Also, for a given joining temperature, lowering the melting temperature of the interlayer alloy improves its spreading characteristics. This is due to the fact that as the excess temperature above the solder's melting temperature increases, the area of

[1] All alloy compositions throughout the rest of the paper will be given in wt.% unless otherwise specified.

spreading increases [43]. This is especially important for Bi-rich alloys, as Bi has been observed to diminish the wettability of certain solders on Cu substrates [44]. The thermodynamic data used for the In-Sn-Bi-Cu systems studied in this work were calculated by Dr. Raymundo Arroyave. Figure 2. [6] shows the ternary In-Sn-Bi phases diagrams that Dr. Arroyave calculated using Thermo-Calc®. The bold red lines represent a range of alloy compositions near the eutectic which have melting points between 60-110 °C, and therefore are potential candidates as interlayers for LTTLP bonding. Two alloy compositions were chosen as interlayers for

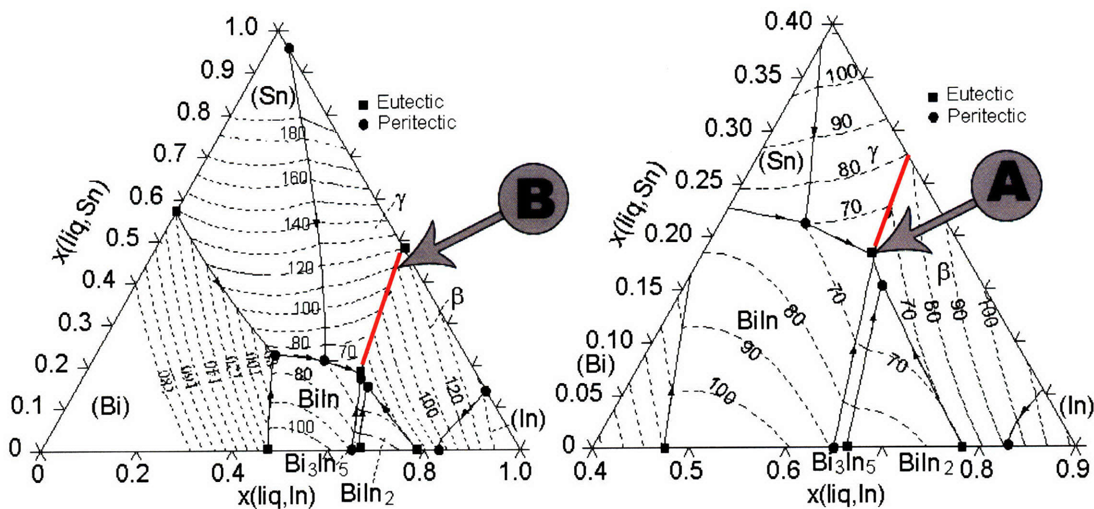

Figure 2.2: Calculated In-Sn-Bi ternary phase diagrams. The points 'A' and 'B' represent the eutectic and low-bismuth interlayer alloys, respectively. (From Ref. [6])

studying the In-Sn-Bi-Cu TLP process. The first alloy, labeled 'A' in Figure 2. is the eutectic alloy 48.3In-15.6Sn-36.1Bi which, according to thermodynamic calculations, has a melting temperature of about 60 °C. The other alloy, labeled 'B', is a low-Bi alloy with the composition 50In-43.6Sn-6.4Bi and has a melting temperature of 110 °C according to the calculated phase diagram. The reason for choosing the second alloy with a lower bismuth content is due to some of the known deleterious effects of Bi-rich solders [45, 46] . For example, it has been found that the thermal fatigue life and ductility of Sn-3.5Ag solders are degraded due to the precipitation of fine bismuth particles [46]. Also, copper has no solubility for bismuth which may limit its use as

a MPD in the In-Sn-Bi-Cu TLP process. Therefore, in addition to the Bi-rich eutectic alloy, it was advisable to study another low melting alloy within the In-Sn-Bi system with a lower bismuth content.

2.3 Novel Approaches to TLP Bonding

2.3.1 Addition of Base Material to Interlayer Alloy

One way to improve the TLP joining process is to reduce the amount of dissolution (see Fig. 2.1b) by adding varying amounts of the base material to the interlayer alloy. Having an interlayer that is partially composed of some of the base material would lessen the amount of substrate that needs to be dissolved in order for the liquid interlayer and solid substrate to come into equilibrium. Decreasing the dissolution volume during the early stages of TLP bonding would effectively reduce the required holding time by shortening the diffusion distances, and thus the time for the bond to mature and homogenize. A reduction in bonding time is extremely important in making TLP bonding an economically viable, large-scale process for electronic packaging.

Another potential advantage of adding base material to the interlayer alloy can be seen from Figure 2. which shows plots, calculated by Dr. Arroyave, of temperature versus liquid fraction for four alloys with the composition of 16Sn-6.4Bi-XCu (In bal.), where X represents the amount of copper added to the interlayer alloy. In the case of equilibrium solidification, it is seen that increasing additions of copper result in a lower solidification temperature. With regard to LTTLP bonding, this means that at reduced bonding temperatures (for example, below 120 °C), the interlayers with a higher composition of base material (i.e. Cu in this case) will contain a larger fraction of liquid phase which enhances the TLP bonding process. According to the Scheil equation, or non-equilibrium, solidification calculations, all of the alloys have very similar

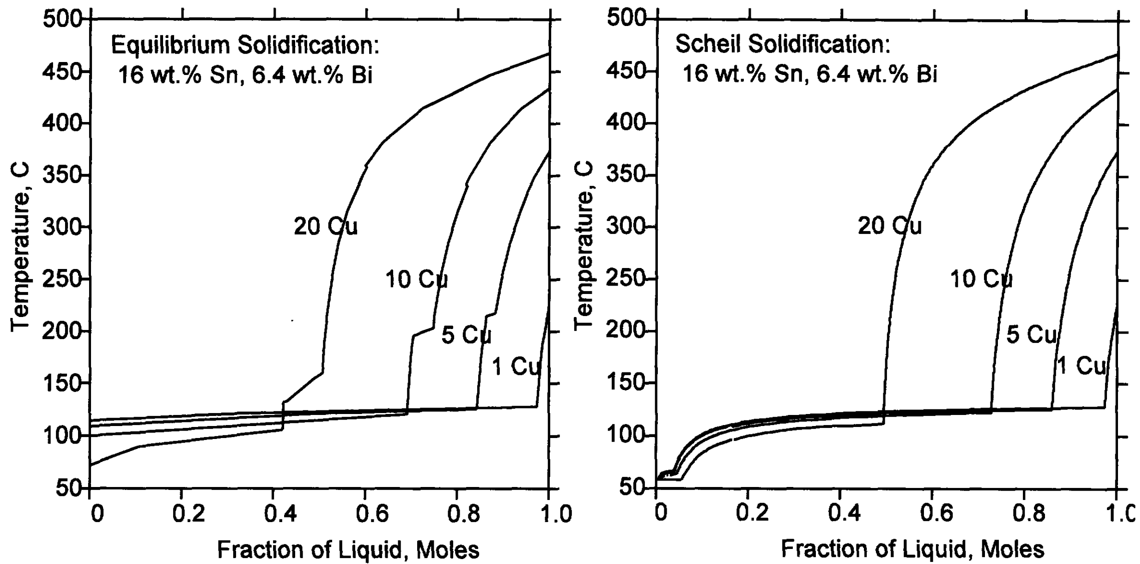

Figure 2.3: Liquidus Calculations for 16Sn-6.4Bi-XCu (In-balance) alloys. For equilibrium solidification conditions, larger additions of Cu result in lower solidification temperatures. Scheil solidification calculations predict very similar solidification patterns for all alloys below 120 °C.

solidification patterns below 120 °C. The actual solidification patterns of these alloys should be somewhere between these two trends. Although these calculations are for alloys which have different compositions than the ones being studied in the present work, a similar type of behavior may be expected. For this reason, an analysis of the effects of copper additions on the solidification behaviors of the aforementioned alloys in the In-Sn and In-Sn-Bi systems were performed in this study.

2.3.2 Diffusional Barrier Layers on Substrate

Various phenomena can occur during the course of TLP bonding which complicate the kinetics of the process. One problem that may be encountered during TLP bonding is surface roughening of the substrate due to solid-state diffusion. Such a phenomenon was observed by MacDonald et al. [18] who noted the formation of a rough cellular solidification surface of a diffusion brazed Cu-Ag couple, as shown in Figure 2. The evidence of the protrusions was attributed to grain boundary grooving caused by surface tension coupled with the migration of

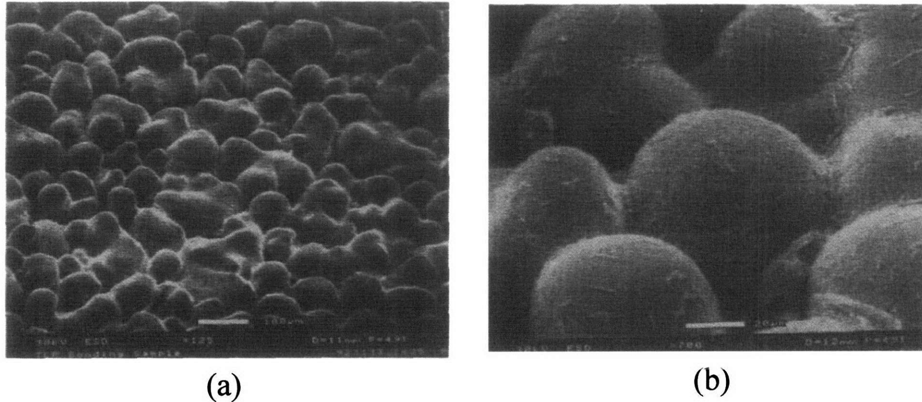

(a) (b)

Figure 2.4: Solidification surface of a diffusion brazed Cu-Ag couple: (a) 125x; (b) 700x. A rough, cellular surface due to grain boundary grooving effects is observed on the Cu-Ag couple. (From Ref. [18])

the solid-liquid (S/L) interface [18]. Surface roughening can limit the ability to achieve thin joints during TLP bonding if the protrusions connect across the joint.

A similar phenomenon in which the planarity of the S/L interface is broken down during TLP bonding occurs during intermetallic formation from the substrate interface. When heating to the target bonding temperature, solid state reactions between the interlayer and the substrate can lead to the formation of intermetallics from the substrate surfaces. If intermetallic phases are formed in a non-planar manner, their continual growth and eventual contact across the joint can isolate the liquid phase in a manner which prevents the diffusion of the MPD necessary for the TLP bonding to proceed. Bosco et al. [47] studied the growth of Cu_6Sn_5 (η) intermetallic grains during a Cu-Sn TLP bonding process and noted that contact of the grains and subsequent consumption of Sn through reaction with Cu lead to void formation near the bond mid-plane when the interlayer was below a certain critical thickness. The existence of a critical interlayer thickness to prevent void formation also limits the thickness of joints that can be attained from the TLP process. In the In-Sn-Cu TLP system, Sommadossi et al. [42] observed similar growth behavior of the η [Cu_2(In,Sn)] intermetallic phase. Figure 2. [42] shows the duplex microstructure of the η phase, with the coarse grains being produced by diffusion of Cu atoms

through the solid η phase and continued reaction with the liquid at the liquid/grain interface. The fact that the thickness of the region of coarse grains is about twice that of the fine-grained region suggest that the mobility of the Cu atoms through the η phase is higher than that of the In and Sn atoms through the same phase [42]. The growth of the coarse grains can lead to similar effects as described previously for the Cu_6Sn_5 intermetallic grains (i.e. void formation and large joint thicknesses). Moreover, the interface between the η sublayers of large and small grains has been observed to be the critical location for fracture development [48].

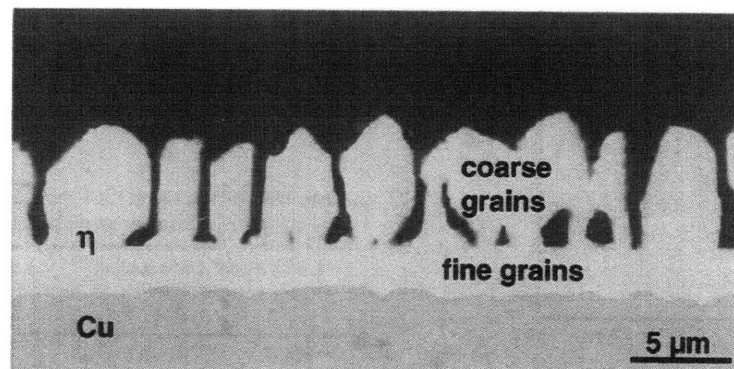

Figure 2.5: Cross-section of a Cu/In-48 at.%Sn/Cu sample diffusion soldered at 200 °C for 30 min. The η phase is formed with a duplex microstructure containing both coarse and fine grains. (From Ref. [42])

Undesirable effects such as surface roughening and brittle intermetallic formation are usually unavoidable in the TLP process, especially when bonding at low temperatures where slow solid state diffusion takes place. However, with clever processing design, the degree of which such phenomena occur can be controlled. In this work, a method is proposed by which a diffusion barrier layer is placed on the substrate surfaces in order to limit the amount of solid state diffusion which occurs during the initial stages of TLP bonding. Specifically, the use of electroless nickel plating on copper substrates will be studied as a means to minimize or prevent surface roughening and/or formation of coarse-grained η phase during the heating and dissolution stages of the TLP process. In order to accomplish this, the nickel layer must prevent

the interdiffusion and subsequent reaction between the substrate and interlayer. In addition, the nickel layer must also breakdown after the first stages of the TLP process to permit the interdiffusion required for isothermal solidification to complete. With respect to the In-Sn-Cu and In-Sn-Bi-Cu LTTLP processes, the formation of the η phase is necessary in order to achieve stable joints at elevated temperatures. Therefore, an optimum thickness for the nickel layer is sought which allows it to fulfill both of these requirements in order to minimize the joint thickness while producing mechanically stable joints.

2.4 Summary of Target Goals

In summary, the overall goal of this work is to develop a lead-free, LTTLP bonding process within the In-Sn-Bi-Cu and In-Sn-Cu systems which requires:

- Maximum bonding temperature of 125 °C; secondary target maximum bonding temperature is 75 °C
- Maximum bonding time of 2 hrs.
- Minimal bonding pressure (preferably less than 100 psi, although larger pressures were studied)
- No chemical flux

Additionally, the joints produced by the LTTLP bonding process should display the following characteristics:

- Reflow temperatures of at least 200 °C
- Minimal joint thickness (preferably less than 25 μm)
- Mechanical integrity at elevated temperatures (defined to be 100 °C, which is representative of the service temperatures typically undergone by these joints)

Chapter 3: Experimental Procedure

3.1 Sample Preparation

3.1.1 Alloy Production for TLP Interlayers

The two compositions of alloys that were used as TLP interlayers in the In-Sn-Bi-Cu system were 50In-43.6Sn-6.4Bi (low Bi alloy) and the eutectic 48.3In-15.6Sn-36.1Bi. For the In-Sn-Cu system, the interlayer was composed of the eutectic 50.9In-49.1Sn alloy. In addition, to study the effects of adding base material to the interlayers, various quantities of copper additions were added to the standard interlayer alloys for each system. In every case, as copper was added to the interlayer, the quantity of each of the other constituents used in the interlayer was decreased by a respective amount which left the ratio of the standard interlayer (i.e. with no copper additions) the same.[2] The form and purity of the raw materials that were used to make the interlayer alloys were: indium bar (99.99%), tin granules (99.99%), 5-20mm bismuth needles (99.99%), and 4-6mm copper shot (99.999%). Lead-tin eutectic alloys (63Sn-37Pb) were also produced using 3mm lead shot (99.9999%) and the tin granules mentioned previously. These alloys were used to make Pb-Sn soldered joints which were used as a comparison to the TLP joints made in this study.

Once the materials for each of the standard interlayer alloys were weighed (± .005 g), they were encapsulated inside of a quartz tube that was evacuated to a pressure below $1*10^{-6}$ torr and then backfilled with argon. This was to prevent oxidation of the materials during the melting process. During the melting process, the quartz tube was placed inside of a box furnace at 700 °C for 8 hours. The long melting time was used to ensure homogeneity of the alloy. After the

[2] All alloy compositions throughout the rest of the paper will be designated as either In-Sn-Bi-XCu or In-Sn-XCu depending on the material system. The ratios (not actual composition) of the In-Sn-Bi and In-Sn will be assumed to be the same as those described for the base alloys (i.e. 50In-43.6Sn-6.4Bi and 50.9In-49.1Sn, respectively).

melting process was complete, the tube was removed from the furnace at the melting temperature and allowed to air cool to room temperature. Once cooled, the bar of solidified alloy was removed from the quartz tube. This same process was performed for the production of the Pb-Sn alloy.

Production of the interlayer alloys with copper additions was slightly different than the process previously described. In order to homogeneously dissolve copper into the alloys, a master alloy of composition 70Cu-30Sn was made first. The encapsulation process for the master alloy was the same as for the standard interlayer alloys. The master alloy was melted inside of a box furnace at 1100 °C for 8 hours and air cooled in the same manner as the standard alloys. To make the interlayers with copper additions, pieces from the master alloy were added to other raw materials of the standard interlayer alloys in order achieve the corresponding percentage of copper addition while keeping the ratio of the standard interlayer the same. These materials were then melted in the same fashion as described for the standard interlayer alloys. Energy dispersive spectroscopy (EDS) was performed after every melting step to evaluate the composition of the alloys. All of the alloys had bulk compositions within 2 wt.% of the expected values.

3.1.2 Differential Scanning Calorimetry

In order to verify the melting temperatures of the interlayer alloys, differential scanning calorimetry (DSC) was performed on the alloys using a PerkinElmer® PYRIS Diamond DSC. This is a power compensation DSC which allows it to resolve closely occurring thermal transitions. In addition, it uses platinum resistance thermometers rather than conventional thermocouples to make extremely accurate temperature measurements. In one calorimeter of the DSC, small pieces of each alloy (≈ 5-15 mg) were placed inside an aluminum pan so that they

completely contacted the base of the pan. An empty aluminum pan was placed in the second calorimeter as a reference. The heating profile for the samples was the following: hold at 50 °C for 1min; heat from 50 °C to 450 °C at 10 °C/min; cool from 450 °C to 30 °C at 10 °C/min; and a final hold for 1min at 30 °C. The heating (and cooling) rates were 10°C/min, which is the same as those used during the TLP bonding procedure (see Section 3.1.3 iii). After each test, a graph of the heat flow (mW) versus temperature (°C) was generated, from which the melting temperatures of various phases were calculated. This way, one could observe the presence of phases which melt below the bonding temperature (and thus produce the transient liquid phase necessary for the TLP process) and those which melt above this temperature and do not contribute to forming the TLP phase. Results from the DSC tests were compared equilibrium solidification paths which were derived through *ab initio* thermodynamic calculations.

3.1.3 Production of TLP Joints

i) Substrate Preparation and Nickel Plating

The first step in producing the TLP joints was to cut out copper substrates using an electron discharge machine (EDM). Copper coupons of dimensions 0.5"x 0.5" (.062" thick) were EDM cut from an Alloy 110 copper sheet with mirror-like (#8) finish (from McMaster-Carr®). The copper coupons were then cleaned with 30%HCl and rinsed with deionized water and ethanol.

An electroless nickel plating solution, produced by Alfa Aesar®, was used to nickel plate the surfaces of the copper substrates. The solution bath was kept a temperature of 95 °C using a hot plate, while the pH was maintained between 2-8-3.5. Although a range of plating times was tested in this study, it was the 1, 2, and 3 minute plated copper substrates that were used to produce the TLP joints in this study (in addition to the non-plated samples). The thicknesses for

the 1, 2, and 3 minute platings were approximately 1.5 μm, 2.2 μm, and 3.1 μm, respectively, as measured using SEM image analysis tools. The reason for choosing these plating times (and corresponding thicknesses) will be discussed in Section 4.2 of the results section. The composition of the deposits was 90%Ni-10%P according to the manufacturer's specifications, but EDS measurements were made to verify the compositions. After being plated, the copper substrates were cleaned with deionized water and ethanol to remove any excess solution from the surfaces prior to the bonding procedure.

ii) Bonding Procedure – Application of Interlayer Alloy

After the copper substrates were prepared, as described in the previous section, the next step was to make sandwich copper-to-copper (Cu/Cu) bonds using the desired interlayer alloy, as shown in Fig. 3.1 (note that the figure is not drawn to scale). For the bonding procedure, the

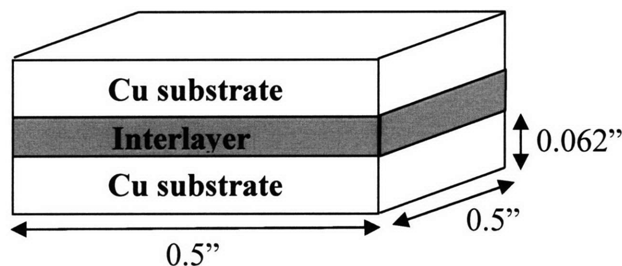

Figure 3.1: Schematic of copper-to-copper sandwich bonds used to create TLP joints.

copper coupons were taken to a glove box which contained an atmosphere of nitrogen and forming gas (95%N-5%H). Figure 3.2 shows the experimental set-up within the glove box for the bonding procedure. An aluminum fixture containing small wells was used to hold the copper pieces in place while a hot plate heated the fixture to the desired bonding temperature of either 75 °C (for the In-Sn-Bi-XCu eutectic based alloys) or 125 °C (for the In-Sn-Bi-XCu low-Bi and In-Sn-XCu alloys). Once the copper pieces reached the set temperature, small beads of the interlayer alloy were placed on the polished (mirror-like) side of the copper pieces and allowed

to melt. The alloy was then spread over the entire surfaces of the copper substrates using an ultrasonic lapper with a half-inch copper tip. The ultrasonic lapper slightly scored the surfaces of the copper pieces and used mechanical agitation (i.e. high frequency vibrations) to ensure complete wetting of the substrates. A different tip was used for each different interlayer alloy in order to prevent contamination of the alloy's composition. To create the Cu/Cu bonds, two of the substrates with melted alloy were sandwiched together while tweezers were used to make

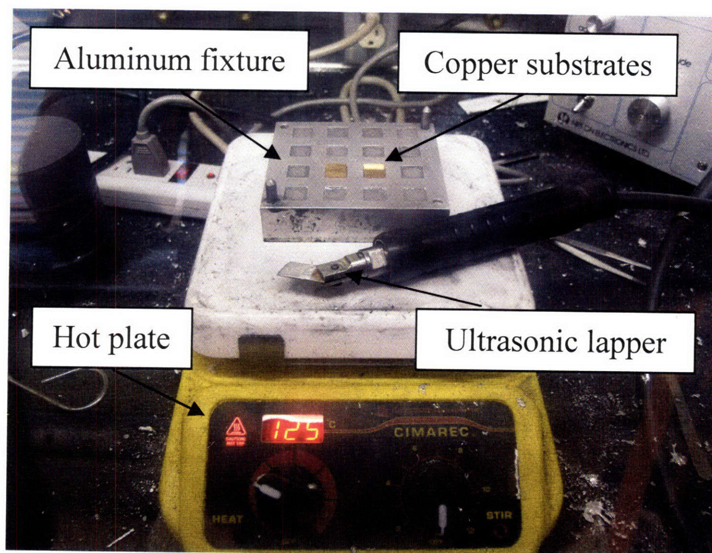

Figure 3.2: Experimental set-up for bonding procedure. Beads of interlayer alloys were spread on the heated surfaces of copper substrates using an ultrasonic lapper. The bonding procedure was done within a glove box containing an atmosphere of pure nitrogen and forming gas (95%N-5%H).

sure that the two opposing substrates remained parallel to one another. After creating the sandwich bonds, the samples were quickly removed from the aluminum fixture to prohibit as much diffusion from occurring before the pressing stage of the TLP joint production. The same bonding procedure, as described in this section, was also used to make the Pb-Sn soldered samples. In the case of these samples, the copper pieces were heated to 190 °C in order to melt the Pb-Sn eutectic alloy and allow it to be spread on the surfaces of the substrates.

iii) Pressing Procedure

The final stage of TLP joint production was the pressing stage. Two different apparatuses were used for producing the TLP joints for reasons that will be described shortly. Figure 3.3 shows the pressing apparatus used for producing all of the TLP joints in the In-Sn-Bi-Cu system. Prior to pressing the Cu/Cu sandwich bonds, a dual-platen hot press (Fig. 8a) was pre-heated to the desired bonding temperature. An Omega® 871 digital thermocouple thermometer was used to measure the temperature of the platens. Once the platens reached the bonding temperature, the press automatically maintained the temperature (±2 °C). The Cu/Cu

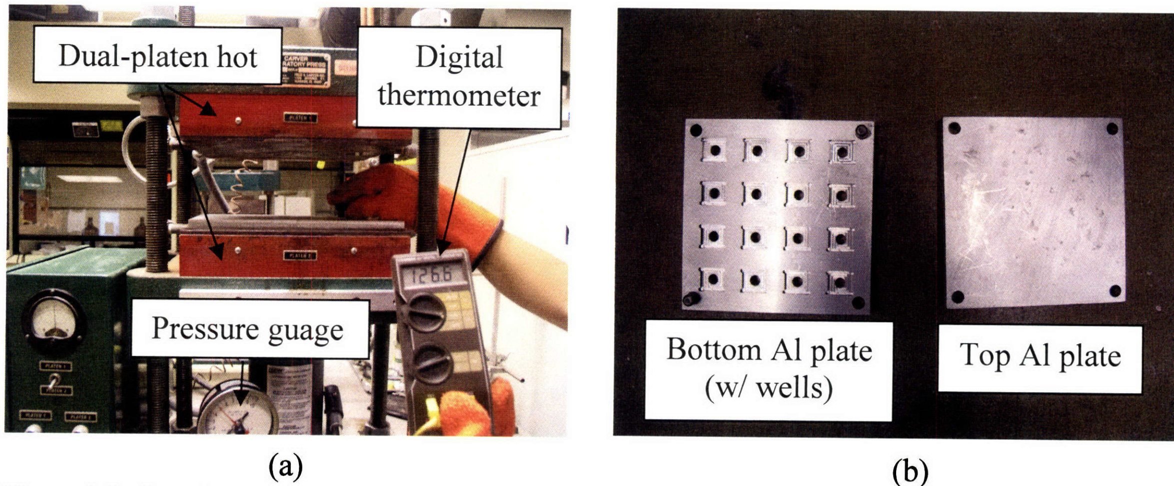

Figure 3.3: Pressing apparatus used to press the In-Sn-Bi-Cu TLP joints: (a) Dual-plate hot press used to press the Cu/Cu sandwich bonds to create TLP joints; (b) aluminum plates used to hold samples together during the pressing stage of the TLP process.

sandwich bonds were then placed in an aluminum plate with smalls wells (Fig. 3.3b) and placed on the hot press. The aluminum plate was allowed to heat at a rate of 10 °C/min to the bonding temperature before placing a second, flat aluminum plate on top of it. Small metallic pegs on corners of the bottom aluminum plate were placed through holes in the top plate to ensure the two plates remained parallel to one another during pressing. Finally, the entire fixture of Cu/Cu bonded samples sandwiched between two aluminum plates was pressed between the two platens of the hot press for the designated bonding pressure and time (a Carver® pressure guage was

used to monitor the pressure). After pressing was completed to create the Cu/Cu TLP joints, the aluminum plates were taken off of the press so that the samples could be removed and allowed to air cool to room temperature.

During the course of research, a new method of pressing samples was developed in order to optimize this stage of TLP joint production. One problem with the previously described method was the inability to press the samples under an inert atmosphere, thus allowing oxidation to occur. Also, the pressure had to be controlled manually, making this method laboriously inefficient. Figure 3.4 shows the apparatus used the press all of the TLP joints from the In-Sn-Cu system. The apparatus consisted of three aluminum plates, two compression springs (spring force rate = 110 lbs/in.), and two knobs attached to threaded rods. The Cu/Cu sandwich bonds (with In-Sn-XCu interlayers) were placed between the bottom two plates as shown in the figure.

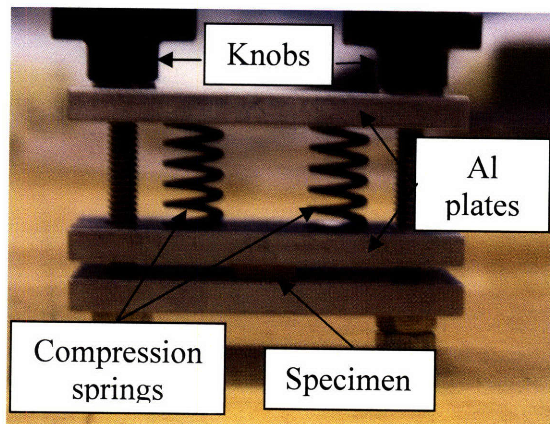

Figure 3.4: Pressing apparatus used to press the In-Sn-Cu TLP joints.

The two knobs were then turned to compress the upper aluminum plate, which in turn compressed the springs to obtain the desired pressure on the specimen. Four of these apparatuses, each containing an individual specimen, were placed on a heating plate within a furnace which was filled with 95%N-5%H forming gas. The specimens were heated to their

bonding temperature of 125 °C at a rate of 10 °C/min. A type K thermocouple was coupled to the heating plate through a programmable control in order to control the TLP bonding temperature. The thermocouple was placed within the furnace in the vicinity of the samples in order to monitor the temperature (±3 °C). After pressing was completed, the four apparatuses were removed from the furnace so the samples could be removed and allowed to air cool to room temperature.

The Pb-Sn samples were not pressed because they were to be studied as conventional soldered joints as opposed to TLP joints.

3.2 Microstructural and Phase Analysis

3.2.1 Metallographic Preparation

Before analyzing the resulting microstructures and phases of the various TLP joints, a specimen from each set of uniquely prepared joints had to be metallographically prepared. The specimens were first cut through the center using a high speed diamond saw. One of the halves was then mounted in an epoxy media containing conductive filler so that the cross-section of the joints could be analyzed using scanning electron microcopy (SEM) techniques. The mounted samples were then prepared using the following grinding and polishing schedule: 500 grit (~30 μm) and 1200 grit (~14 μm); 5 μm, 1 μm, and 0.3 μm MicroPolish® II alumina suspension; and 0.05 μm MasterPrep® alumina suspension.

3.2.2 Scanning Electron Microscopy

A Leo® 438 variable pressure (VP) SEM was used for microscopic analysis of the TLP joints. In order to obtain the most clearly resolved micrographs, secondary electron images were taken using the following setting: 400 μA beam current, 250 pA probe current, and 20 kV

acceleration voltage. These images provided sufficient contrast to identify the different phase regions within the joints without the need for using additional back scattered imaging techniques. Although the samples were not etched to reveal grain boundaries, the morphology of the various phase regions was observed. The microstructures of some of the phases were deduced by comparing the micrographs in this work to those described in related technical literature. Imaging analysis tools associated with the SEM system were used to measure joint thicknesses as well. In addition to studying the microstructure of the TLP joints, failure analysis of the joints was performed by studying the resulting fracture surfaces of mechanically tested joints (See Section 3.3).

3.2.3 Energy Dispersive Spectrometry

Chemical characterization of the TLP joints was performed using an energy dispersive x-ray spectroscopy system within the SEM. Several types of data were collected from the samples in order to fully characterize the compositional make-up of the joints. The first type of data that was collected was the x-ray spectra of the individual phases of the joint. These spectra were used to determine (semi-quantitatively) the chemical compositions of the phases. By comparing the composition of individual phases with relevant phase diagrams, an assessment of the thermal stability of the joints could be made. That is, the mechanical properties of the joints at elevated temperatures (see Section 3.3) could be related to the degree of low melting point phases which remained in the joint after the TLP bonding process.

A second EDS technique used to chemically analyze the TLP joints was to take diffusion profiles of the joints using a line scan method. The method employed in this work, however, differed from typical line scan measurements. Figure shows an illustrative sketch of the difference between the two types of scans using a schematic Cu/Cu TLP bonded joint as an

example. In conventional line scans (Fig. 3.5a), spectrum measurements taken from many single points across the specimen are used to obtain a linear diffusion profile. However, in the profiling method used in this work (Fig. 3.5b), x-ray spectra were taken from small rectangular areas instead of singular points. The data obtained from each of the area scans was then used to graph the diffusion profile. The reason for measuring the diffusion profiles in this way was due to inhomogenity observed in the joints, as will be discussed further in the Section 4.4.2.

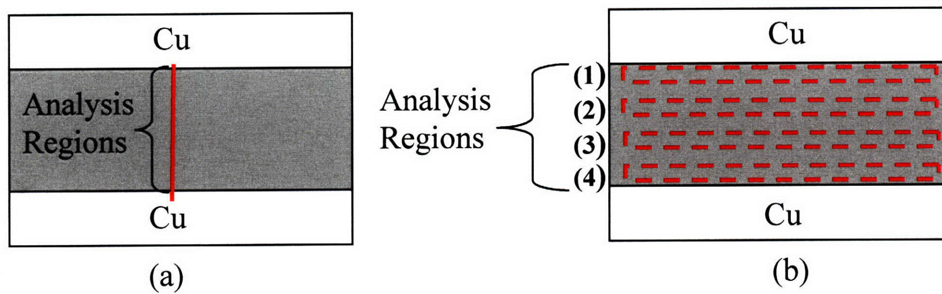

Figure 3.5: Two EDS diffusion profiling methods: (a) Typical line scan measurement; (b) Rectangular area scan technique used in the present work. Composition data obtained from each rectangular area was used to plot the diffusion profile of each elemental constituent across the TLP joint.

Lastly, an EDS analysis method known as compositional mapping was also performed on some of the TLP joints. During compositional mapping, x-rays produced from each of the elemental constituents in the specimen are used to create individual, usually color-coded, maps of the intensity patterns. From these patterns, one can observe the topography (i.e. location) of each element in order to better understand the diffusion and segregation behavior during the TLP bonding process. Compositional mapping was used, as will be shown in Section 4.2, to determine the optimal nickel layer thicknesses used as diffusion barriers for TLP bonding.

3.3 Mechanical Testing

3.3.1 Shear Tests

The mechanical integrity of the TLP joints was evaluated by performing both room temperature and elevated temperature shear tests. A shear testing fixture, shown in Fig. 3.6a, was designed to hold the specimens for these tests. The test specimen was loaded in the small well (Fig. 3.6a) so that one of the copper substrates sat inside of the well, while the other substrate was exposed to a rectangular shear column (Fig. 3.6b). The shear column rested on only the one exposed Cu substrate so that the area of the specimen being tested was 0.5in. x 0.062 in. , or 0.031 $in.^2$ (refer to Fig. 3.1). After loading the specimen into the testing fixture, the fixture was placed on the stage of an Instron® 5500R (Fig. 3.6c) which was used to run the shear tests. A load cell of 1,000 lbs was used for these tests. A cylindrical crosshead was used to transfer the load to the test specimen through the rectangular shear column (Fig. 3.6c,d) at a rate of .02 in/min. Also, a small stainless steel marble was placed in a small groove that was machined into the center of the top of the shear column (Fig. 3.6d) to make sure that the load was evenly distributed to the test specimen.

During the room temperature tests (≈ 25 °C), the shear fixture was placed directly onto the Instron® stage. For the elevated, or service, temperature tests (100 °C), the shear fixture was placed on a heating plate which was then put onto the stage (see Fig. 3.6d). A type K thermocouple was placed through the back of the shearing fixture (where the sample ejector is inserted in Fig. 3.6b) so that it just touched the substrate of the test specimen which sat inside of the well, as seen in Fig. 3.6d. This was the most accurate way to monitor the test temperature of the specimens. The heating apparatus and thermocouple were the same as those used for the pressing procedure of the In-Sn-Cu TLP joints (Section 3.1.3 *iii*) and maintained the test

temperature ±3 °C. Data from the tests was collected through a Bluehill® software program associated with the Intron® machine.

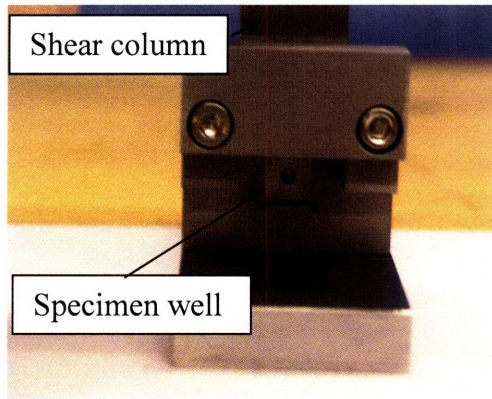

(a)

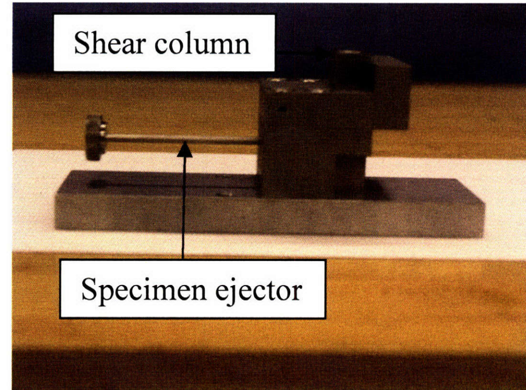

(b)

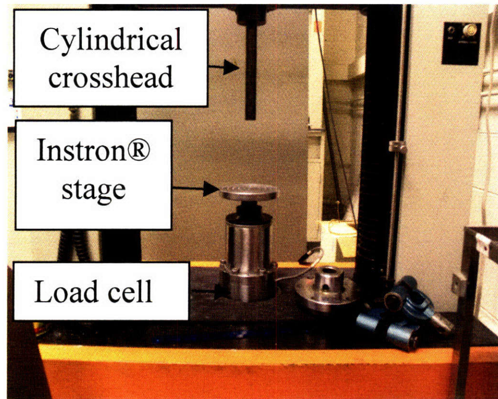

(c)

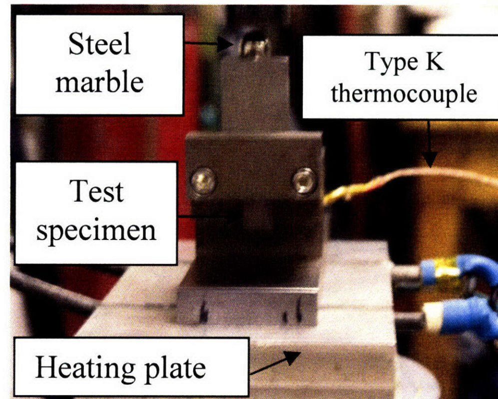

(d)

Figure 3.6: Shear testing experimental set-up: (a) Shear testing fixture (front view); (b) Shear testing fixture (side view); (c) Instron® machine; (d) Set-up for elevated temperature (100 °C) shear tests.

Chapter 4: Results and Discussion

4.1 Interlayer Alloy Melting Behavior

Figure 4.1a shows typical output from a DSC test (in this case, for the 50In-43.6Sn-6.4Bi alloy) which plots heat flow (mW) versus temperature (°C). The peaks on the graph represent phase transitions which occur during the heating (top portion of graph) and cooling (bottom portion of graph) stages of the test. Figure 4.1b shows an equilibrium solidification path for the same alloy that was calculated by Dr. Arroyave using Thermo-Calc®. The colored lines represent different phases, each of which is defined in the key on the upper-left portion of the graph. To compare these two sets of data, the first large peak in Fig. 4.1a (circled), which represents the formation of the transient liquid phase, can be related to the liquid line (black) in Fig. 4.1b. According to the DSC results, TLP formation begins at temperature of 93.9 °C and completes at a temperature of 108.0 °C. Comparatively, the thermodynamic calculations predict the first liquid to form in the alloy is at a temperature around 80 °C and complete melting of the alloy to occur around 110 °C. Although the onset temperatures for TLP formation, as determined both experimentally and computationally, differ by around 10-15 °C, the end temperatures are in very close agreement (within 1 °C).

The most pertinent data gathered from the DSC tests, in regard to the TLP process, was an understanding of the effect of Cu additions on the amount of transient liquid phase which forms upon reaching the bonding temperature of 125 °C. In the case of the low-Bi alloy shown in Fig. 4.1, for example, the alloy completely melts before the bonding temperature is reached. As observed in Fig. 4.1a, the initial peak, which represents TLP formation, is actually made of two "humps" which indicate the presence of multiple phase transitions occurring very close together. Within this temperature range, as shown by Fig. 4.1b, there is an increase of InSn(β)

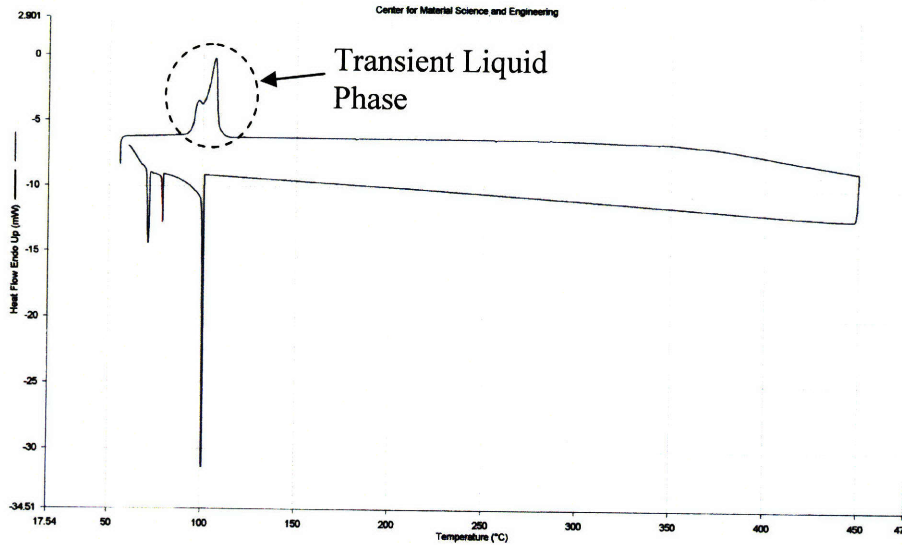

(a)

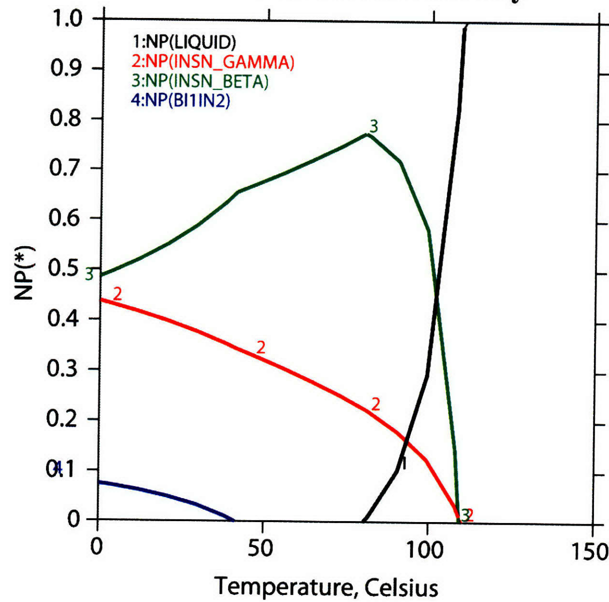

(b)

Figure 4.1: Melting behavior of 50In-43.6Sn-6.4Bi interlayer alloy: (a) DSC output of heat flow (mW) vs. temperature (°C); (b) Calculated equilibrium solidification path. Experimental determination (top graph) of the melting behavior of the interlayer alloy agrees very closely with that predicted through thermodynamic calculations (bottom graph).

phase and a decrease of In_2Bi and InSn(γ) which occurs through the redistribution of In upon heating (InSn(β) being the indium-rich phase in the In-Sn binary system). The first liquid starts to form when the InSn(β) curve reaches a maximum. At this point, the fraction of phases present is about 78 % InSn(β) and 22 % InSn(γ), which is very close to the fraction of phases upon reaching the In-Sn binary eutectic temperature (≈ 85 % InSn(β) and 15 % InSn(γ)). This difference is due to the presence of bismuth which becomes redistributed in the In-Sn phases from the In_2Bi intermetallic..

Table I shows the effects of Cu additions on TLP formation for both the In-Sn-Bi and In-Sn based interlayer alloys. For both the low-Bi and In-Sn eutectic alloys, an increase in the amount of Cu addition results in a decrease in the amount of TLP formed upon reaching the bonding temperature. This decrease was observed both experimentally (DSC) by measuring the enthalpy change upon the first phase transition (assuming larger ΔH values corresponded to greater fractions of liquid formation) and computationally through solidification paths similar to that seen in Fig. 4.1b. The reason for the decrease in TLP formation upon increases in base material addition to the interlayer alloy is that the copper promotes the formation of high melting intermetallics during heating which consume the MPDs responsible for TLP formation (mainly

Table I: Effect of copper additions on TLP formation in the In-Sn-Bi and In-Sn systems

Interlayer Alloy	Cu Addition (wt%)	Onset Temp (°C)	End Temp (°C)	ΔH (J/g)	Pct. Liquid (Calc.)
50In-43.6Sn-6.4Bi (low-Bi)	0	93.9	108.0	26.6	100
	5	99.4	106.7	23.6	86
	10	98.4	108.3	23.2	70
	20	96.0	107.7	13.3	42
48.3In-15.6Sn-36.1Bi (eut.)	0	60.5	66.3	31.4	100
50.9In-49.1Sn (eut.)	0	118.4	120.7	27.3	100
	2.5	117.7	120.2	27.2	93
	5	117.5	120.5	25.9	86

In and Sn) during their growth. Thus, by the time the bonding temperature is reached, there is less MPD available to form the TLP necessary for bonding. Figure 4.2 illustrates this for the In-Sn-Bi-20Cu and In-Sn-5Cu alloys. In the case of the In-Sn-Bi-20Cu alloy (Fig. 4.2a), copper promotes the formation of Cu_6Sn_5 and $Cu_{11}In_9$ at the expense of the In-Sn (β+γ) phases which form the TLP. Most of the intermetallics are stable above the melting temperature and either melt around 200 °C or are eventually transformed into other intermetallics phases. In fact, the alloy does not completely melt until a temperature of around 370 °C. Similar behavior can be seen in Fig. 4.2b, where Cu_6Sn_5 is again formed at the expense of the In-Sn (β+γ) low melting phases. Solidification paths for the other interlayer alloys listed in Table I can be found in Appendix A, except for the In-Sn-Bi (eutectic) alloy. Although the effects of Cu additions on the melting temperature of this alloy were not studied in this work, the melting temperature for alloy as measured by DSC (60-65 °C) agree very well with that predicted by thermodynamic calculations (≈ 60 °C) (see Fig. 2.2).

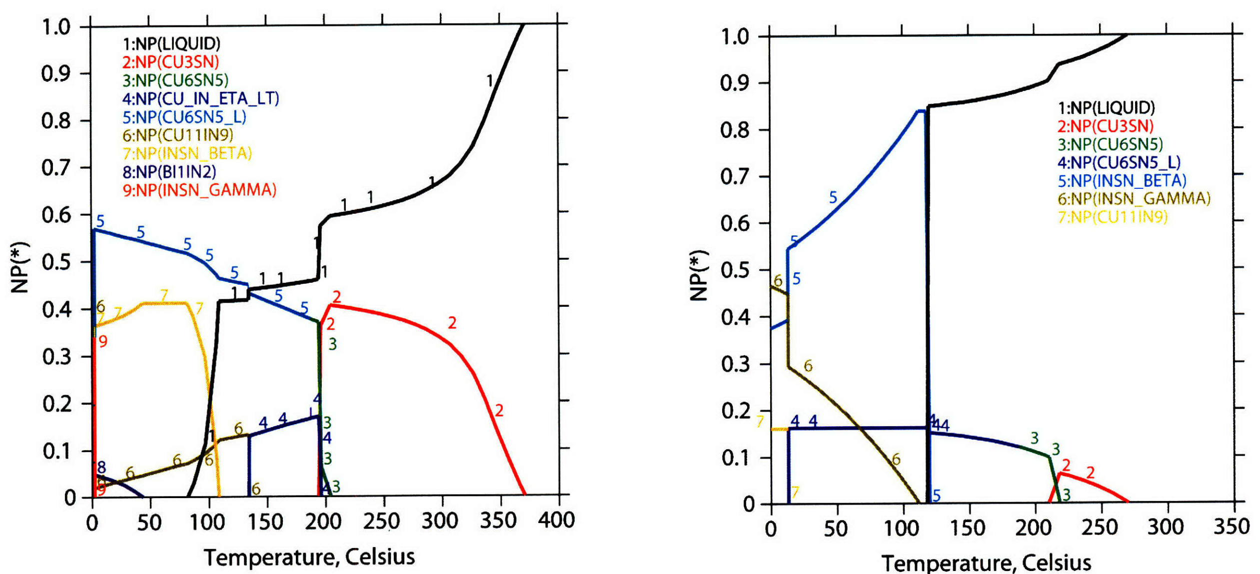

Figure 4.2: Calculated solidification paths for (a) In-Sn-Bi-20Cu; and (b) In-Sn-5Cu interlayer alloys. Increasing amounts of Cu additions to the interlayer alloys decreases the fraction of liquid phase formed upon heating to the bonding temperature as a result of consumption of the MPDs by Cu-rich intermetallic phases.

4.2 Determining Electroless Layer Thicknesses for Study

Prior to analyzing the effects of diffusional barrier layers on the TLP bonding process, an optimal range of layer thicknesses to study had to be chosen. As mentioned in Section 2.3.2, the diffusional layer must fulfill two requirements: (1) prevent formation of non-planar intermetallic grains due to reactions between the liquid interlayer and substrate during the initial stages of TLP bonding; and (2) breakdown in order to allow sufficient interdiffusion for isothermal solidification to complete. Since the joints studied in this work were all from either the In-Sn-XCu or In-Sn-Bi-XCu alloy systems and were produced below 200 °C, it was expected that only the η IP would form at the S/L interface (refer to Section 2.2.2). Also, it was assumed that the diffusion of Cu atoms through the η phase into the interlayer was faster than that of the In, Sn, or Bi atoms through the η phase into the substrate (refer to Section 2.3.2). Based on this assumption, the primary source for isothermal solidification would be the diffusion of Cu into the interlayer. Therefore, in determining the optimal nickel layer thicknesses, the main focuses were on the ability of the layer to allow sufficient Cu diffusion into the interlayer while preventing the formation of the coarse-grained η phase during the initial TLP bonding stages.

Figure 4.3 shows EDS compositional maps for TLP joints made with the In-Sn-Bi interlayer at 125 °C for 2 hours and a pressure of 450 psi. Figure 4.3a shows the compositional map for a TLP joint with no nickel plating. The substrate and joint regions are marked on the SEM image. Notice that there is a significant degree of Cu diffusion (here, marked in green) into the interlayer. Also, there are regions near the center of the interlayer which seem void of copper. These regions are denoted by dotted circles in the image. The reason for this is most likely due to the growth and connection of η phase and other stable (high-melting) intermetallics across the joint which left low-melting phases (having no or little Cu content) constrained,

prohibiting In, Sn, and Bi diffusion away from the joint. Phase formation will be discussed in the Section 4.4.2.

An EDS compositional map for a TLP joint produced with a nickel layer thickness of about 1.8 μm is shown in Fig. 4.3b. A significant amount of Cu diffusion into the joint (here, marked in pink) was also observed in this case. It is seen from the Ni map that the barrier layers on the Cu substrates have almost completely dissolved, thus allowing Cu diffusion to take place. Lastly, a decrease in joint thickness can also be observed in this TLP joint compared to the one made without a Ni layer (Fig. 4.3a). This difference in joint thicknesses may be attributed to the prevention of η and other Cu-rich IP growth across the joint which limits the joint thickness (refer to Section 2.3.2). A more detailed discussion of the effect of barrier layer thickness on joint thickness is presented in the Section 4.4.1.

The last compositional map, Fig. 4.3c, is for a TLP joint made with a nickel layer thickness of about 3.5 μm. It is seen from the Ni map that the thick barrier layers have not broken down by the end of the 2 hr TLP bonding process. The effect, as noted in the Cu map, is that very little copper has been allowed to diffuse into the joint. Therefore, a large increase in the original interlayer's melting temperature is not expected for this joint.

In conclusion, it was found that an increase in the Ni layer thickness decreased the amount of Cu diffusion into the joint, but at the same time, had the potential to decrease joint thickness. A Ni deposition of about 3.5 μm was too thick a barrier layer for the TLP process, as it did not allow any Cu diffusion to occur which is necessary for isothermal solidification to take place. Therefore, it was decided that a range of 1-3 min plating times would be used to deposit the Ni barrier layers for the TLP joints studied in this work. This corresponded to Ni layer thicknesses of 1.5 μm, 2.2 μm, and 3.1 μm, respectively.

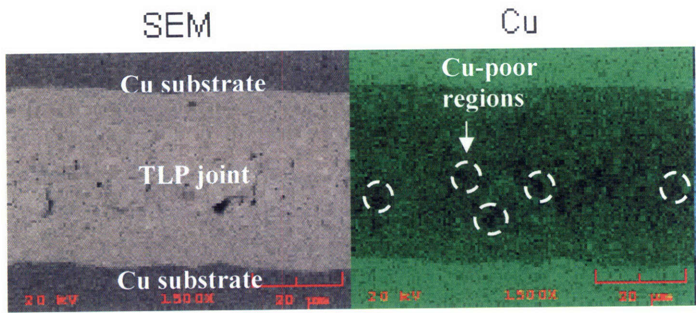

(a) – No Ni layer

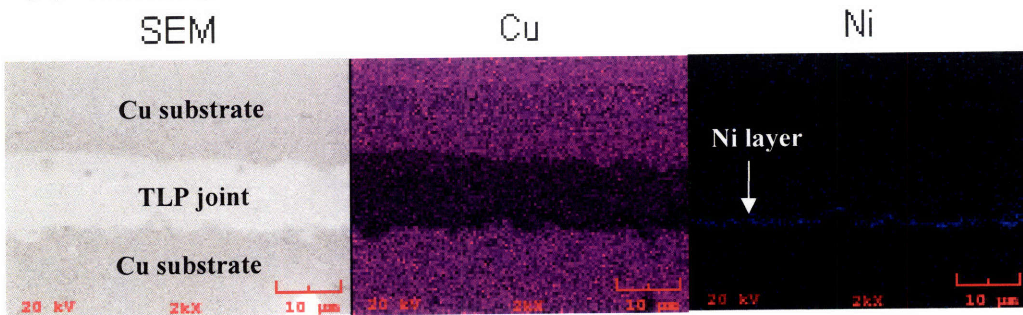

(b) – 1.8µm Ni

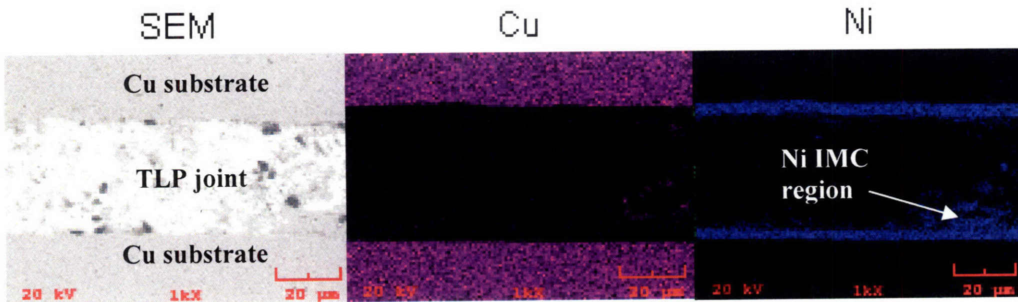

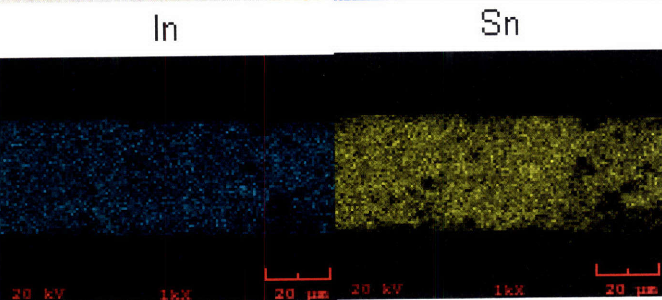

(c) – 3.5µm Ni

Figure 4.3: Effect of Ni layer thickness on Cu diffusion during TLP bonding. As Ni layer thickness was increased, the degree of Cu diffusion into the joint during TLP bonding was decreased. Joints were produced using 50In-43.6Sn-6.4Bi interlayer with the following processing parameters: 450 psi pressure at 125 °C for 2 hrs.

To demonstrate the effect of the Ni barrier layers on Cu diffusion during the beginning of the TLP bonding process, specimens were made in which an interlayer alloy was applied to a Cu substrate at the bonding temperature and was allowed to heat up, melt, and remain on the substrate surface for 10 min (similar to a sessile drop experiment). Afterwards, the specimen was cooled to room temperature. The SEM images in Figure 4.4 show two such samples that were made using the In-Sn eutectic interlayer alloy at 125 °C. The impurities seen in the interlayers of the images are artifacts from metallographic preparation procedure. In Fig. 4.4a, no Ni barrier was deposited onto the Cu substrate prior to the application of the interlayer alloy. A clear diffusion region can be seen by the S/L interface in which the fine-grained η phase (see Fig. 2.5) has grown into the solid substrate and copper has diffused into liquid where the coarse-grained η is formed. An EDS analysis of these regions confirmed the existence of the η phase in

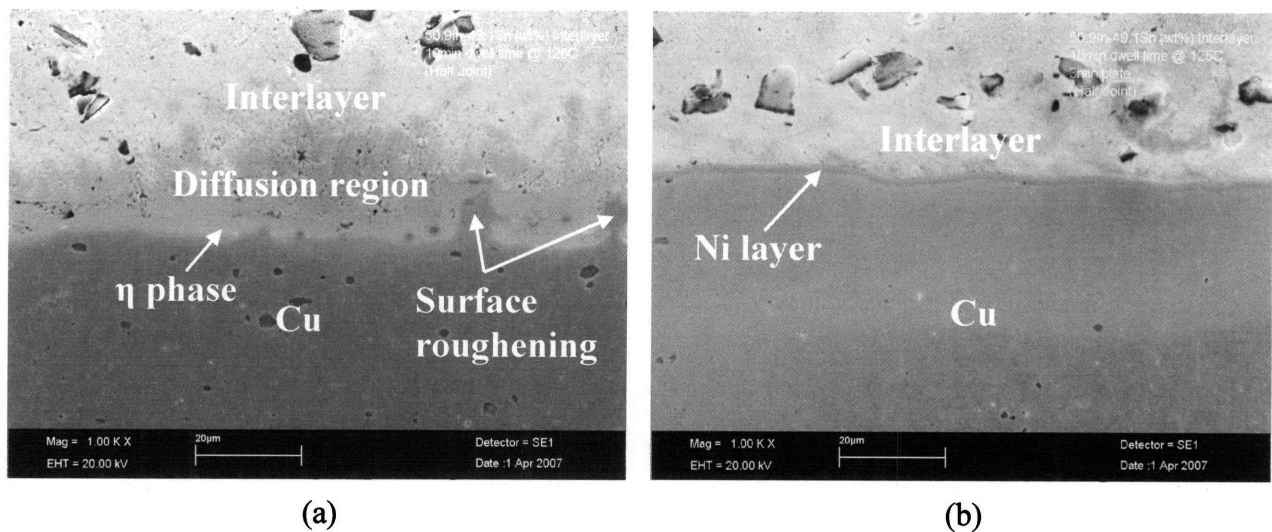

(a) (b)

Figure 4.4: Effect of Ni diffusion barrier layer on TLP process. Half-TLP joints produced with In-Sn eutectic interlayer alloy at 125 °C for 10 min: (a) no Ni layer; (b) 3min Ni plating. In the absence of a diffusion barrier layer, reactions between the solid Cu and liquid interlayer lead to formation of η phase at the S/L interface. No η phase is present when the Ni barrier layer is used.

these regions. Surface roughening was also observed at the interface, although its effect on the TLP process seemed to be negligible compared to the intermetallic formation. Figure 4.4b

shows a specimen in which the substrate was plated for 3 min prior to the application of the interlayer alloy. In this case, no interdiffusion is seen to have occurred and the growth of η phase is eliminated. Thus, the Ni layer was successfully used as a diffusion barrier layer for this TLP system.

4.3 Effect of Cu Additions on Joint Thickness

As was mentioned in Section 4.2, the use of the Ni barrier layer can reduce the joint thickness by prohibiting the formation of η and other Cu-rich intermetallic phases across the joint during the initial stages of TLP bonding. In addition to the effects of the diffusion barrier layer, the amount of Cu addition to the interlayer alloy can also affect the joint thicknesses

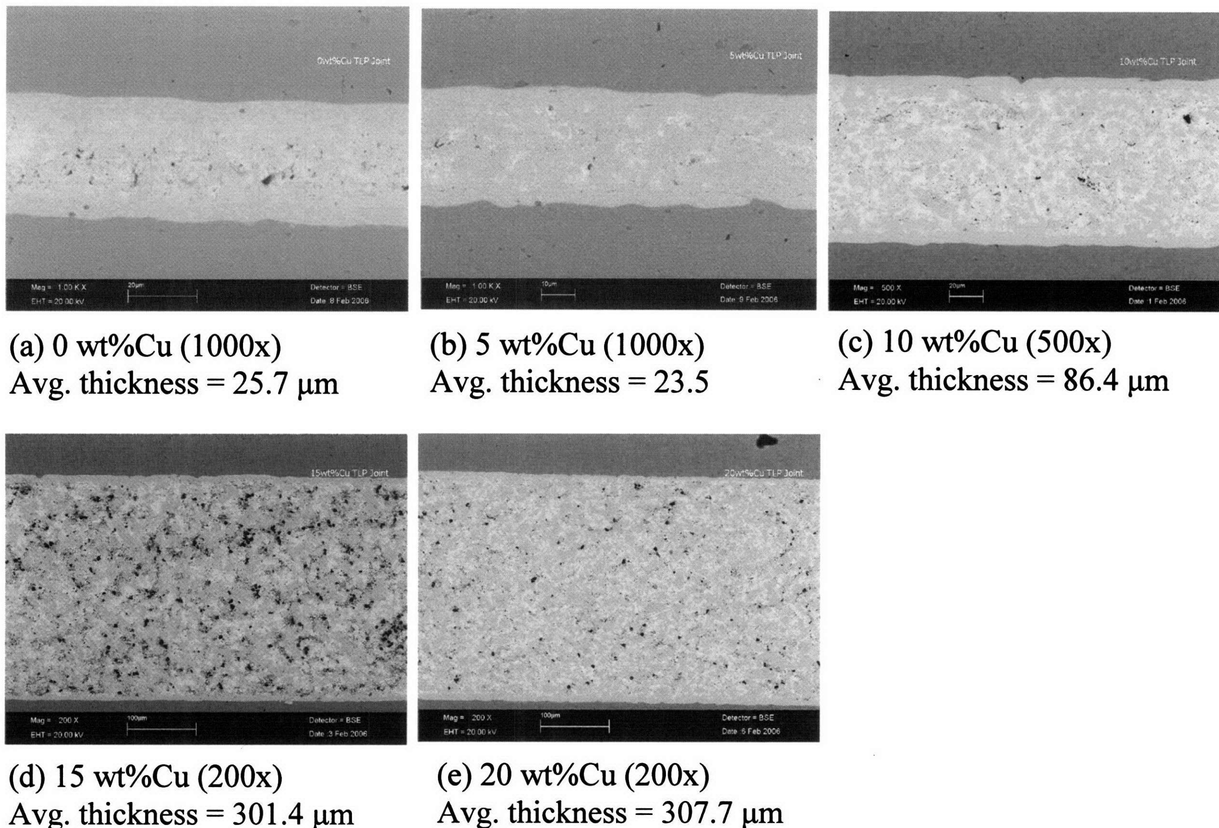

(a) 0 wt%Cu (1000x)
Avg. thickness = 25.7 μm

(b) 5 wt%Cu (1000x)
Avg. thickness = 23.5

(c) 10 wt%Cu (500x)
Avg. thickness = 86.4 μm

(d) 15 wt%Cu (200x)
Avg. thickness = 301.4 μm

(e) 20 wt%Cu (200x)
Avg. thickness = 307.7 μm

Figure 4.5: Effect of Cu additions on resulting joint thickness in the In-Sn-Cu and In-Sn-Bi-Cu LTTLP systems. All TLP joints were made using the In-Sn-Bi-XCu interlayer alloy (constant 50In-43.6Sn-6.4Bi ratio) using 200 psi pressure at 125 °C for 2 hrs. Above 5 wt%Cu, increasing amounts of Cu additions drastically increase resulting joint thickness. The trend of increasing joint thickness with greater Cu additions seems to plateau at very high concentrations of copper (around 15 wt%Cu).

obtained using the TLP bonding process. Figure 4.5 shows five different TLP joints made with the low-Bi In-Sn-Bi-XCu interlayer at 125 °C for 2 hours and a pressure of 200 psi. The amount of copper addition, image magnification, and measured average joint thickness is indicated for each image for ease of comparison between the joints. The measurements for the joint thicknesses include the joint area between the two original S/L interfaces (i.e. excludes thickness of fine-grained η phase regions). From these images, it is observed that for Cu additions above 5 wt%Cu, there is a drastic increase in the resulting joint thickness compared to the joint made without any Cu additions. The trend of increasing joint thickness with increasing Cu additions seems to plateau after 15 wt% Cu additions.

The increase in joint thickness with increasing Cu additions can be attributed to the fact that the Cu additions to the original interlayer alloy promote the formation of Cu-rich intermetallic phases in the bulk of the joint during the TLP process, such as Cu_6Sn_5 and $Cu_{11}In_9$ (see Fig. 4.2 and A.1, 2) in addition to the η intermetallic grains that form at the S/L interface. In the case of no copper additions, the joint thickness is predominately determined by the growth and connection of the largest η intermetallic grains, from opposing Cu surfaces, across the joint. Connection occurs when the two sets of opposing grains grow to some height distribution where the grains in the first few percentiles of each distribution have a high likelihood of contacting similar sized grains. This idea is derived from the explanation of a critical Sn interlayer thickness in the Cu-Sn TLP system given by Bosco et al. [47], which was briefly discussed in Section 2.3.2. Applying this concept in the case of using the In-Sn-Bi-XCu interlayers, it can be argued that the formation of intermetallic grains in the bulk of the joint, due to the Cu additions, makes it more likely that intermetallic grains make contact across the joint and thus increase the joint thickness. In other words, the coarse η intermetallic grains growing from the Cu substrate

surfaces do not have to grow as large of a grain size because they do not have to make contact to grains on the opposing surface, but can alternatively make contact to an intermetallic grain (or group of intermetallic grains) in the bulk of the joint which is connected to an intermetallic grain on an opposing surface. Since the latter situation is much more likely, the joint thickness will increase with increasing Cu additions.

The reason for the plateau in the trend of increasing joint thickness is explained by the fact that the more (or the larger) intermetallic grains that are formed in the bulk of the joint, the smaller the grain size that the η grains (growing from the S/L interface) must achieve to connect to those bulk grains. At a certain level of Cu addition, there is such a large volume fraction of intermetallic grains in the bulk of the joint, than an intermetallic 'bridge' forms across the joint region before any major growth of the interfacial coarse-grained η phase can occur. Additional In-Sn-Cu or In-Sn-Bi-Cu TLP specimens with varying amounts of copper additions to the interlayer alloy should be made, however, to further evaluate the relationship between joint thickness and concentration of base material to the interlayer alloy.

Some additional points should be emphasized in regard to the above explanation for increasing joint thickness with base materials additions. One is that, as we have seen from DSC analysis of the interlayer alloys (Section 4.1), the increase in Cu additions reduces the amount of transient liquid phase which forms upon heating to the bonding temperature. Thus, the increase in joint thickness can also be attributed to the fact that, for interlayers with larger Cu content, a relatively larger portion of the transient liquid phase is being consumed during the formation of the intermetallic phases. As less transient liquid phase is formed during the heating stage, it becomes more likely that either all of the transient liquid phase becomes consumed prior to TLP bonding or that any transient liquid phase existing upon reaching the bonding temperature is

already confined within the intermetallic phase. In either of these cases, the TLP process cannot proceed, leaving behind thick joints with a large fraction of unreacted TLP phase (see Section 4.4.2 for more detail). It should also be noted that the above explanation of does not take the effect of diffusion kinetics into account, such as how the diffusive properties of the constituents in the TLP system change when base material is added to the interlayer. This analysis was beyond the scope of this project. However, kinetic effects may have contributed to the aforementioned trend and should be investigated in future studies for a complete understanding of this phenomenon.

4.4 Optimizing the LTTLP Process Design

The previous three sections of this paper described experiments that were done in order to understand the behaviors and effects of each individual processing element to the LTTLP bonding process. To briefly summarize, Section 4.1 described the melting behaviors of various interlayer alloys and the effects of base material additions. It was determined that increasing amounts of Cu addition to the base interlayer alloy resulted in a decrease of transient liquid phase available for TLP bonding. This was due to the formation and growth of Cu-rich intermetallic phases which consumed the In and Sn MPDs during heating to the bonding temperature Section 4.2 discussed how an optimal range of electroless Ni layer thicknesses (or plating times) were chosen as potential diffusion barriers for the In-Sn-Cu and In-Sn-Bi-Cu LTTLP processes. The plating times ranged from 1-3 min with corresponding thicknesses of about 1.5 μm, 2.2 μm, and 3.1 μm. Finally, Section 4.3 described a set of experiments in which a range of Cu additions (0-20 wt% Cu) to then In-Sn-Bi (low-Bi) interlayer alloy were studied to determine the effects of the interlayer alloy's Cu content to the resulting joint thickness. It was found that above 5 wt% Cu, increasing Cu additions led to an increased joint thickness. At 15 wt% Cu additions, the

joint thicknesses were in excess of 300 µm, at which point the trend of increasing joint thickness seemed to plateau.

The present section discusses the results of a range of studies in which all of these different elements of the LTTLP process (i.e. interlayer alloys, diffusion barrier layers, and additions of base material to interlayer alloy) were combined with one another to determine the optimal processing design for the desired low temperature, lead-free TLP bonding process. The main quality parameters on which the TLP joints were evaluated, based on the target goals mentioned in Section 2.4, were their joint thicknesses (minimal thickness desired), high temperature stability (reflow temperatures of at least 200 °C), and mechanical properties (room/elevated temperature shear strengths). Due to the vast number of experiments needed to characterize every TLP joint with a unique set of processing parameters, some combinations of design parameters were dismissed (based on findings from other experiments) as being unable to achieve the target goals, and were thus not studied. This will be discussed further in the following sections.

4.4.1 Controlling Joint Thickness

i) In-Sn-Bi-Cu Systems

In a previous study of LTTLP bonding in the In-Sn-Bi-Cu system, Williams et al. [6] found that a minimum of a two hour dwell time was needed for joints made with a 50In-43.6Sn-6.4Bi interlayer to achieve reasonable shear strengths at 100 °C. These joints were made using a bonding temperature of 125 °C and pressures in excess of 450 psi. In this study, lower pressures were sought in order to optimize the bonding process. For this study, it was decided that all of the joints to be studied in the In-Sn-Bi-Cu system were to be made using a bonding pressure of 50 psi (at a temperature of 125°C). Since this pressure was much lower than that used in the

experiments performed by Williams et al. (while the temperature remained the same), it was hypothesized that bonding temperatures of at least 2hr were going to be necessary to obtain sufficiently high temperature mechanical properties in the joints. Also, only 0-2 min platings were studied for the joints in this system. As will be seen in Section 4.4.3, this was due to a markedly large degradation in mechanical properties experienced by these joints with increasing barrier layer thickness. Finally, only 5 and 10wt% Cu additions were studied for this TLP system, as larger concentrations of base material to the interlayer alloy produced too little transient liquid phase to be used as a viable interlayer alloy in the TLP process (see Table I).

Figure 4.6 shows a graph of joint thickness versus plating time (related to plating thickness) for the TLP joints made using In-Sn-Bi-XCu interlayers. All of these joints were bonded for 2 hrs at 125 °C under a pressure of 50 psi. There are a couple of observations from this data. One observation, as was previously noted in Section 4.3, was an increase in joint thickness with increasing copper additions. This was attributed to the increase of η formation in the bulk of the joint during TLP bonding. However, this difference in joint thickness seems to be dependent on the barrier layer thickness. With no barrier layer, there is a very large increase in joint thickness upon 5 wt% Cu additions, but a very small difference between 5 and 10 wt% Cu additions. The difference in joint thickness between the TLP joints made with 5 wt% and 10wt% Cu becomes much more apparent when the Ni diffusion barrier layer is added to the Cu substrate prior to bonding.

Another point to consider is the relative effectiveness of the Ni diffusion barrier layer in minimizing the joint thickness for each of the interlayer alloys used in this In-Sn-Bi TLP system. For the In-Sn-Bi-0Cu joint, there was no significant effect of the Ni layer on decreasing the joint thickness under the given bonding conditions. Even so, all the joints made with this interlayer

were below the target joint thickness of 25 μm.. Unlike the low-Bi joint made without any copper additions, there was a considerable decrease (≈50 μm) in the joint thickness for the In-Sn-Bi-5Cu joint upon using a plating time of 2 min. For the In-Sn-Bi-10 Cu, there was actually a drastic increase (> 100 μm) in joint thickness when using a plating time of 1 min. The joint thickness started to decrease after a plating time of 2 min, but did not reduce to a value below the standard joint made without any copper additions. From the above trends, it seems that with longer plating times, the joints made with 5 and 10 wt% Cu additions can potentially reach the target joint thickness of 25μm. Future studies using longer plating times should be performed in order to verify this.

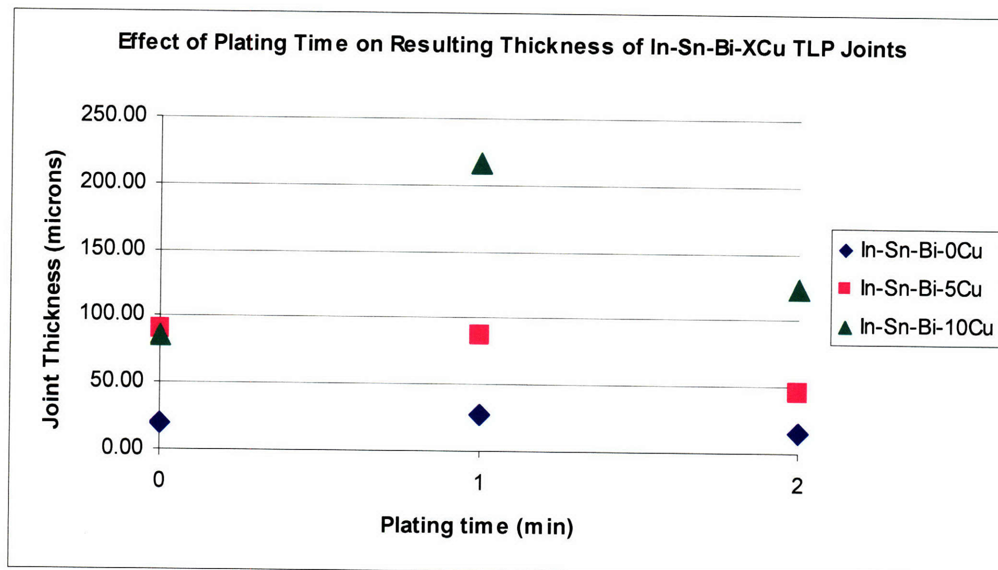

Figure 4.6: Effect of plating time on resulting joint thickness of In-Sn-Bi-XCu joints. The use of a Ni diffusion barrier layer is shown to potentially decrease the thickness of joints made using copper additions. Greater concentrations of base material to the interlayer require longer plating times to reduce the joint thickness to that of the standard In-Sn-Bi joint made with no copper additions. All joints were bonded at 125 °C for 2 hr under 50 psi.

The use of a Ni diffusion barrier layer was not studied for the TLP joints made with the eutectic In-Sn-Bi based interlayer alloys. However, additions of base material to this interlayer alloy were found to have the same effect as was observed for the low-Bi alloy. That is,

increasing amounts of Cu additions lead to large increases in the resulting joint thickness. For this interlayer alloy, additions of 0, 5, and 10 wt% Cu lead to average joint thicknesses of 7.45 μm, 19.2 μm, and 59.1 μm, respectively. It should be noted that each of these thicknesses are smaller than compared to the low-Bi joints made with the same amount of Cu additions.

ii) In-Sn-Cu System

For the TLP joints made within the In-Sn-Cu system, a wider range of bonding times was considered as compared to the joints made in the In-Sn-Bi-Cu system. The bonding times used were 0.5, 1, 2, and 4 hr. Thus, not only were the effects of diffusion barrier layer on resulting joint thickness able to be studied, but its effect on the growth rate was analyzed as well. Also, the bonding pressure was increased to 100psi. Up to 3 min plating times were investigated as a means to optimize the joint thickness obtained while bonding within this TLP system.

Figure 4.7 shows the effect of copper additions and dwell time on In-Sn-XCu joints produced without the Ni barrier layer. In this case, it was found that a small concentration of base material addition (2.5 wt% Cu) actually slightly decreased the joint thickness, as opposed to the larger Cu concentrations. It is thought that this stems from the fact that the smaller concentration of Cu effectively decreases the required amount of dissolution (see Section 2.3.1) required for equilibrium at the S/L interface, while not promoting an excessive degree of intermetallic formation in the bulk of the joint during the heating stage of TLP bonding as was observed for higher Cu additions (see Section 4.3). As can be seen in Fig 4.7, joints made with 5 wt% Cu again result in an increase in joint thickness compared to the TLP joints made with no Cu additions. By comparing this graph with Fig. 4.6, it is seen that the In-Sn based TLP joints produce thicker joints than the low-Bi joints bonded under the similar conditions (i.e. 125 °C, 2hrs, 0 min plate, equal Cu content). For example, the In-Sn-5Cu joint was found to be ≈ 230

μm after a 2 hr dwell time, whereas the In-Sn-Bi-5Cu joint was found to be slightly less than 100 μm after the same dwell time. A similar comparison can be made for the joints made with no Cu additions. The only difference in bonding conditions within the two systems was that the In-Sn joints were bonded under a slightly higher pressure than the In-Sn-Bi joints. However, this difference would have favored the In-Sn joints to be thinner, and so the difference in joint thickness is most likely a result of the corresponding microstructures (see Section 4.4.2(ii)).

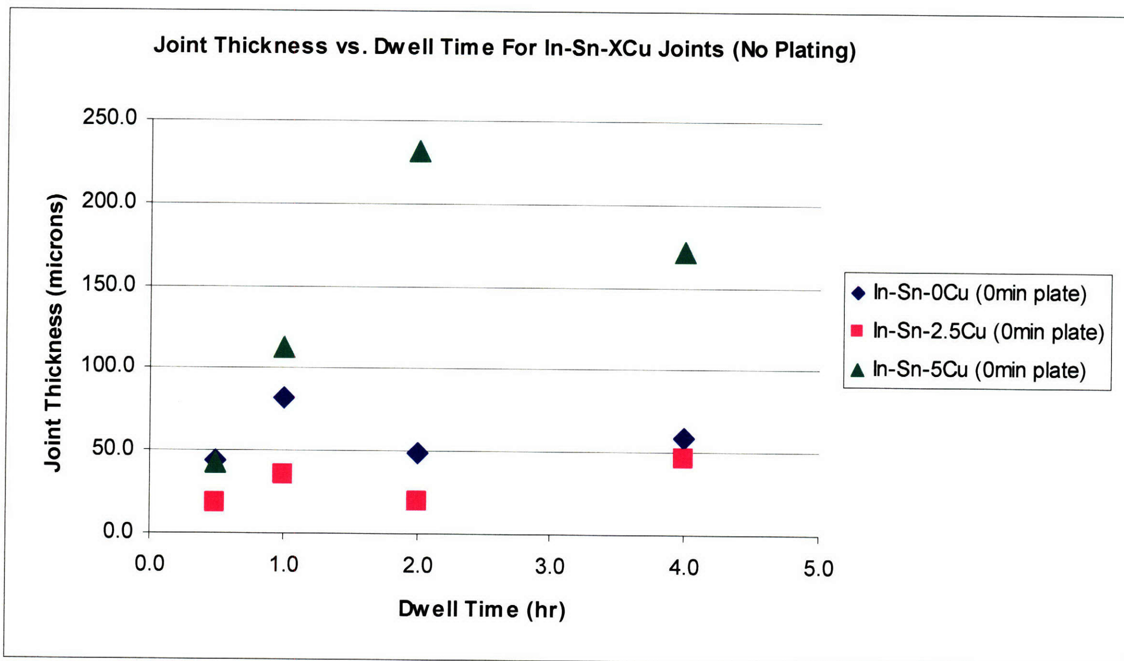

Figure 4.7: Effect of dwell time on TLP joints made with In-Sn-XCu interlayers without Ni plating. Joint thickness of TLP joints made with 0 and 2.5 wt% Cu additions do not significantly change with bond time. Larger concentration of Cu (5 wt%) lead to a drastic increase in growth rate of the joints due to rapid growth of η phase from the S/L interface. All joints were bonded at 125 °C under 100 psi.

A second interesting point is the growth of the joints with dwell time. Figure 4.7 shows that the thickness of In-Sn-0Cu and In-Sn-2.5Cu joints did not significantly vary with dwell time, although a slight increase in thickness seemed to be observed. However, there was a much more noticeable increase in joint thickness for the In-Sn-5Cu over the 4 hr time span. This increase in joint thickness with bond time is to be expected since the diffusion of copper through the η phase

is faster than that of the In or Sn (Fig. 4.4a). Hence, more material is being added to the joint region during bonding, resulting in larger joint areas. Also, since the bonding temperature is below 200°C, the formation of the ζ ($Cu_{10}Sn_3$) phase is suppressed. The ζ phase has been shown to be responsible for allowing In (ζ has the ability to dissolve In) and Sn to diffuse into the Cu substrates through decomposition of the phase into each of these elements at the S/L interface [42]. Thus, the suppression of this phase also contributed to the trend of increasing joint thickness with dwell time.

The fact that the TLP joints with 5 wt% Cu additions grew much more rapidly than either of the joints made with 0 or 2.5 wt% Cu suggests that the Cu-rich intermetallics (see Section 4.1), which formed prior to the solidification stage, provided significant sources of atoms from which the η phase could grow. The rate at which the η phase forms from the redistribution of In and Sn atoms from intermetallics such as $Cu_{11}In_9$ or Cu_6Sn_5, respectively, can be much faster than that from consumption of In and Sn atoms from the liquid phase. Therefore, higher nominal concentrations of Cu to the interlayer alloy result in much more rapid growth of the joint region. However, this explanation is only hypothetical and a much more thorough analysis of the kinetics in Cu/In-Sn/Cu TLP joints must be performed in order to fully understand this phenomenon.

As was mentioned at the beginning of this section, the use of Ni barrier layers was also studied as a means of optimizing the joint thickness obtained using the In-Sn-Cu TLP system. The use of Ni plating did not have much of an effect on the growth of the joints made without any Cu additions, as shown in Fig. 4.8. This was to be expected since growth rate of the In-Sn-0Cu was minimal even without the use of the nickel plating. It should be mentioned that the existence of the stray data point for the joint made with the 3 min plating time for 1 hr was most

likely due to experimental error (such as poor plating quality), and was emitted from the this analysis. Although not shown here, the Ni layer was also not found to have an effect on the growth rate of the In-Sn-2.5Cu joints.

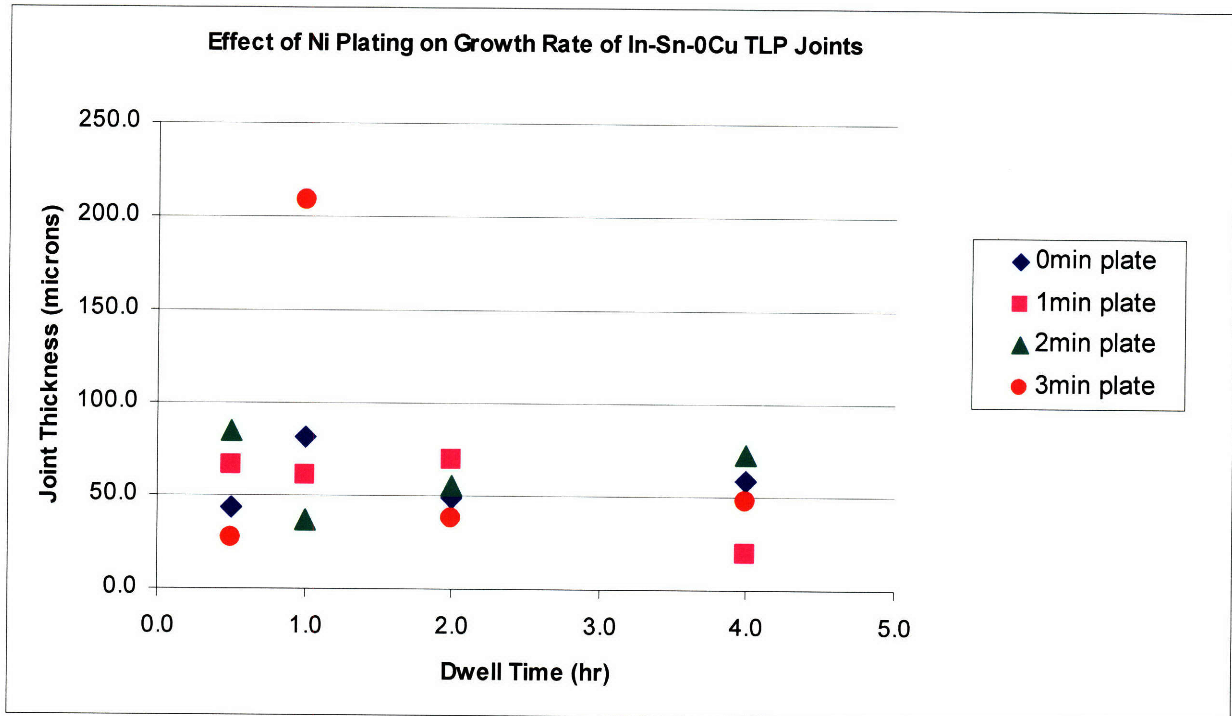

Figure 4.8: Effect of Ni plating on growth rate of In-Sn-0Cu TLP joints. Use of a Ni diffusion barrier layer does not significantly effect the growth rate of joint made without Cu additions. The same observation was made for the In-Sn-2.5Cu joints. All joints were bonded at 125 °C under 100 psi.

Unlike the In-Sn-0 and In-Sn-2.5Cu joints, the use of a diffusion barrier layer was seen to have a significant effect on the growth of In-Sn-5Cu joints, as shown in Fig. 4.9. Each of the sets of data were fitted to power law trend lines ($\Delta x = kt^n$), where it was assumed that the growth of the η intermetallic (which was assumed to control joint thickness) was described by such equations. Here, Δx would represent the thickness of the η layer, t the dwell time, k the growth rate constant, and n an exponent which depends on the rate controlling mechanism [42, 49]. It is important to stress that these lines are not meant to be an exact fit or quantitatively predictive in any way, but rather a means to more clearly compare the *overall* behaviors of the different sets of

joints. As was shown in Fig. 4.7, and again shown here, joints made with the In-Sn-5Cu interlayer without plating (blue line) experienced rapid growth during bonding. Through use of

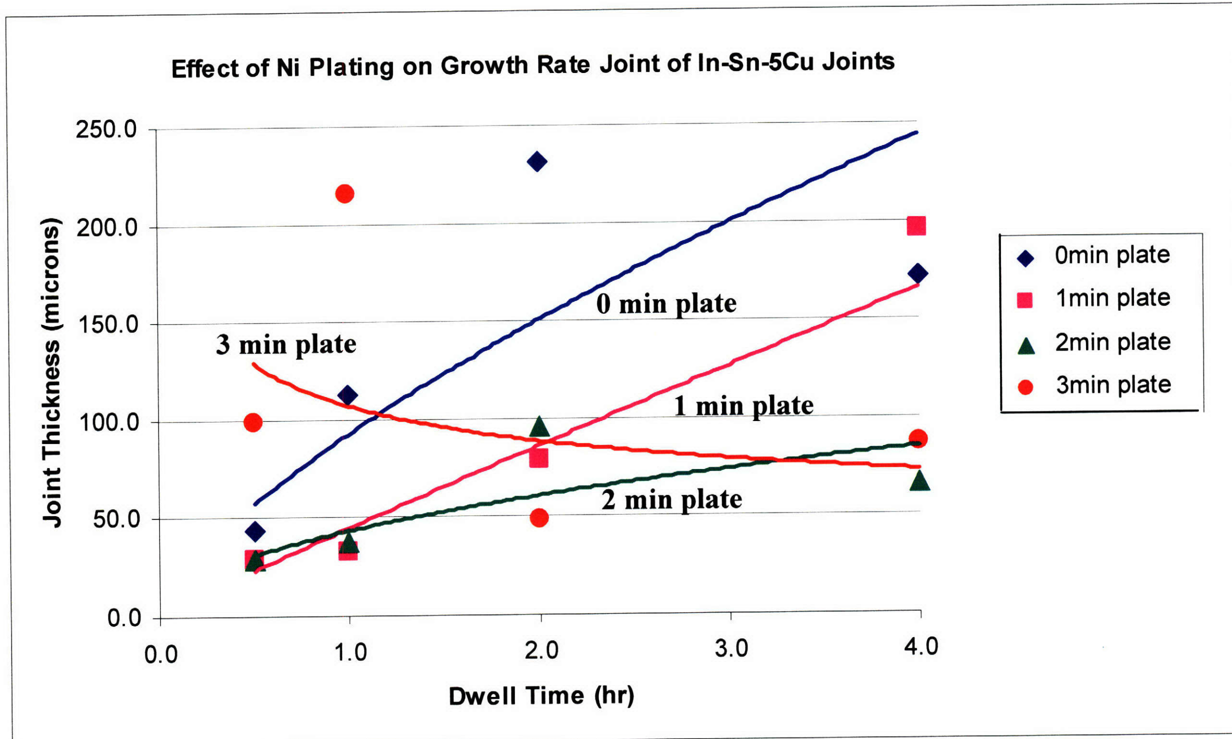

Figure 4.9: Effect of Ni plating on growth rate of In-Sn-5Cu TLP joints. Use of a Ni diffusion barrier decreases growth rate of joint made 5 wt% Cu additions due the suppression of η phase growth into the joint region during bonding. The growth rate decreases with increasing Ni layer thicknesses because of longer dissolution times for the thicker Ni layers. All joints were bonded at 125°C under 100 psi.

the Ni barrier layer, this growth was retarded by prohibiting the diffusion of Cu, and hence the growth of η phase, into the joint. As the Ni plating thickness was increased, the growth rate of the joints decreased, as marked by the decreasing slopes of the growth trend lines for increasing plating times. In fact, the 2 and 3 min platings reduced the growth rate of the joints enough so that after a dwell time of 2 and 4 hrs, the thicknesses were close to those observed for the In-Sn-0 and In-Sn-2.5Cu joints after the same bonding time (Fig. 4.8). The reason for the decreasing growth rates is that the thicker Ni platings take a longer time to dissolve, and thus prevent diffusion of Cu for a longer period of time (see Fig. 4.3). The fact that the 3 min plated samples

show a negative growth rate (i.e. the thickness decreases with time) is most likely due to the scattering of the data from experimental variability in processing these thicker Ni layers. It is more likely that the joint thickness should remain about constant (or increase very slowly) given the observed trends from the other sets of data.

4.4.2 Compositional and Phase Analysis

Due to the inability to perform accurate reflow tests on the TLP specimens, the high temperature stability of the joints were evaluated based on compositional and phase analysis of the joints. Since the η phase has a melting point around 500 °C, it is reasonable to assume that greater volume fractions of η phase present in the joint will lead to higher reflow temperatures. Likewise, increasing Cu content inside of the joint should lead to greater high temperature stability due to the likelihood of high melting Cu-rich intermetallic phases present in the joint region.

i) In-Sn-Bi-Cu System

Prior to discussing the results of the experimental compositional and phase analysis of the TLP joints, it is very useful to discuss the expected joint microstructures as predicted by thermodynamic calculations. The expected microstructural evolution of the In-Sn-BiXCu joints during TLP bonding at 125 °C is shown in Fig. 4.10a. It should be noted that these graphs assume equilibrium conditions and do not account for segregation of the individual constituents of the materials system. In other words, for every composition of copper (at%) plotted on the graph, the corresponding ratio of the other three elements of the system are 50In-43.6Sn-6.4Bi. In relating such a graph to the Cu/In-Sn-Bi-Cu TLP system, the right side of the graph corresponds to the regions nearest the substrate/interlayer interface where the Cu concentration is

expected to be highest. The left regions of the graph correspond to the bulk of the joint where low Cu concentrations are expected due to the longer diffusion distances from the substrate. At the moment the alloy reaches the bonding temperature, the interlayer will be made of liquid with a fraction of Cu_6Sn_5 depending on the nominal concentration of Cu in the interlayer alloy and the degree of solid state diffusion which takes place during heating to the bonding temperature. As isothermal solidification takes place and Cu diffuses into the joint, the fraction of liquid decreases as Cu-rich intermetallics, such as Cu_6Sn_5, $Cu_{11}In_9$, and η (arbitrarily labeled as Cu_In), are formed in the joint. Thus, based on the Fig. 4.10a, the regions near the center of the joint (lower Cu content) are expected to be made up of Cu_6Sn_5, $Cu_{11}In_9$, and liquid (or unreacted TLP phase), while the regions near the substrate should be composed of η. The absence of any Bi phases suggests that this component is dissolved into the other phases and does not form any new phases with the other elements. Although this graph only shows up to 70 at% Cu concentrations, experimental results showed that larger Cu concentrations within the joint were not obtained during bonding and so the higher temperature phases were neglected from this analysis.

Figure 4.10b shows the expected microstructure of the joint after the TLP process has been completed and the joint is cooled down to room temperature (25 °C). It is observed that the liquid phase (Fig. 4.10a) which remained unreacted during bonding, solidifies to form InSn(β), InSn(γ), and In_2Bi, which are all low melting phases (all $T_m < 225$ °C). Also, the fraction of the Cu_6Sn_5 is increased, while the η phase only exists at Cu concentrations in excess of 50 at%. Taking into account solid-state transformations of the intermetallic phases, the only high melting phases ($T_m > 400$ °C) expected to be contained in the joint are therefore η, Cu_6Sn_5, and $Cu_{11}In_9$.

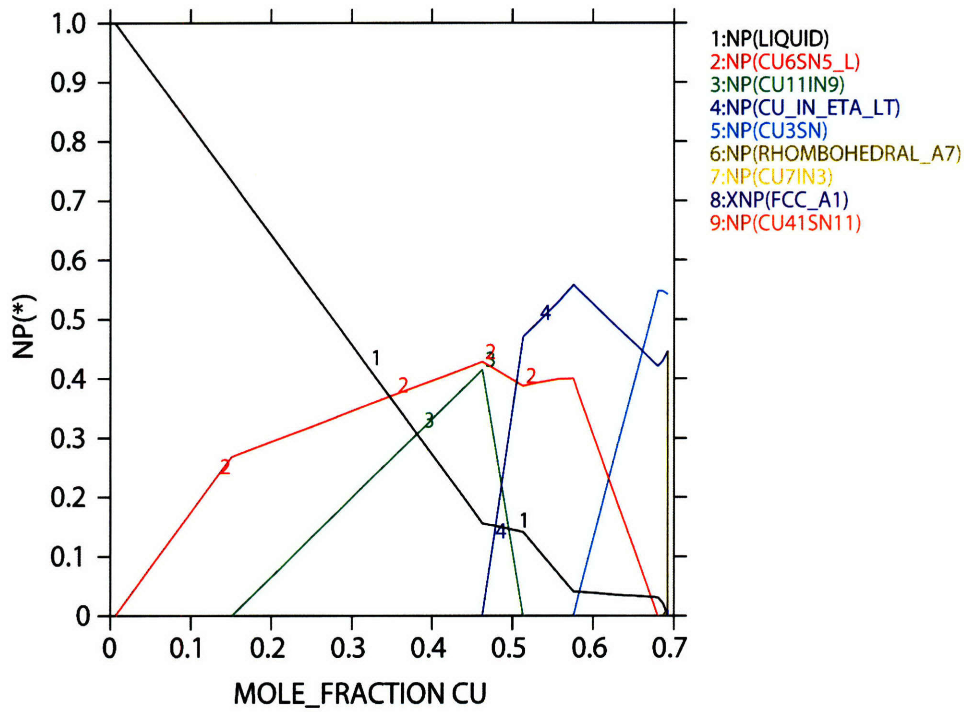

(a)

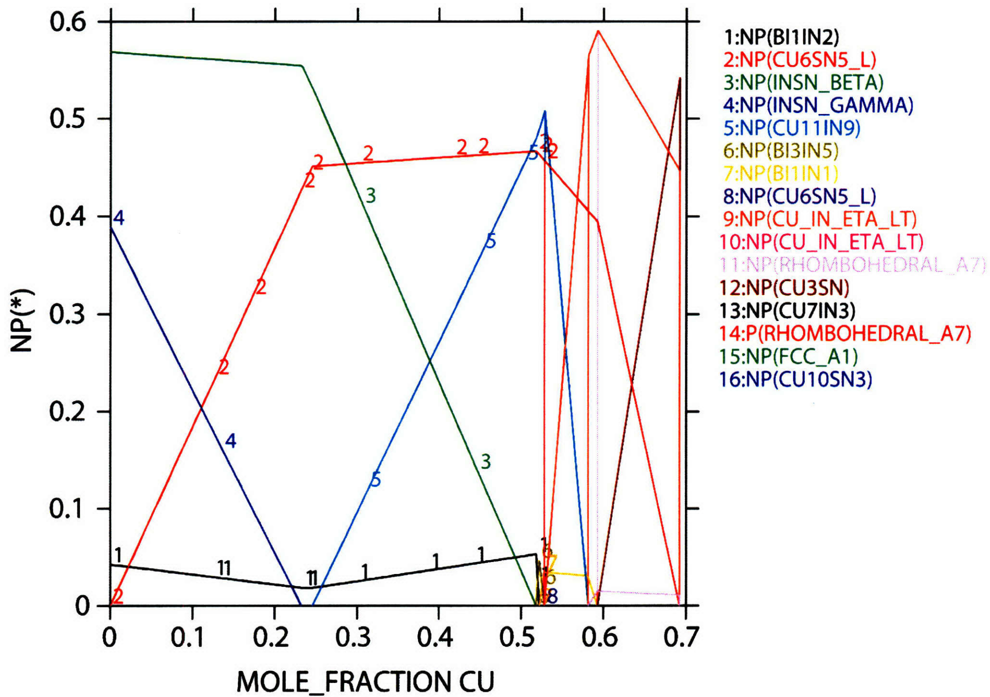

(b)

Figure 4.10: Prediction of phase fractions in In-Sn-Bi-XCu TLP joints (a) during bonding (T=125 °C); and (b) at room temperature (T=25 °C)

A SEM micrograph of the low-Bi TLP joint (Fig. 4.11) clearly demonstrates the microstructure which was expected from thermodynamic considerations. Coarse η grains (Fig. 4.11a) are observed to have grown from each of the substrate interfaces until they eventually

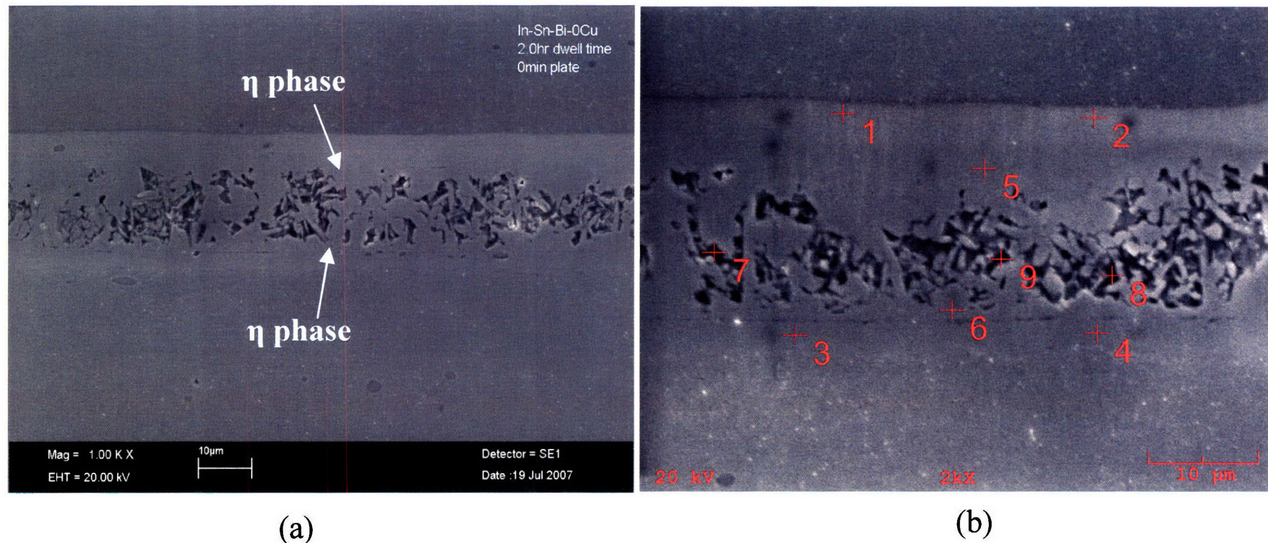

Figure 4.11: (a) SEM micrograph of low-Bi TLP joint. Regions of EDS analysis are shown in (b). Joint was bonded at 125 °C for 2 hr under 50 psi.

connected across the joint. In the central portion of the joint are regions of low melting phases which are constrained by the surrounding intermetallic grains. Figure 4.11b shows various regions from which EDS measurements were taken. The average composition of regions 1-4 was found to be around 23In-27Sn-1Bi-Cu (at %), which according to the In-Sn-Cu ternary diagram [50] (neglecting the small Bi content), lies in the η region. These regions correspond to the fine grain η phase which grew into the Cu substrate through the outward diffusion of In and Sn atoms. Regions 5 and 6 were measured to have compositions extremely close to those in regions 1-4, and thus verified that these coarse grains were in fact the η phase. Regions 7-9 were found to have compositions (at %) ranging from (40-53)In-(18-30)Sn-(2-5)Bi-(22-27)Cu. Referring back to Fig. 4.10b, these compositions most likely correspond to a combination of

phases: primarily $InSn(\beta)$ and Cu_6Sn_5 with a small fraction of In_2Bi, $InSn(\gamma)$, and $Cu_{11}In_9$. A more quantitative compositional analysis, such as x-ray diffraction (XRD), should be performed in order to more accurately determine the fraction of phases present in the joint.

The influence of the interlayer's nominal copper composition on the resulting microstructure can be seen in Fig. 4.12, which shows a SEM micrograph of the In-Sn-Bi-5Cu joint. Like the In-Sn-Bi joint without copper additions (Fig. 4.11), fine and coarse η grains were observed to have grown in the regions near the substrate interface. However, a significant difference between these two microstructures is that there was growth of η phase (identified by EDS) in the bulk of the joint as well. The Cu-rich phase regions in the bulk of the joint may also contain Cu_6Sn_5 and $Cu_{11}In_9$ (see Fig. 4.10b), but the two phases were not able to be distinctively identified through EDS. The existence of Cu-rich intermetallic phases in the bulk of the joint confirms the explanation for larger joint thicknesses with increasing Cu additions as discussed in Section 4.3 and 4.4.1. Another difference between the two joints is that the low melting phases are isolated in more separated regions as compared to Fig. 4.11, which shows the low melting regions all segregated to the central region of the joint. This is a direct result of the IPs which formed in the interior of the joint, resulting in the confinement of unreacted TLP. All of the low-melting regions had Cu contents equal to or less than 5 at% Cu. The black-colored, low-melting regions were found to be very rich in In ($\approx$ 80In-10Sn-5Bi-Cu), which corresponds closely to the $InSn(\beta)$ phase. However, there is likely some In_2Bi present in these regions as well. The bright white phases located at the $\eta/InSn(\beta)$ phase boundaries had compositions of about 34In-56Sn-5Bi-Cu, which, according the calculated In-Sn-Bi ternary phase diagram (Fig. 2.2), refers to the $InSn(\gamma)$ phase. Again, this microstructure agrees very well with the

thermodynamic predictions shown in Fig. 4.10b. The microstructure for the In-Sn-Bi-10Cu joint was very similar to that seen in Fig. 4.12.

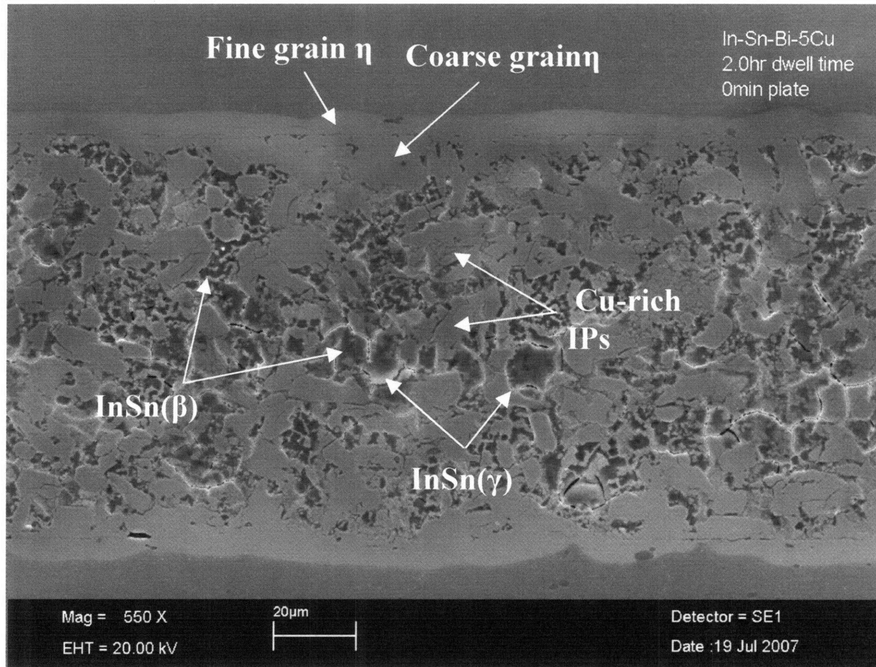

Figure 4.12: SEM micrograph of In-Sn-Bi-5Cu joint. A similar microstructure was also seen for the In-Sn-Bi-10Cu joint. Joint was bonded at 125°C for 2 hr under 50psi.

The effect of Ni plating on the microstructural evolution of the In-Sn-Bi-XCu TLP joints can be seen from the SEM micrographs shown in Fig. 4.13. Figure 4.13a shows an In-Sn-Bi-5Cu joint with that was plated for 2 min prior to bonding. One clear microstructural difference between this joint and that bonded with the same interlayer without the Ni layer (Fig. 4.12) is that there is less fine-grain η present on the Cu side of the Cu/interlayer interface due to the prevention of In and Sn atoms out of the joint. Instead, these atoms formed intermetallics with the Ni (this is what causes the retardation of Cu diffusion into the joint). Also, the micrograph shows that the interior of the joint is made up primarily of three different phase regions with the following compositions (at%): light (≈ 31In-60Sn-6Bi-1Cu), dark (≈ 15In-35Sn-4Bi-42Cu), and

black (≈ 85In-3Sn-5Bi-4Cu). These compositions (which neglect small amounts of Ni and P that were detected from the Ni layer) primarily refer to InSn(γ), η, and InSn(β), respectively. Note that even though the measured composition of the dark phase regions lies in the η region of the In-Sn-Cu ternary diagram [50], the average composition of the η in this joint had a lower Cu and much higher Sn content than the typical η phases formed in the joint without plating (Cu-23In-27Sn-1Bi (at %)). This suggests that the Cu-intermetallic will not be stable to temperatures as high as those in the non-plated joints.

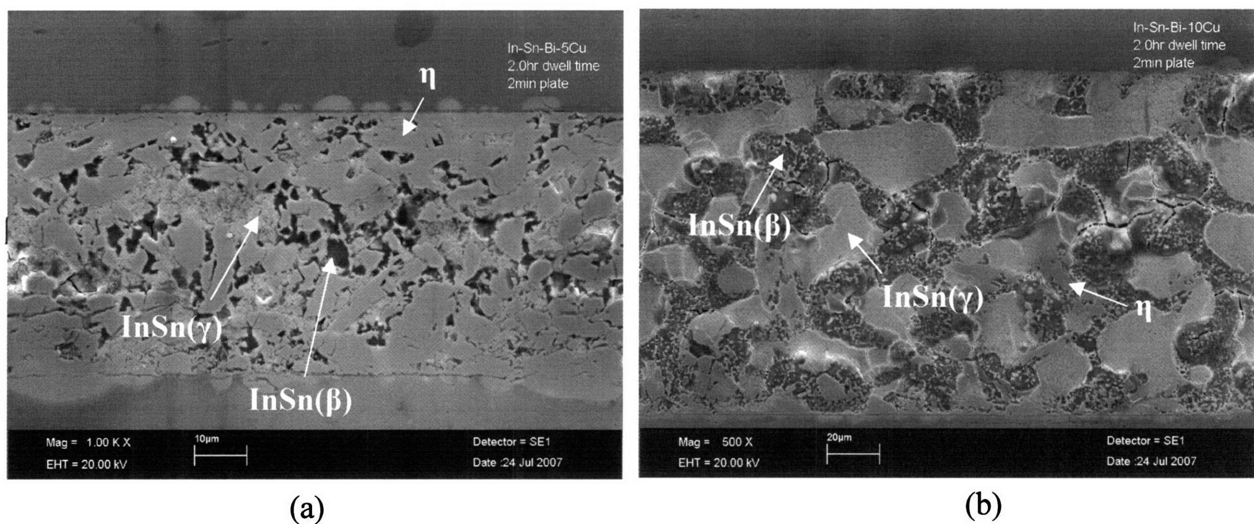

Figure 4.13: SEM micrograph of (a) In-Sn-Bi-5Cu (2 min plate); and (b) In-Sn-Bi-10Cu (2 min plate) joints. Joints were bonded at 125 °C for 2 hr under 50 psi.

The resulting microstructure of the In-Sn-Bi-10Cu joint that was plated for 2 min prior to bonding is shown in Fig. 4.13b. Like the microstructure seen in Fig. 4.13a, minimal amounts of fine-grain η had formed during TLP bonding. The large 'island-shaped' regions were found to be composed of InSn(γ) and η. The coarse morphology of these phases explains why the joint thickness was actually measured to increase with the use of Ni plating for the In-Sn-Bi-10Cu joints (Fig. 4.6).

The effect of Ni plating on Cu diffusion during TLP bonding in the In-Sn-Bi system can be seen from the diffusion profiles shown in Fig. 4.14 for the low-Bi joints bonded with and without Ni plating. As mentioned in Section 3.2.3, these diffusion profiles represent average composition measurements taken across the joint. This takes into account the inhomogenity of the joint microstructures as was observed in Figs. 4.11-4.13. For the low-Bi joint without plating (Fig. 4.14a), the average Cu content was measured to be around 45-50 at% in the regions extending from the substrate interface towards the center of the joint. In the central region of the joint the average composition of Cu dropped below 40 at%, while an increase in the average In content was also observed. This diffusion profile makes sense when referring back to the microstructure observed for this joint (Fig. 4.11), which showed the Cu-rich η phase growing from the substrate interface and the Cu-poor low melting regions located in the center of the joint (constrained by the η phase). Also, the fact that the center region was found to be more rich in In than Sn, suggests the presence of more In-rich low melting phases such as InSn(β). This is in agreement with the thermodynamic predictions shown in Fig. 4.10b for the Cu-poor side of the diagram.

When the low-Bi joint was plated for 2 min prior to bonding (Fig. 4.14b), there was negligible diffusion of Cu into the joint even after a 2 hr dwell time (< 5 at% Cu). In fact, the compositions measured in the diffusion profile were very close to the nominal composition of the interlayer alloy (which is 52.3In-44.1Sn-3.6Bi (at.%)) meaning that the extent of isothermal solidification undergone during bonding was minimal. Accordingly, the reflow temperature of the joint was not expected to be much greater than the original melting temperature of the interlayer (T_m = 110° C). The effect of the Ni plate on Cu diffusion in the In-Sn-Bi joints with 5

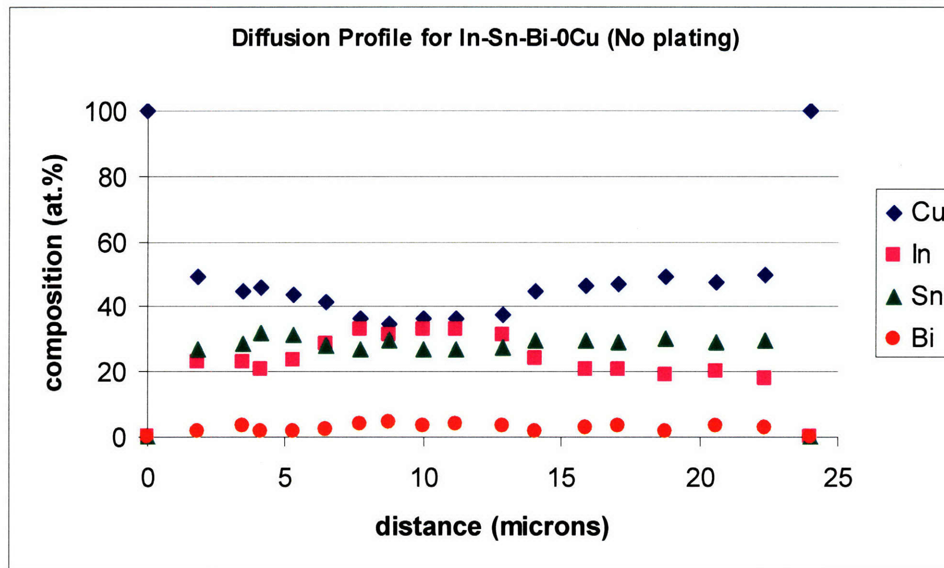

(a)

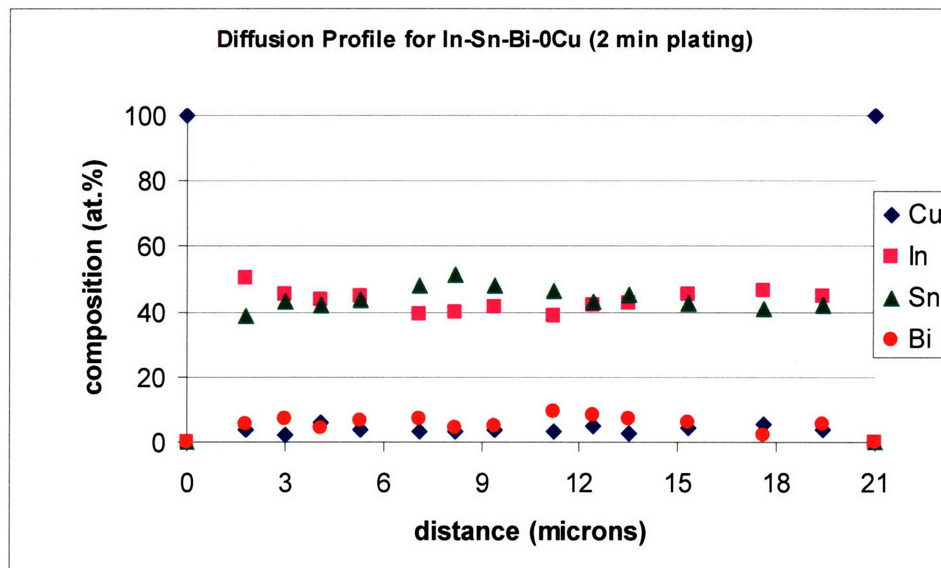

(b)

Figure 4.14: Diffusion profiles for In-Sn-Bi-0Cu TLP joints with (a) no Ni plating; and (b) 2 min Ni plating. The Ni diffusion barrier layer was observed to severely retard Cu diffusion into the joint necessary for isothermal solidification. Joints were bonded at 125 °C for 2 hr under 50 psi.

and 10 wt% Cu additions was observed to be the similar to that shown for the joint without Cu additions. That is, thicker Ni plates reduced diffusion of Cu into the joint during TLP bonding, and thus prevented the formation of high-melting Cu-rich intermetallics in the joint region.

However, the extent to which the average Cu composition of the joint was reduced was less than for the In-Sn-Bi-0Cu joint due to the ability of these joints to form Cu-rich intermetallics from the original Cu additions in the interlayer alloy. Overall, the diffusion barrier layer seemed to have a negative effect on achieving high temperature stability for the In-Sn-Bi-XCu TLP joints.

The resulting microstructures for the eutectic In-Sn-Bi based TLP joints are shown in Fig. 4.15. Figure 4.15a shows a micrograph for the In-Sn-Bi eutectic (48.3In-15.6Sn-36.1Bi) TLP joint made without any Cu additions. Similar to the microstructures observed for the low-Bi joints, fine and coarse-grain η phase was found to exist near the Cu substrate interface. However, the bulk of the joint primarily consisted of low-melting In-Bi intermetallic phases (bright regions in micrograph). According to EDS measurements, these phase regions had compositions (at. %) around 51In-34Bi-15Cu which, neglecting the Cu content, refers to the InBi and In_5Bi_3 phases. Thus, the relatively high Bi content in the interlayer promoted much slower Cu diffusion rates (due to Cu-Bi segregation) which caused a lack of Cu-rich intermetallic growth into the joint during TLP bonding. The microstructure for the eutectic In-Sn-Bi-5Cu TLP joint was found to be very similar to that shown in Fig. 4.15a. The presence of Cu-Bi segregation can be observed more clearly in Fig. 4.15b which shows the microstructure of the eutectic In-Sn-Bi-10Cu joint. The compositions (at. %) of the dark phase and bright phase regions were found to be 31In-11Sn-2Bi-Cu (η phase) and 60In-37Bi-3Cu (InBi + In_5Bi_3), respectively. The fact that the Cu and Bi containing phases become segregated results in it being more difficult for the η phase to grow and connect across the joint. This is the reason why these joints were observed to be thinner than their low-Bi counterparts as was discussed in Section 4.4.1(i). However, the high temperature stability of the joints is compromised by the large fraction of low-melting In-Bi phases ($T_m \approx 90 - 110$ °C) present in the joint.

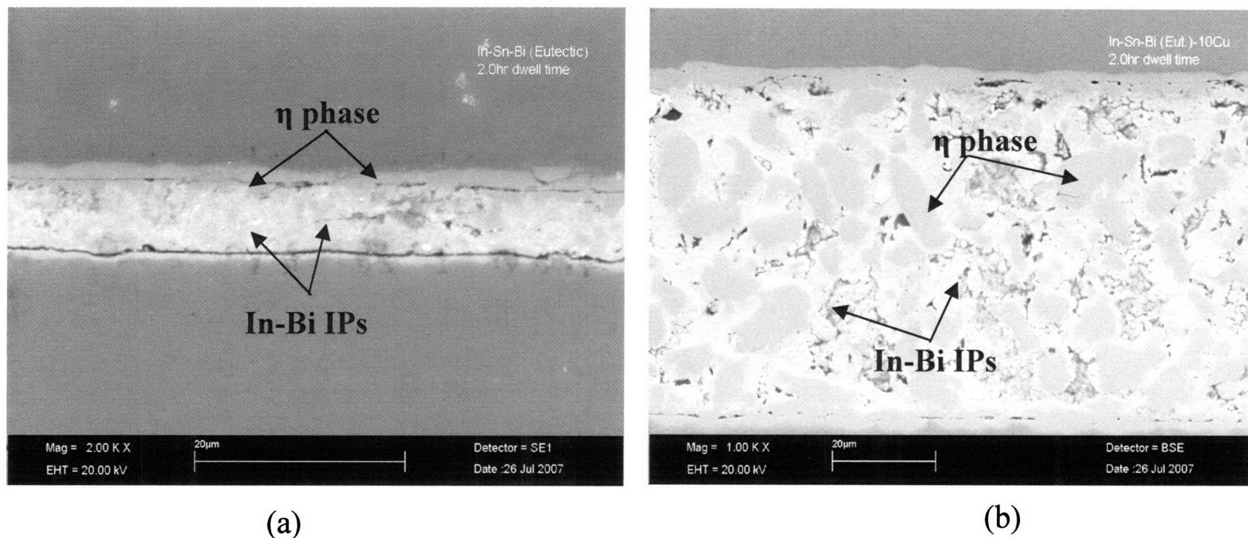

Figure 4.15: SEM micrograph of (a) eutectic In-Sn-Bi; and (b) eutectic In-Sn-Bi-10Cu TLP joints. Joints were bonded at 75 °C for 2 hr under 50 psi.

ii) In-Sn-Cu System

According to thermodynamic calculations, the microstructures for the TLP joints bonded using the eutectic In-Sn based interlayer were expected to be very similar to the joints bonded within the In-Sn-Bi system. The expected Cu-rich (high-melting) phases were η, Cu_6Sn_5, and $Cu_{11}In_9$, while the Cu-poor (low-melting) phases were InSn(β) and InSn (γ). The only significant difference expected between the microstructures was the absence of the low-melting In_2Bi phase. The corresponding thermodynamic calculations can be referred to in Appendix A.

Despite having similar equilibrium solidification paths, there were some noticeable microstructural differences between the TLP joints made in the In-Sn-Cu and In-Sn-Bi-Cu systems. The experimentally observed microstructures for the In-Sn-0Cu and In-Sn-5Cu joints bonded for a dwell time of 2 hr can be seen in Fig. 4.16. Comparing the microstructure of the In-Sn-0Cu joint (Fig. 4.16a) to that in Fig. 4.11 for the In-Sn-Bi-0Cu joint, it is seen that there is no central region of low-melting phases. Instead, the InSn(β) phase is isolated into very small

regions as pointed out in the micrograph. The other phase regions were found to have compositions closely referring to η and InSn(γ).

A similar microstructural difference can be observed between the In-Sn-5Cu joint (Fig. 4.16b) and the In-Sn-Bi-5Cu joint (Fig. 4.12). The fraction of InSn(β) phase present in the In-Sn-5Cu joint was observed to be much less than in the In-Sn-Bi-5Cu jont. Also, the presence of the InSn(γ) phase (bright white regions) at the η/InSn(β) phases boundaries is more prominent in the In-Sn-5Cu joint as compared to the In-Sn-Bi joint made with the same concentration of Cu additions. This microstructural difference is due to the fact that there is no Bi in the interlayer to react with the In to form In-Bi intermetallic phases, such as In_2Bi. Therefore, there is more In readily available to react with the Cu during bonding to form the η phase, and consequently more η phase to dissolve any unreacted Sn present in the joint. Upon solidification, thin regions of unreacted liquid phase form InSn(β) and InSn(γ). Notice that most of the InSn(β) and InSn(γ) exist in the central portion of the joint (away from the Cu interface), where the Cu concentration is expected to be the lowest. The increase in Cu-rich intermetallic formation due to the elimination of Bi from the TLP system serves to explain why, under similar bonding conditions, the In-Sn based TLP joints were found to be larger than the corresponding In-Sn-Bi joints made with the same Cu content as discussed in Section 4.4.1(ii).

The resulting microstructure of the In-Sn-2.5Cu joint after a dwell time of 2 hr (Fig. 4.17) displayed a much higher degree of homogeneity than observed for the In-Sn-0Cu joint (Fig. 4.16a). The only two phases identified in this joint were η and InSn(β). Other phases may have been present in the joint, but were too small in fraction to be individually identified using EDS. In considering the target goals of the TLP process being developed, this microstructure seems to be optimal because it is both thin ($\approx$ 20 μm) like the In-Sn-0Cu joint (Fig. 4.16a), but is more

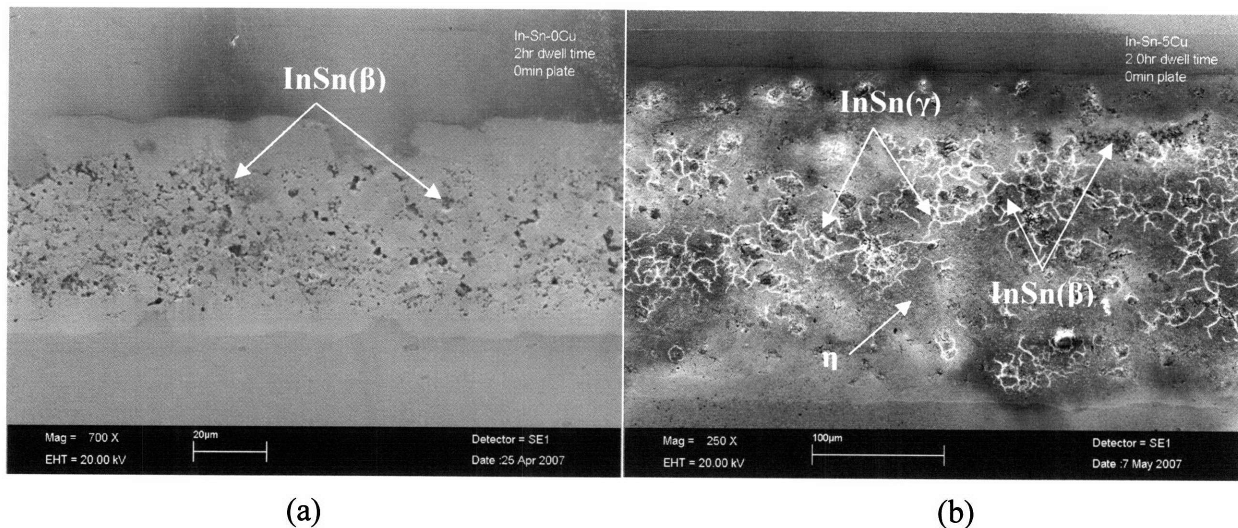

(a) (b)

Figure 4.16: SEM micrograph of eutectic (a) In-Sn; and (b) In-Sn-5Cu TLP joints. Less In-rich, low-melting phases were present in the In-Sn joints (as compared to those bonded in the In-Sn-Bi system) due to the elimination of In-Bi intermetallic formation during TLP bonding. Joints were bonded at 125 °C for 2 hr under 100 psi.

homogenous and contains a larger fraction of high-melting Cu-rich intermetallic phases like the In-Sn-5Cu joint (Fig. 4.16b). As was mentioned in Section 4.4.1(ii), it is thought that the smaller addition of Cu effectively reduces the time of dissolution without growing excessively large intermetallic grains in the bulk of the joint. Instead of forming solid intermetallic bridges across the joint, more liquid phase is produced which allows the joint to thin down as it is pressed and excess liquid is squeezed out of the joint. By the time the η grains growing from the substrate interfaces connect with the Cu-rich intermetallic grains in the bulk of the joint, most of the In and Sn have been consumed in forming the η phase. Only a small amount of residual liquid phase is left which is constrained within the intermetallic grains which solidifies into InSn(β).

Compositional analysis of the In-Sn-Cu joints at different dwell times gave further insight into the microstructural evolution of the joints during TLP bonding. Only the data for joints bonded for 1 hr and 4 hr will be discussed here since the microstructures and diffusion profiles for these joints closely resembled those for the joints bonded for 0.5 hr and 2 hr, respectively.

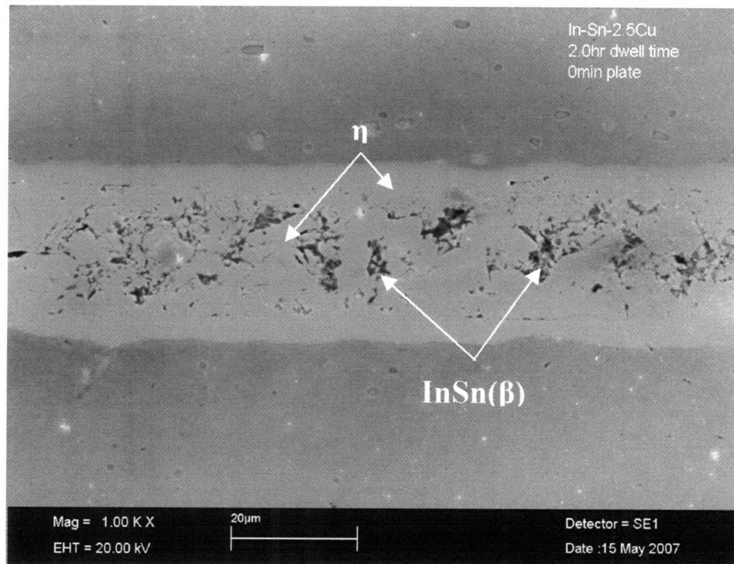

Figure 4.17: SEM micrograph of In-Sn-2.5Cu joint. Joint was bonded at 125 °C for 2 hr under 100 psi.

The microstructure of the In-Sn-0Cu joint after a 1 hr dwell time is shown in Fig. 4.18a. As shown in the micrograph, the microstructure was primarily composed of InSn(β) and InSn(γ), although there were small regions of η detected in the joint as well. The microstructure suggests that a relatively small amount of Cu diffusion took place in the 1 hr time span. This is verified by the diffusion profile of the joint (Fig. 4.18b) which shows a low content of Cu (≈ 2-10 at.%) throughout the joint region as well as very high compositions of In and Sn. (Fig. 4.18b). After bonding the same joint for 4 hr (Fig. 4.19), the composition profile (Fig. 4.19b) shows a large increase of Cu concentration (≈ 20 at.%) and decrease in In concentration. The increase in Cu concentration signifies an increased amount of Cu diffusion into the joint and corresponding growth of the η phase, while the decrease in In content is a result of the smaller sized InSn(β) regions formed from solidification of the unreacted liquid. Also, the high levels of Sn measured in the joint suggest that some InSn(γ) is still present in the joint after the bonding process (most

of the measured Sn is from that dissolved in the η phase). This microstructure, shown in Fig. 4.19a, is very similar to that in Fig. 4.16a for a dwell time of 2 hr.

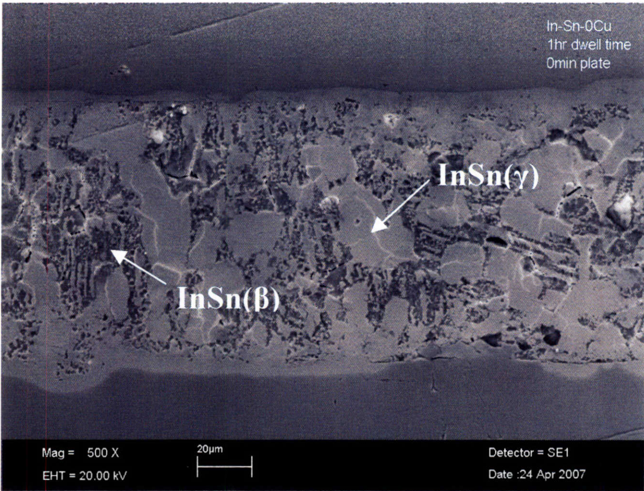

(a)

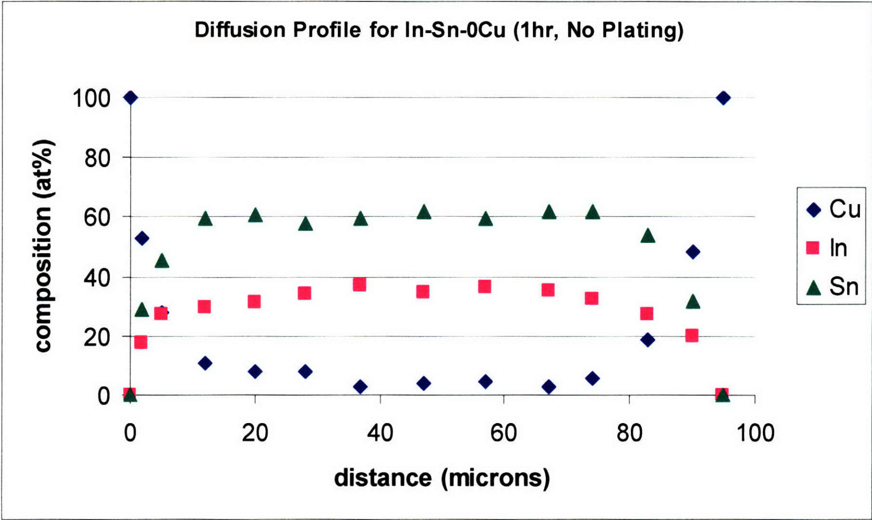

(b)

Figure 4.18: (a) SEM micrograph and (b) diffusion profile of eutectic In-Sn joint after 1 hr dwell time. Joint was bonded at 125 °C under 100 psi.

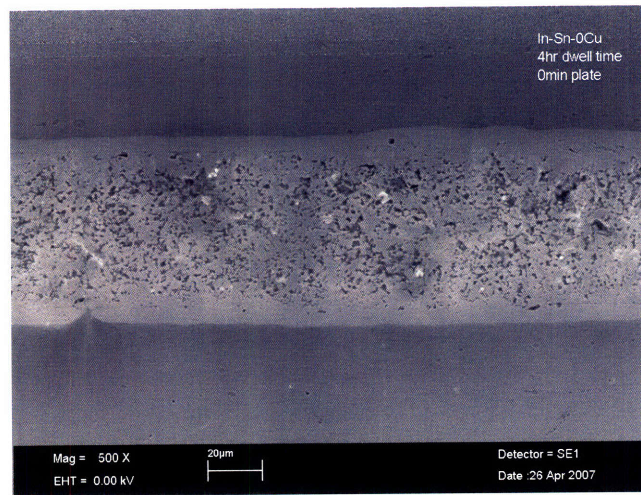

(a)

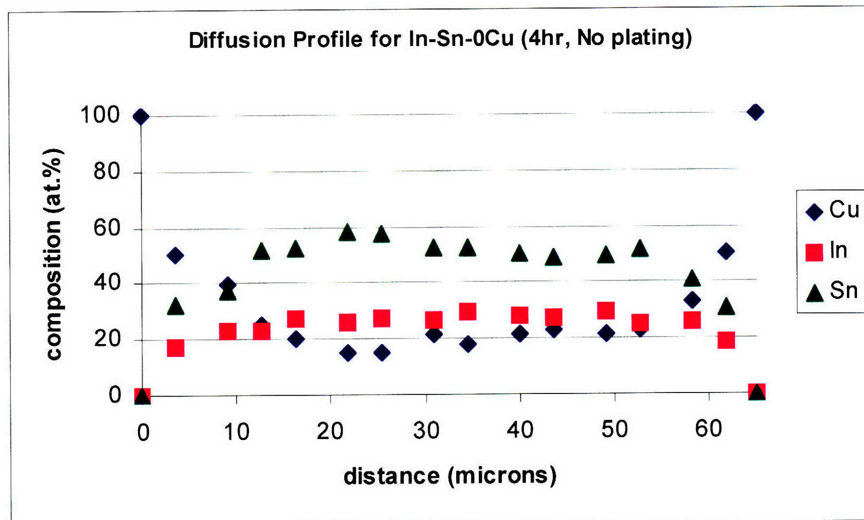

(b)

Figure 4.19: (a) SEM micrograph and (b) diffusion profile of eutectic In-Sn joint after 4 hr dwell time. Joint was bonded at 125 °C under 100 psi.

A SEM micrograph and diffusion profile for the In-Sn-2.5Cu joint after bonding for 1 hr is shown in Fig. 4.20. Interestingly, the microstructure shown in Fig. 4.20a is very similar to that of 4.17, which shows the microstructure for the same joint after a 2 hr dwell time. In addition, the diffusion profile in Fig. 4.17 shows a substantial level of Cu content (≈ 40 at.%) across the

entire joint, signifying that a large portion of the joint is made up of the η phase. This is a big improvement over the TLP joint made with the eutectic In-Sn interlayer which showed a negligible degree of Cu-rich intermetallic growth in the same bond time (Fig. 4.18). In fact, this joint is seen to have more Cu content than the eutectic In-Sn joint that was bonded for 4 hr (Fig. 4.19). Thus, it is shown that adding 2.5 wt.% Cu additions to the eutectic In-Sn interlayer alloy has the potential to greatly decrease the time necessary to produce a high temperature stable microstructure without increasing the joint thickness. The microstructure for the In-Sn-2.5Cu joint after a 4 hr dwell time (Fig. 4.21a) looks very similar to the same joint bonded for 1 hr (Fig. 4.20a), except that there seems to be more InSn(β) present in the joint in case for the 4 hr dwell time. Also, the diffusion profile measured after 1 hr and 4 hr bond times were found to be very similar to one another. Compared to the 1 hr dwell time (Fig. 4.20b), the diffusion profile in Fig. 4.21b shows the same average Cu composition across most of the joint with only slight changes in In and Sn content. However, this joint was also larger than compared to the In-Sn-2.5Cu joint bonded for 1 hr which means that Cu diffusion into the joint continued to occur throughout the entire bonding period.

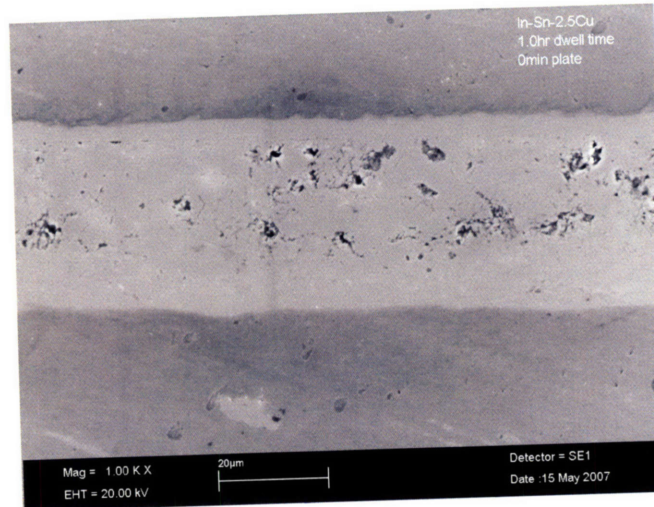

(a)

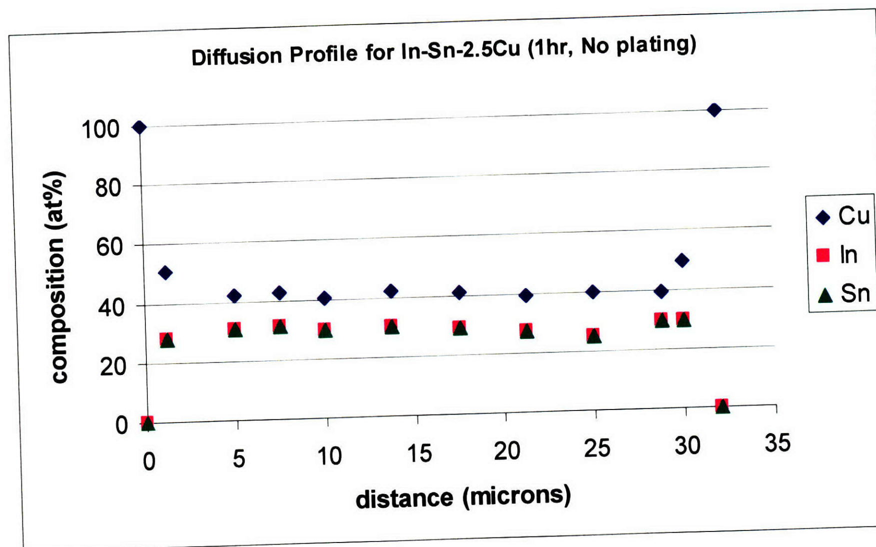

(b)

Figure 4.20: (a) SEM micrograph and (b) diffusion profile of In-Sn-2.5Cu joint after 1 hr dwell time. Additions of 2.5wt% Cu to eutectic In-Sn interlayer alloy was seen to decrease the bond time necessary to obtain a high temperature stable microstructure. Joint was bonded at 125 °C under 100 psi.

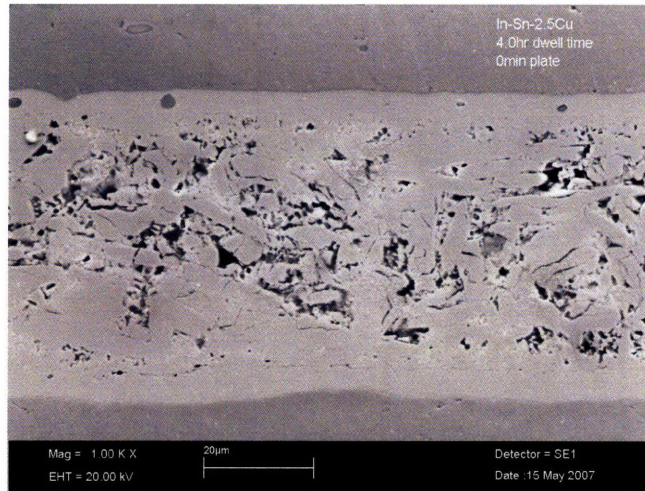

(a)

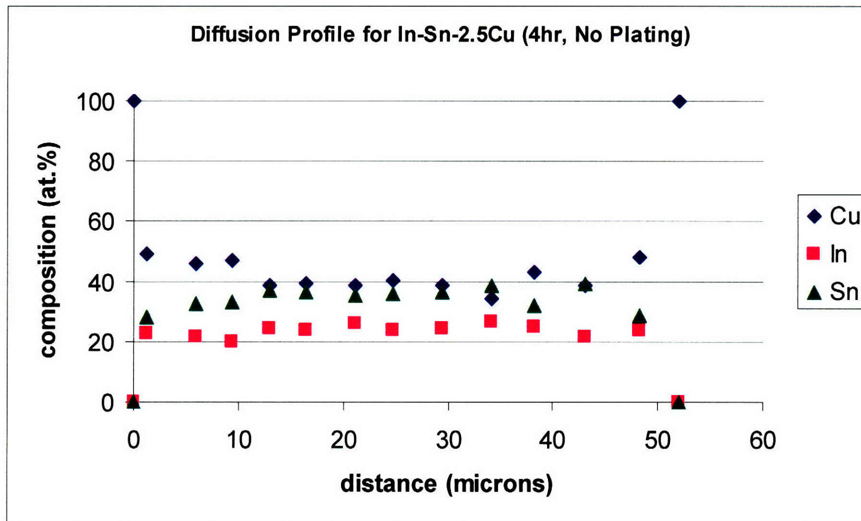

(b)

Figure 4.21: (a) SEM micrograph and (b) diffusion profile of In-Sn-2.5Cu joint after 4 hr dwell time. Joint was bonded at 125 °C under 100 psi.

The resulting microstructure and composition profile for the In-Sn-5Cu joint after a 1 hr dwell time is shown in Fig. 4.22. According to the diffusion profile in Fig. 4.22b, the average composition of Cu the In-Sn-5Cu varied between 30-40 at.% at regions close (≤ 20 μm) to the Cu substrate interface and around 20 at.% in the central region. This is noticeably different than the profile measured for the In-Sn-2.5Cu joint bonded for the same time (Fig. 4.20b), which

shows that the average Cu composition is 40 at.% throughout the bulk of the joint. It is thought that the increase in nominal Cu concentration accelerates the rate at which intermetallic bridges form across the In-Sn-5Cu joint. Not only does this lead to thicker joints (see Section 4.3), but it also leads to an increase in constrained liquid phase upon reaching the bond temperature. As a result, the Cu diffusion distances become larger and it takes a longer time for the joint form η across the entire reaction zone (i.e. joint region). During isothermal solidification, Cu continues to diffuse into the joint and form the η phase. As mentioned in Section 4.4.1(ii), it is suggested that Cu-rich intermetallics which form in the bulk of the joint promote the rapid growth of the joint region through redistribution of In and Sn atoms into the η phase. The additional η phase reactions with the In and Sn in the unreacted liquid resulting in the microstructure, and corresponding composition profile, seen in Fig. 4.23. Thin regions of low-melting, Sn-rich phases (mostly InSn(γ)) were present due to undissolved Sn in the η phase (along with small InSn(β) regions), just as was observed in Fig. 4.16b for the same joint bonded for 2 hr.

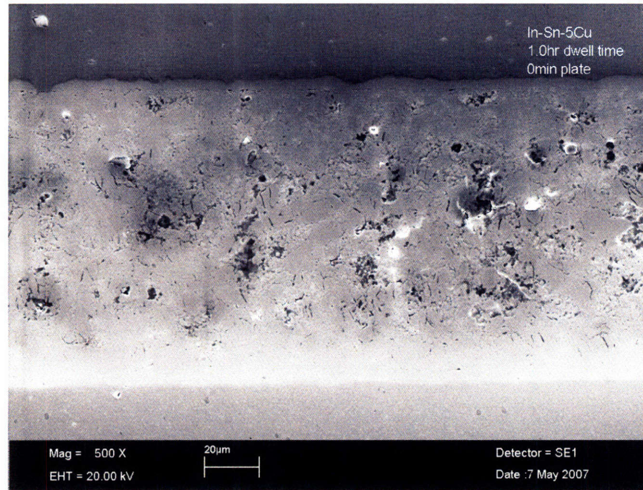

(a)

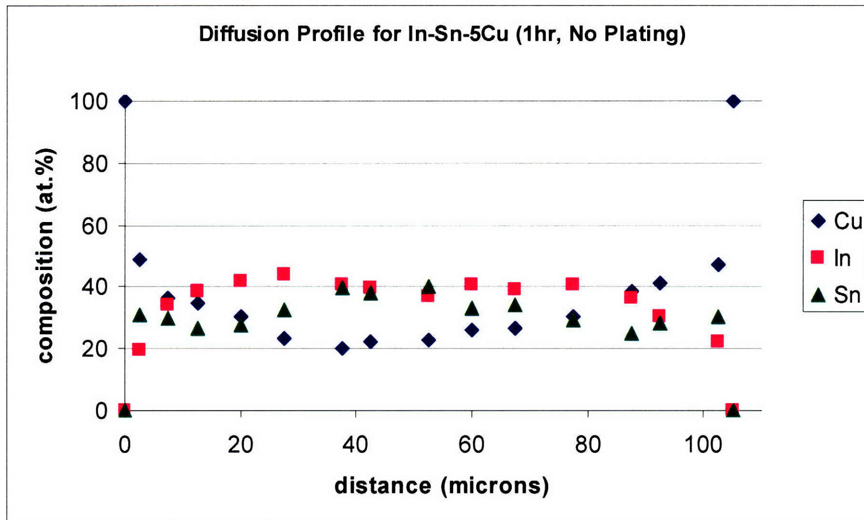

(b)

Figure 4.22: (a) SEM micrograph and (b) diffusion profile of In-Sn-5Cu joint after 1 hr dwell time. Joint was bonded at 125 °C under 100 psi.

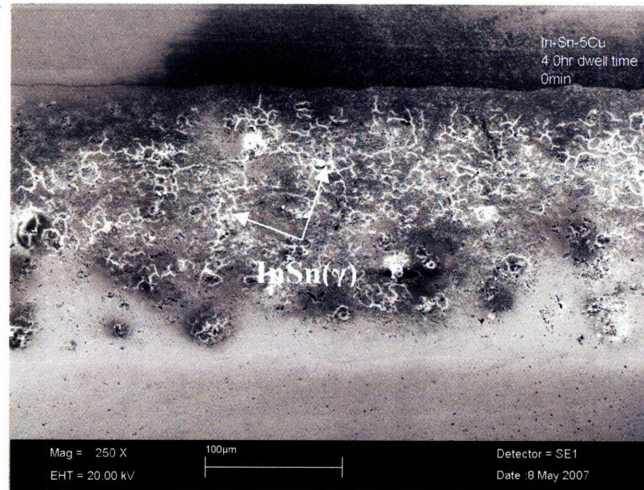

(a)

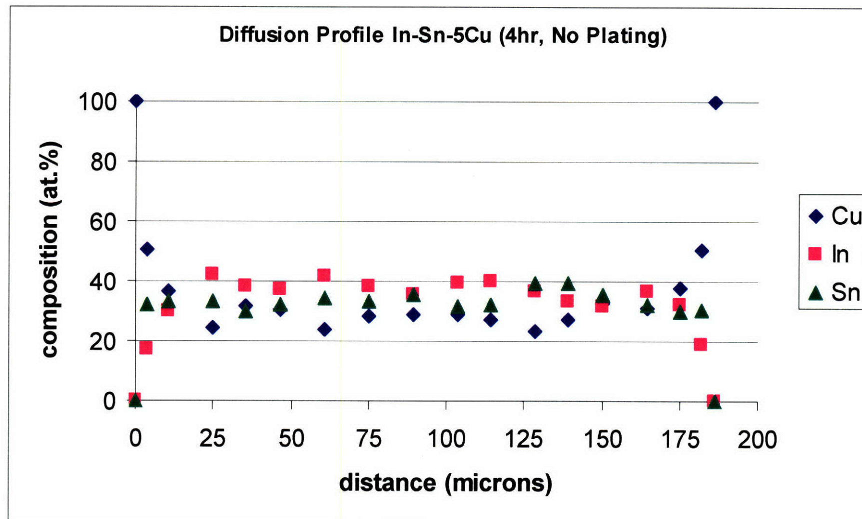

(b)

Figure 4.23: (a) SEM micrograph and (b) diffusion profile of In-Sn-5Cu joint after 4 hr dwell time. Joint was bonded at 125 °C under 100 psi.

As was discussed in Section 4.4.1(ii), the Ni layer did not have any significant effect on the growth rates on either the eutectic In-Sn or In-Sn-2.5Cu joints. Due to the relatively small content of Cu in the interlayers of these joints, excess formation of Cu-rich intermetallics in the joint (which form intermetallic bridges) while heating to the bonding temperature was prevented. Since these joints were already relatively thin (30-70 μm) prior to the Ni plating (Fig. 4.8), the

use of a diffusion barrier layer was a less crucial parameter in optimization of these joints. It is for this reason that the effect of the diffusion barrier layer on the microstructural evolution of these joints was not analyzed in detail in this study. However, a couple of observations should be mentioned. One is that, as was observed for the In-Sn-Bi joints, increasingly thicker Ni layers reduced the average Cu composition of the joint, signifying a smaller presence of Cu-rich intermetallics. Also, the effect of the Ni layer on reducing η formation was a lot less prominent in the In-Sn-2.5Cu joints than the eutectic In-Sn joints, especially at low plating times. The reduction in average Cu composition was witnessed to start occurring after a 1 min plating time for the eutectic In-Sn joints, whereas a noticeable decrease in average Cu composition was not observed until a 2 min plating time for the In-Sn-2.5Cu joints. This is likely a result of the ability of the In-Sn-2.5Cu joint to promote rapid growth of η phase in the joint region from the presence of Cu-rich intermetallics such as Cu_6Sn_5 and $Cu_{11}In_9$ which can redistribute In and Sn atoms to form a continuous η layer upon Cu diffusion into the joint. Finally, longer dwell times resulted in higher average Cu compositions for both joints regardless of plating time. This is to be expected since longer dwell times allow the Ni layer to dissolve and thus Cu to diffuse into the joint.

For larger Cu additions of 5 wt%, the use of a diffusion barrier layer was found to greatly reduce the growth rate of the TLP joints (Fig. 4.9). However, it was important to study the microstructure of these joints in order to assess whether the decrease in growth rate was also correlated to a sacrifice in the amount of high-melting η phase formed in the joint region due to lack of Cu diffusion. According to the microstructure and corresponding diffusion profile observed for the In-Sn-5Cu joint plated for 2 min prior to bonding (Fig. 4.24), there was a relatively high degree of Cu diffusion into the joint after a 1 hr dwell time. There were areas

near the Cu substrate where the Ni layer was observed to break down that consisted of phase regions that were extremely rich in Cu (> 90 at.%). These regions of Cu solid solution (α) were presumably formed during rapid diffusion of Cu into the joint through the regions where the Ni layer broke down. The diffusion profile in Fig. 4.24b shows nearly the same average Cu composition in the joint as was observed for the In-Sn-5Cu joint bonded without Ni plating for the same 1 hr dwell time (Fig. 4.22b). From these observations, it is reasoned that the Ni layer prevented enough Cu diffusion from the substrates to provide sufficient time for liquid to form before the growth of the intermetallic bridges. Thus, the liquid was not constrained within intermetallic grains upon reaching the bonding temperature, and the joint could be pressed thinner by expelling excess liquid out of the joint (in a similar manner as the In-Sn and In-Sn-2.5Cu joints). By the time the Ni layer started to decompose, the diffusion distances were reduced to a point where the η phase could form throughout the entire reaction zone. As in the case for the In-Sn-2.5Cu joints, the growth of the η phase was accelerated by the presence of Cu-rich intermetallics such as Cu_6Sn_5 and $Cu_{11}In_9$. After bonding for 4 hr, the Ni layer is dissolved further (as noted by the increase in η phase formed on the Cu side of the joint/substrate interface) and Cu diffusion into the joint continues to proceed (Fig. 4.25a). Also, there is a decrease in the amount of the Cu(α) phase near the substrate which has transformed into η due to the diffusion of In and Sn into those regions. The diffusion profile (not including Ni and P from the barrier layer) in Fig. 4.25b shows that the average Cu composition is 25-30 at.% across the entire joint which is similar to that of the non-plated joint bonded for 4 hr (Fig. 4.23b). It is concluded, therefore, that the Ni layer was used successfully in reducing the growth rate of the In-Sn-5Cu joints without sacrificing the ability to achieve a high temperature stable microstructure.

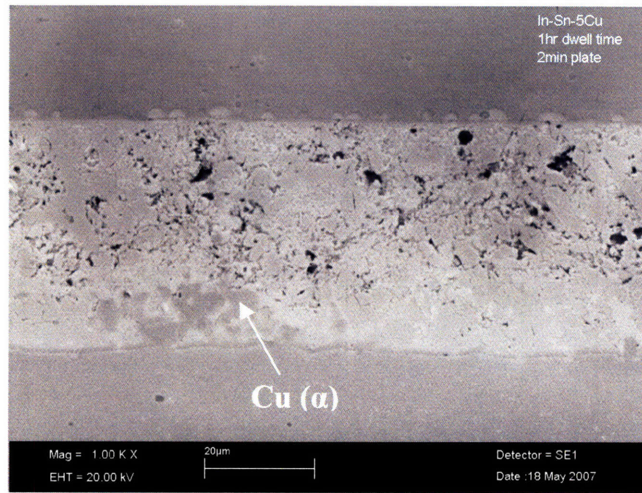

(a)

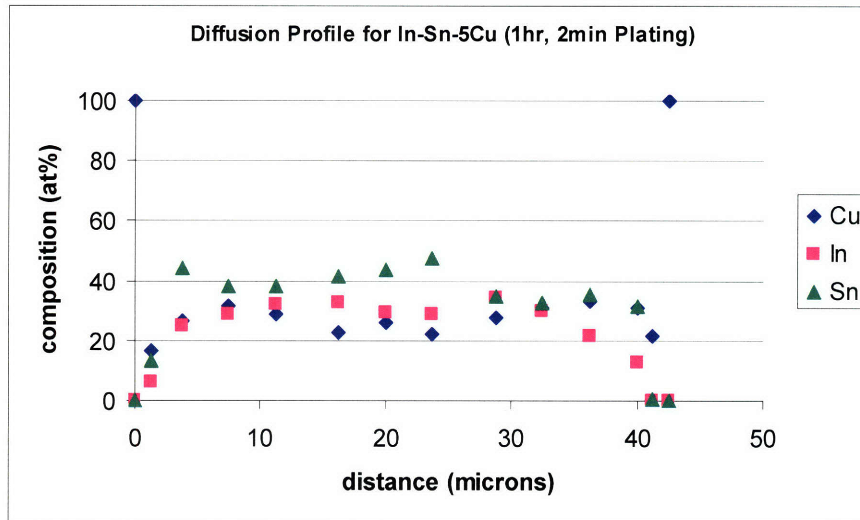

(b)

Figure 4.24: (a) SEM micrograph and (b) diffusion profile of In-Sn-5Cu joint (2 min plate) after 1 hr dwell time. Joint was bonded at 125 °C under 100 psi.

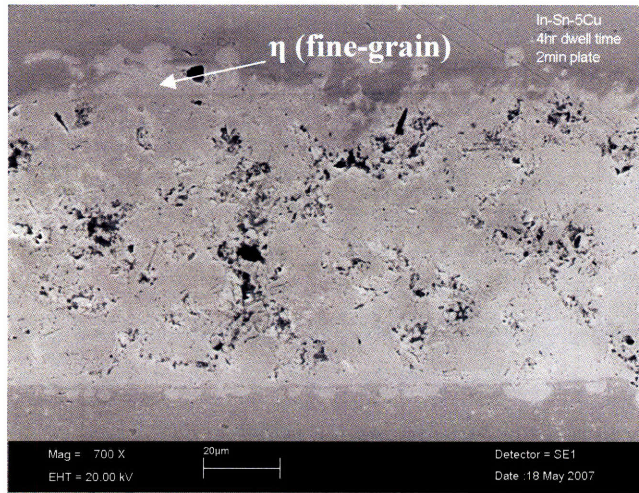

(a)

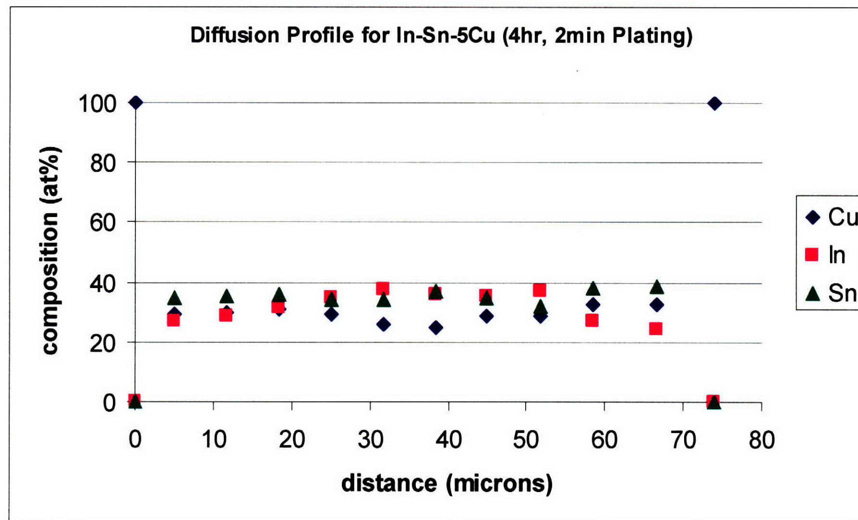

(b)

Figure 4.25: (a) SEM micrograph and (b) diffusion profile of In-Sn-5Cu joint (2 min plate) after 4 hr dwell time. Joint was bonded at 125 °C under 100 psi.

4.4.3 Mechanical Behavior and Failure Analysis

i) In-Sn-Bi-Cu Systems

Table II lists the shear strength values measured for the low-Bi In-Sn-Bi-XCu joints at both room temperature (25 °C) and operation temperature (100 °C). The room temperature (R.T.) shear strengths ranged from around 10,000 – 20,000 psi (≈ 70 – 140 MPa), which was

about half of that measured for the eutectic Pb-Sn soldered joint (30,410 psi ≈ 210 MPa). Taking into account experimental variation of the measurements, there does not seem to be any concrete evidence of an effect of Cu content or plating time on the room temperature shear strengths of the TLP joints made in the In-Sn-Bi-Cu system. This suggests that the room temperature shear strength depends primarily on the Cu-rich intermetallics (i.e. either Cu_6Sn_5 or η) at the substrate/joint interface which was found to be present in all of the various joint microstructures, regardless of the initial interlayer composition or plating thickness. The room temperature shear strength did not seem to be affected by the joint thickness or the presence of low temperature phases in the bulk of the joint region. This agrees well with shear test observations made by Sommadossi et al. who noted that rupture always occurred through the η phase when it was present in Cu/In-48Sn/Cu (at.%) TLP joints [48]. It was not possible to perform microscopic analysis of the fracture surfaces of the specimens that were tested at room temperature since the Cu substrates did not completely separate at failure.

The shear strengths of the low-Bi TLP joints produced in the In-Sn-Bi-Cu system were observed to decrease by one to two orders of magnitude when tested at the operating temperature (O.T.) as seen in Table II. This sharp decrease in strength is due to the presence of low-melting phases which remained in the joint after bonding. Unlike the room temperature shear strengths, the shear strengths measured at operating temperature showed some signs of dependency on interlayer composition and Ni plating thickness. Comparing the average values of operating temperature shear strengths measured for the low-Bi joints made with different nominal Cu contents (without plating), it is seen that joint made without Cu additions displayed strengths around twice that of the joints made with 5 or 10 wt.% Cu additions; although this difference may be less when considering the experimental variation. The decrease in strength with

increasing Cu additions may be attributed to the large increase in joint thickness with increasing nominal Cu concentration of the interlayer alloy (Fig. 4.6). Also, in comparing the joints made with and without Cu additions, it is shown that the Ni layer has a much more prominent effect on the operating temperature shear strength of the joints made without Cu additions. As shown in Table II, the operating temperature shear strength of the In-Sn-Bi-0Cu joint reduces by more than half after using a plating time of 1 min, and reduces even further after plating for 2 min. This makes sense when referring back to Fig. 4.14 which showed that the Ni plating severely reduced the amount of Cu diffusion into the low-Bi joint, and hence the amount of Cu-rich intermetallics which formed to provide high temperature mechanical stability. The operating temperature shear strengths of the low-Bi joints made with 5 and 10 wt.% Cu additions, on the other hand, were not found to be highly affected by the Ni plating. As was mentioned in Section 4.4.2(i), this is because these joints, having had Cu present in the interlayer prior to bonding, were able to form the necessary IPs needed for high temperature mechanical stability even with the reduced amount of Cu from the substrates into the joint region.

Although microscopic analysis of the fracture surfaces of the was not performed for these specimens, physical visualization of the fracture surface immediately after failure (i.e. substrate separation) revealed shiny, liquid-like regions on the fracture surface. These melted regions are most likely the low melting In-Bi IPs (T_m = 90 – 110 °C) which were present in the interconnect zone post solidification of the joints as their melting points are around the test temperature (100 °C). These phases are a major cause for the observed degradation in the high temperature mechanical properties of the joints. Regardless of the TLP bonding parameters used in this system, all of the low-Bi joints performed poorly under the service-like conditions compared to the eutectic Pb-Sn solder joint which had an operating temperature shear strength value

measured to be 15,140 psi (≈ 100 MPa). Thus, further optimization of the TLP bonding process within the In-Sn-Bi-Cu system must be done in order to make it a viable replacement for conventional soldering methods used in the electronics packaging industry,

Table II: Shear strength values measured for the low-Bi In-Sn-Bi-XCu TLP joints

Interlayer Alloy	Plating Time (min)	R.T. Shear Strength (psi)	O.T. Shear Strength (psi)
In-Sn-Bi-0Cu	0	16,420 ± 3,950	1,230 ± 530
	1	15,920 ± 2,220	380 ± 170
	2	14,220 ± 2,790	210 ± 80
In-Sn-Bi-5Cu	0	13,690 ± 3,130	620 ± 110
	1	13,110 ± 4,190	740 ± 310
	2	10,680 ± 770	520 ± 230
In-Sn-Bi-10Cu	0	14,330 ± 2,410	470 ± 160
	1	17,100 ± 4,130	380 ± 100
	2	18,710 ± 2,520	340 ± 80

Values for the room temperature shear strengths of the eutectic In-Sn-Bi TLP joints made with 0, 5, and 10 wt% Cu additions were found to be 11,360 ± 3,780 psi (78 ± 26 MPa) , 13,350 ± 5,270 psi (92 ± 36 MPa), and 18,200 ± 6,010 psi (125 ± 41 MPa), respectively. These values are comparable to those made with the low-Bi interlayer, which again suggests that the room temperature strengths were dependent on the presence of the η intermetallic grains at the substrate/joint interface. However, none of the eutectic-based In-Sn-Bi TLP joints were able to sustain any load at the operating temperature because the interlayers melted prior to application of the load at 100 °C. This is due to the extremely large fraction of low melting In-Bi IPs which remained in the joint following the bonding procedure (Fig. 4.15). Thus, the benefit of increasing the Bi content of the interlayer alloy in order to depress its melting temperature (and thus the bonding temperature) is negated by the segregation of Cu-rich and Bi-rich phases which stablizes the presence of In-Bi IPs. This, in turn, severly inhibits the ability of the TLP joint to

increase its reflow temperature during the bonding process, leading to poor high temperature mechanical behavior.

ii) In-Sn-Cu System

Figure 4.26 shows the resulting room temperature shear test values measured for the TLP joints made with the eutectic In-Sn interlayer alloy. Since only a single measurement was made for each sample in this system, experimental variation was assumed to be the same as found for room temperature shear strengths of the joints made in the In-Sn-Bi-Cu system (i.e. on the order of 10^3 psi). At room temperature, most of the shear strengths were measured to be within the 10,000 – 16,000 psi ($\approx$ 70 – 110 MPa) range, with no obvious dependence on either the plating time or dwell time. These values are of the same magnitude as the low-Bi TLP joints made without Cu additions (Table II). Since the room temperature shear strengths are mostly dependent on the properties of the same interfacial Cu-rich intermetallics that were found in the In-Sn-Bi-XCu joints, a significant change in the mechanical response of the joints at this temperature was not expected.

A marked increase in room temperature shear strength was found for the In-Sn-2.5Cu TLP joints which displayed strengths mostly within the 20,000 – 25,000 psi ($\approx$ 140 – 170 MPa) range (Fig. 4.27). Some of the joints even had shear strengths about the same as the Pb-Sn soldered joint denoted by the large red square at 0 hr dwell time. Although the exact reason for the observed improvement in room temperature shear strength for these joints is uncertain, it is believed that it is due to a change in the microstructure of the intermetallic grains at the substrate/joint interface. For example, from the micrographs presented in Section 4.4.2(ii), the microstructure of the interfacial η grains of the non-plated In-Sn-2.5Cu joints (Figs. 4.17, 4.20, and 4.21) seem to be more homogenous than those observed for the non-plated In-Sn-0Cu joints

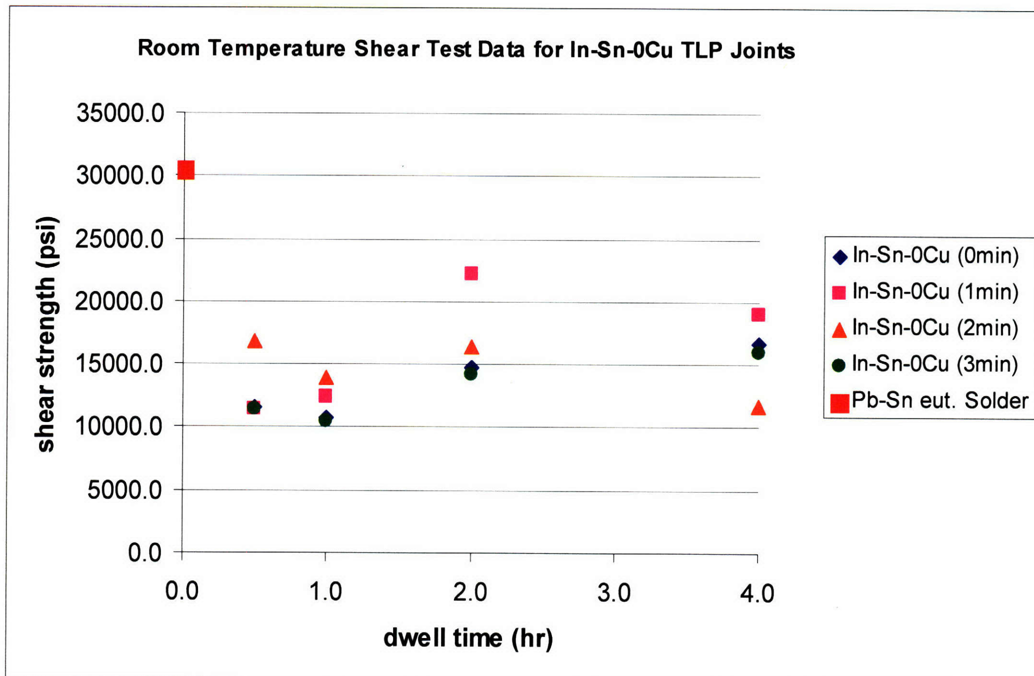

Figure 4.26: Room temperature shear strengths for TLP joints made with eutectic In-Sn interlayer using various dwell times and plating times.

(Figs. 4.16a, 4.18, and 4.19) which display a more well-defined boundary between the fine and coarse η grains. This difference in the microstructural homogeneity at the interface suggests a difference in the size of the coarse η grains. That is, the coarse η grains of the In-Sn-2.5Cu joint are smaller in size than those in the In-Sn-0Cu joints, which makes them appear similar in microstructure to the fine η grains on the solid Cu side of the substrate/joint interface – making the interface appear more homogenous. Since the interface between the sublayers of fine and coarse η grains is most likely one of the mechanically weaker regions of the interconnect region [48], it is possible that the finer the coarse grain η grains grow in order to minimize the grain size difference at the interface, the more mechanically stable the joint will be. A similar argument may be made for the plated joints as well. It is important to recognize that a more accurate

determination of the grain size and more rigorous fractography of these joints must be performed to confirm this explanation.

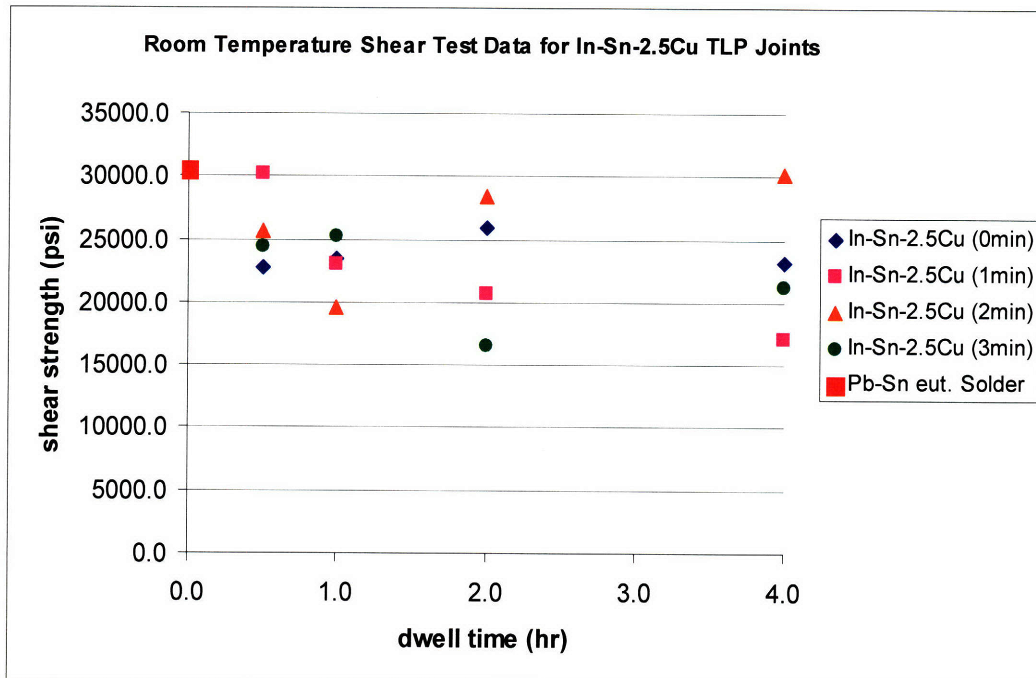

Figure 4.27: Room temperature shear strengths for TLP joints made with In-Sn-2.5Cu interlayer and using various dwell times and plating times. Similar results were observed for the In-Sn-5Cu joints.

The room temperature shear strength values for the In-Sn-5Cu joints were found to be in the same range as those found for the In-Sn-2.5Cu, suggesting a similar microstructure of the intermetallic grains at the substrate/joint interface. This agrees with the microstructures in Figs. 4.16a, 4.22, and 4.23 for the In-Sn-5Cu non-plated joints. Also, the fact that the much larger In-Sn-5Cu (Figs. 4.7-4.9) joints displayed the same range of strengths as compared to the In-Sn-2.5Cu further implies that the joint thickness is not as large a factor as the joint microstructure in determining the room temperature mechanical response of the joints.

When tested at the operating temperature, the majority of the eutectic In-Sn TLP joints displayed shear strengths between 4,000 – 5,500 psi (≈ 30MPa – 40MPa), although a few joints

had operating temperatures approaching values as low 2,300 psi (16 MPa) and as high as 8,800 psi (60 MPa), as shown in Fig. 4.28. Although these strength values are about half of those found for the same joints at room temperature (Fig.4.26), they are about an order of magnitude better than the joints made using the low-Bi based interlayer at the same temperature (Table II). This is most likely a result of the elimination any low melting In-Bi IPs from the joint region from the removal of Bi from the interlayer alloy. Also, the Ni platings do not seem to have the same detrimental effect as was seen in Table II for the low-Bi TLP joints made without any Cu additions in which the strength decreased by more than a factor of two upon application of the diffusion barrier layer. Thus, this data further supports the findings that increasing Bi additions to the interlayer alloy has a negative effect on the high temperature mechanical behavior of Cu/Cu TLP joints. Additionally, the data suggests that the low-melting InSn(γ) and InSn(β) phases have the ability to sustain significant load at elevated temperatures. Despite the improved high temperature stability of these joints, however, they still compared poorly to the conventional Pb-Sn solder joint.

A further improvement in operational temperature mechanical behavior of the TLP joints was observed for the In-Sn-2.5Cu joints (Fig. 4.29), with most of the measured shear strength values falling between 6,000 – 7,500 psi ($\approx$ 40 – 50 MPa). The lines shown in Fig. 4.29 are linear fits to each of the sets of data whose purpose are to ease the qualitative evaluation of the graph given the degree of variation in the results. They are not meant to be an exact fit to the data nor quantitatively predictive. According to these trends, the overall mechanical response of the joints at elevated temperatures is degraded (i.e. the shear strength decreases) with increasing Ni plating times. Shear strengths for the joints made with no Ni plating, a one min plating, and a two min plating were found to reach as high as 15,940 psi (110 MPa), 11,970 psi (83 MPa), and

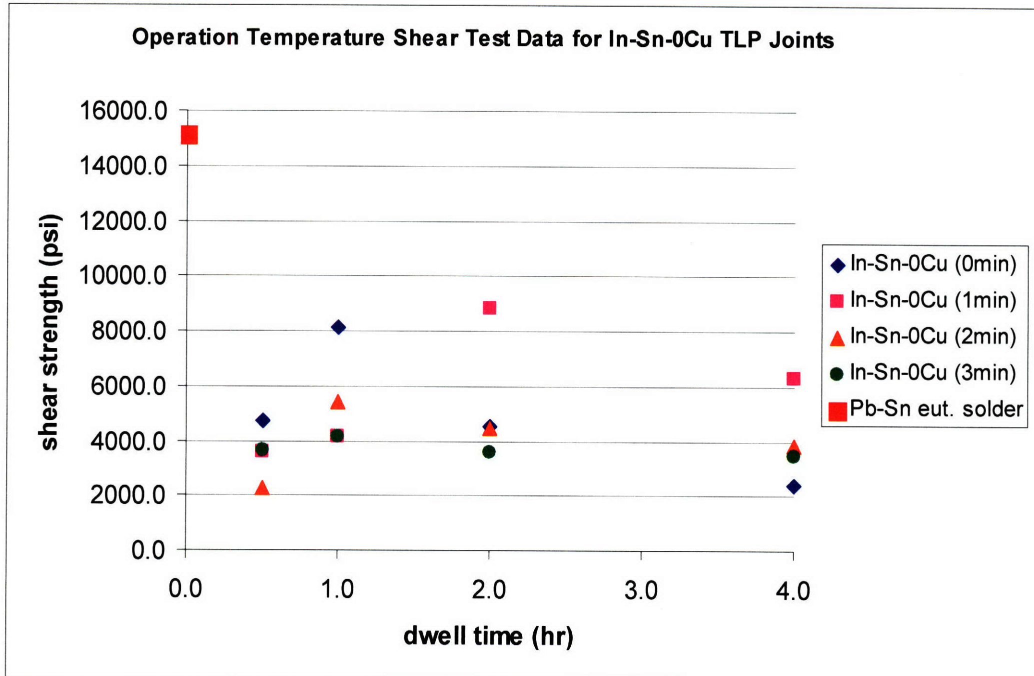

Figure 4.28: Operation temperature shear strengths for TLP joints made with In-Sn-0Cu interlayer and using various dwell times and plating times.

10,730 psi (74 MPa), respectively. On the other hand, most of three min plated joints had shear strengths which fell below the average range, reaching as low as 3,680 psi (25 MPa). This makes sense according to the compositional analysis discussed in Section 4.4.2(ii) which shows that the use of Ni plating seems to decrease the overall Cu content of the TLP joints (i.e. the fraction of high melting Cu-rich intermetallics within the joint) which reduces the mechanical stability of the joints at elevated temperatures. Of course more measurements must be made in order to more accurately define the shear strength of these joints at the operating temperature.

Another trend seen from Fig. 4.29 is a slight decrease in operating shear strength values with increasing dwell time (except for the three min plated joint which remains practically constant). Although this can be due to a small increase in joint thickness with longer bonding times, the analysis of the growth rate of the In-Sn.2.5 Cu joints (Section 4.4.1(ii)), which found the thickness of the In-Sn-2.5Cu joints to remain relatively constant, does not support this

explanation. It is more likely, therefore, that the observed decrease is likely a result of experimental variation and that the average shear strength for each plating time should remain relatively constant.

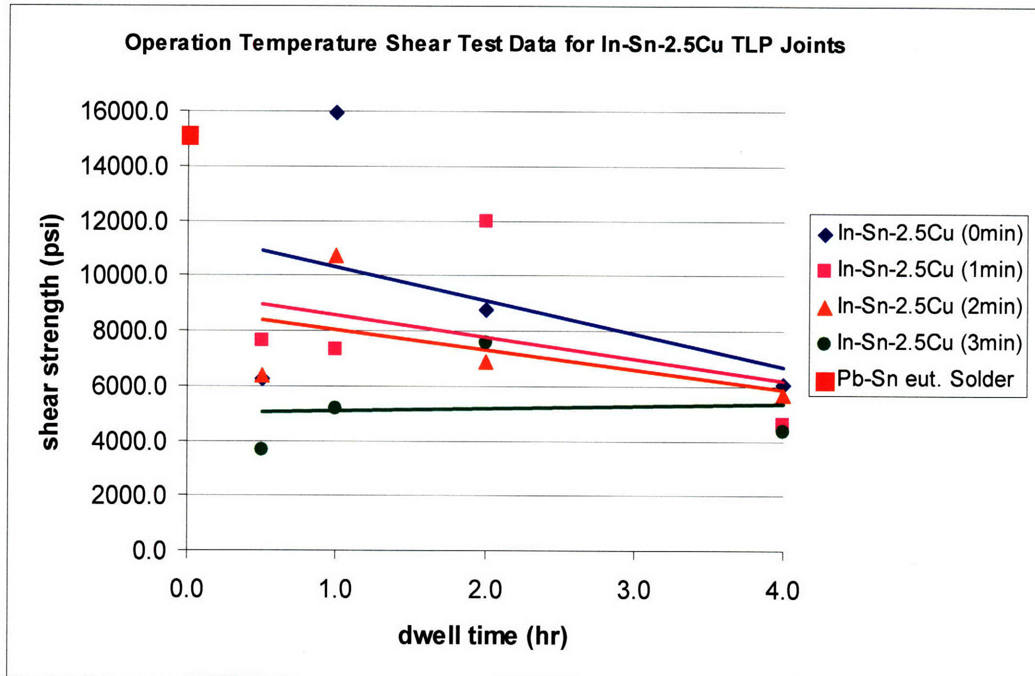

Figure 4.29: Operation temperature shear strengths for TLP joints made with In-Sn-2.5Cu interlayer and using various dwell times and plating times. Increased plating times seem to degrade the overall high temperature mechanical behavior of the In-Sn-2.5Cu joints.

Operating shear strength measurements made for the In-Sn-5Cu joints (Fig. 4.30) again suggest an improvement in high temperature mechanical behavior of the joints with further increases in nominal Cu composition of the interlayer alloy. For the In-Sn-5Cu joints, the operating temperature shear strength measurements mostly fell within a range of 7,500 – 9,500 psi (≈ 50 – 65 MPa), with some values falling both above (maximum of 13,530 psi = 92 MPa) and below (minimum of 4,070 psi = 28 MPa) this range. Also, the trend lines, which are solely qualitativie in nature, show some other differences between these joints compared to those made

with only 2.5 wt% Cu additions (Fig. 4.29). First, a much larger decrease is observed for the non-plated joints with increasing dwell time than was observed for the non-plated In-Sn-2.5Cu joints. Up to a bonding time between 1-2 hr, the overall shear strength of the non-plated joints appears to be greater than the strengths of the plated ones. Upon longer bonding times, the shear strength of the non-plated joints continues to decrease until its trend line falls below those of the plated joints. This is most likely a result of the much more rapid growth rate of the In-Sn-5Cu joints with dwell time (Fig. 4.9) as compared to joints made with lesser Cu additions (Fig. 4.8). Thus, the advantage of increasing the degree of intermetallic formation for high temperature stability is negated by the fact the joint thicknesses are very large due to the intermetallic bridges formed across the joint.

Another difference between the trends observed for the In-Sn-5Cu joints compared to the In-Sn-2.5Cu joints is that the overall mechanical response of the joints at elevated temperatures seems to improve with increasing Ni plating times. Improved mechanical behavior with increasing Ni plating times is due to the fact that the thicker diffusion barrier layers (i.e. longer plating times) more greatly reduce the growth rate of these joints. This contrasts with the case of the In-Sn-2.5Cu joints (Fig. 4.29), in which thicker Ni platings weakened the operating temperature shear strengths of the joints due the prohibition of Cu diffusion, and the resulting intermetallic formation, into the joint region. This difference suggests that upon reaching some critical level of Cu additions to the interlayer alloy, the ability to reduce the growth rate of the joint through the use of diffusion barrier layers becomes crucial in optimizing the high temperature shear strength than in allowing Cu to diffuse into the reaction zone to form intermetallic phases. However, it should be reiterated that more measurements must be made in order to verify the accuracy of the given data, and thus the analysis presented in this section.

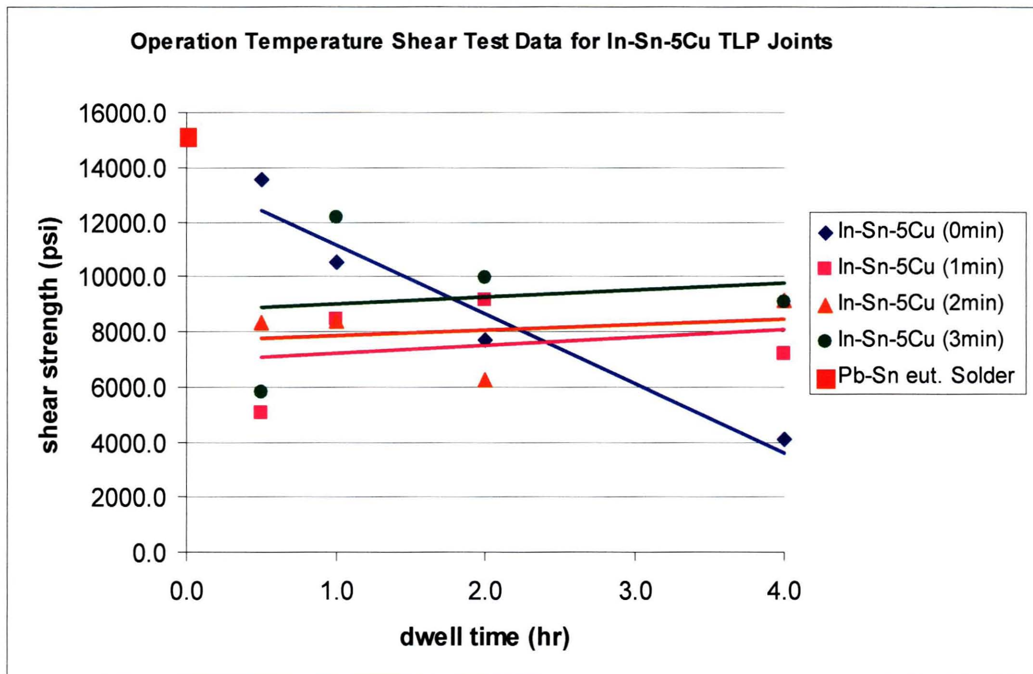

Figure 4.30: Operation temperature shear strengths for TLP joints made with In-Sn-5Cu interlayer and using various dwell times and plating times. In contrast to the In-Sn-2.5Cu joints, increased plating times seem to improve the overall high temperature mechanical behavior of the In-Sn-2.5Cu joints.

To reiterate, Figs. 4.28 – 4.30 show that increases in the nominal Cu concentration improve the overall mechanical behavior of the In-Sn-XCu TLP joints at elevated temperatures. It was presumed that this improvement was a result of larger degrees of Cu-rich intermetallic formation in the joints with larger Cu concentrations in the interlayer alloy (i.e. higher Cu additions result in smaller fraction of low melting phases after bonding). In other words, it was expected that failure at elevated temperatures was predominately governed by the low melting phases present in the interconnect region. A typical fracture surface observed for the In-Sn-XCu TLP joints tested at 100 °C is shown in Fig. 4.31 for the In-Sn-5Cu joint bonded for two hr. Two different regions (labeled A and B) of the fracture surface were observed: Region A being a smooth fracture surface indicative of brittle failure and B appearing more fibrous in nature which

is indicative of ductile behavior. Indeed, EDS analysis of these regions indicated that region A corresponded to the brittle η intermetallic phases and B to the low melting InSn(β) and InSn(γ) phases which may be expected to behave in such a ductile manner at high homologous temperatures (T/T_m). In analyzing the entire fracture surface of the joint, it was found that a much larger portion of the fracture took place within region B, which confirms the previous assumptions that the low melting phases governs the mechanical response of the TLP joints at elevated temperatures.

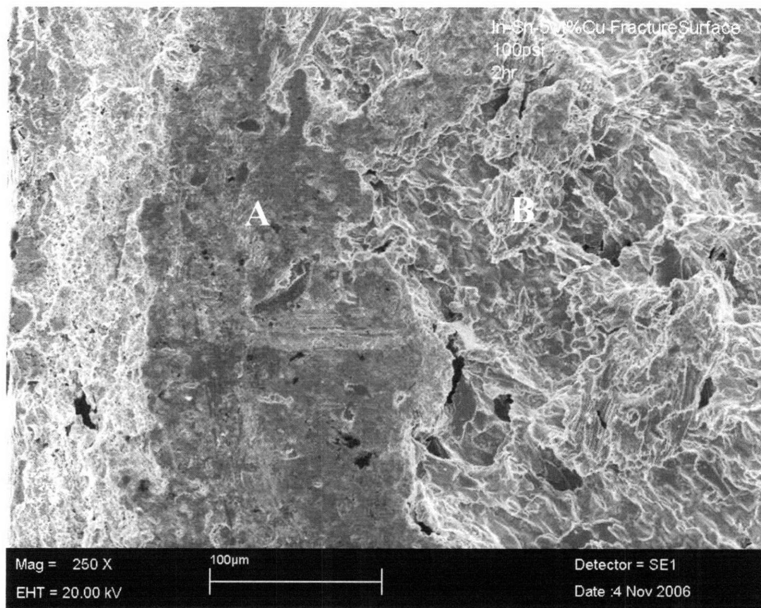

Figure 4.31: SEM micrograph showing fracture surface of non-plated In-Sn-5Cu TLP joint shear tested at 100 °C. The fracture surface revealed two regions: A (η phase) and B (InSn (γ+β) phases). Fracture occurred mainly in the low melting B regions. Joint was bonded for 2 hr under 100 psi.

Chapter 5: Concluding Remarks

5.1 Conclusions

In this work, a lead-free low temperature joining process to be used in electronic packaging applications was sought which could potentially replace conventional Pb-Sn soldering methods presently used in the industry. Specifically, a fluxless low temperature transient liquid phase (LTTLP) bonding process was studied as a means to create robust Cu/Cu TLP joints. The target bonding temperature for the process was to be below 125 °C (with a secondary goal of below 75 °C) The target maximum bonding pressure and dwell time was 100 psi and 2 hr, respectively. Two different TLP systems, In-Sn-Bi-Cu and In-Sn-Cu, were studied as a choice of interlayer alloy used in the TLP bonding process. A 50In-43.6Sn-6.4Bi (T_m = 110 °C) (referred to as low-Bi alloy) and a eutectic 50.9In-49.1Sn (T_m = 120°C) alloy were used as interlayers for the target bonding temperature of 125°C, while a eutectic 48In-15.6Sn-36.1Bi (T_m = 60 °C) alloy was used for the target bonding temperature of 75 °C. In addition, novel approaches to TLP bonding such as the addition of base material to the interlayer alloy and the use of a diffusion barrier layer was studied as a means of optimizing the LTTLP process. The following section briefly summarizes the results discussed in Section 4 and discusses the implications of these results on the ability this project to successfully achieve the target goals.

5.1.1 Validation of Thermodynamic Database

The first, and most important, design element in any TLP bonding process is the choice of the interlayer alloy. In order to design an interlayer alloy for a given TLP joining process, it is necessary to be able to predict not only the melting temperature of the alloy, but also the microstructure that will develop as a result of the reactions between the constituents of the

interlayer alloy and the substrate material. Therefore, one primary goal of this research was to develop a complete and reliable thermodynamic database of the TLP systems under consideration. In Section 4.1, the melting behavior of various interlayer alloys as predicted by calculated equilibrium solidification paths were compared to those observed using DSC. Although the onset melting temperature of the primary TLP varied by 10-15° C, the end melting temperature were observed to agree within 1 °C. Furthermore, the thermodynamic calculations predicted that increases in Cu addition to the low-Bi and eutectic In-Sn interlayer alloys would decrease the fraction of transient liquid phase available for bonding due to consumption of the melting point depressants by Cu-rich intermetallic phases (such as Cu_6Sn_5 and $Cu_{11}In_9$) during heating to the bonding temperature. This decrease in TLP formation with increasing nominal Cu additions to the interlayer alloy was observed experimentally by noting the decrease in enthalpy change upon the first phase transition (TLP formation) for alloys with higher Cu content.

Computational prediction of the equilibrium microstructures for the low-Bi and eutectic In-Sn TLP joints was discussed in Section 4.4.2 along with the experimental microstructural analysis of the TLP joints. According to thermodynamic predictions, the high melting, Cu-rich η phase (Cu_2In with dissolved Sn) was expected to form near the S/L interface where the Cu content is expected to be high, while phases such as Cu_6Sn_5 and $Cu_{11}In_9$ form in the central regions of the joint where Cu content is expected to be much lower due to the longer diffusion distances. Any unreacted liquid phase present in the joint after the bonding procedure was expected to solidify into low melting phases such as InSn(β), InSn(γ), and In_2Bi. The In_2Bi phase was only expected for the joints made with the low-Bi interlayer alloy. SEM micrographs showed microstructures closely resembling those predicted by the thermodynamic calculations, where η (both coarse and fine-grain) existed at the S/L interface and the other lower melting

phases existed in the bulk of the reaction zone. Upon adding base material to the interlayer alloy, Cu-rich IPs were observed to exist within the joint region as well as at the S/L interface. Identification of the various phases was performed through EDS analysis. Experimental validation of the In-Sn-Bi-Cu thermodynamic ensures the accuracy of the phase diagrams developed from this database which may be used in future research to further optimize the TLP bonding processes studied in this work or to develop entirely new ones. Furthermore, dissemination of the information contained within the thermodynamic database into the preexisting materials knowledge base of electronic packaging industries has the potential to greatly expedite the development of a reliable large-scale lead free joining process.

5.1.2 Overall Evaluation of LTTLP Processes

All of the LTTLP processes studied in this work were assessed based on their abilities to achieve certain desired characteristics of the joint within the target bonding parameters previously defined. These characteristics of the joint were a minimal joint thickness (preferably less than 25 μm), a high reflow temperature ($T_m > 200$ °C), and robust mechanical properties at both room temperature (T = 25 °C) and a temperature typical of service conditions (T = 100 °C). Each of the individual design elements of the TLP process (interlayer alloy, Ni layer thickness, and amount of Cu additions) affected the resulting characteristics of the joints in different ways. The current section compares the overall physical and mechanical attributes of joints made within each of the TLP systems.

i) Thickness of TLP Joints

The resulting thickness of the joints studied in this work was very dependent on the composition of the interlayer alloy. One significant finding was that the more Bi-rich interlayer

alloys produced the thinner joints. That is, TLP joints made with the eutectic In-Sn-Bi interlayer (36.1 wt% Bi) were found to produce the thinnest joints, while the joints made with the eutectic In-Sn interlayer (no Bi) produced the thickest joints. The joints made with the low-Bi joint were found to produce joints with intermediate thickness values. Based on microstructural and phase analysis of the joints, it is thought that increased Bi content in the joint causes Cu-Bi segregation which slows the diffusion of Cu into the joint region and prevents the formation of Cu-rich intermetallic bridges across the joint – two phenomena which were observed to be the leading cause of large joints. Another relation between the resulting joint thickness and interlayer composition was that greater additions of Cu to the interlayer alloy resulted in larger joints. This was due to the promotion of Cu-rich intermetallic growth within the bulk of the joint region which facilitated intermetallic bridging across the joint. The thickness of joints made with higher Bi contents was less affected by the additions of Cu due to the Cu-Bi segregation effects previously mentioned. Without the use of Ni plating, the only joints within the In-Sn-Bi-Cu TLP system that were able to obtain the target joint thickness of around 25μm were the eutectic In-Sn-Bi (7.45 μm) and In-Sn-Bi-5Cu (19.2μm) joints, as well as the low-Bi joint made without any Cu additions (20.5 μm). Within the In-Sn-Cu system, the non-plated In-Sn-2.5Cu joints were found to have thicknesses close to the 25 μm target thickness. This joint was the only exception to the trend of increased joint thickness with increased interlayer Cu concentration. It is thought that this is due to the ability of such small base material additions to successfully reduce the amount of dissolution that occurs during TLP bonding without promoting excess intermetallic formation within the joint region.

The use of a Ni diffusion barrier layer was analyzed as a means to reduce joint thickness by retarding Cu diffusion into the joint and hence the growth rate of the Cu-rich intermetallic

grains across the joint. It was found that the choice of an optimum diffusion barrier layer thickness is dependent on composition of the interlayer being used for the particular TLP system. This is to be expected as the joint thickness was also found to depend on interlayer alloy composition. In the case of the low-Bi TLP system, the use of a Ni diffusion barrier layer was only potentially effective at decreasing the joint thickness when the amount of Cu additions was around 5 wt%. Below this content (i.e. 0 wt%Cu), the joint was already thin and so further reduction in Cu diffusion did not make a significant difference; above this content (i.e. 10 wt% Cu), there was such a large degree of intermetallic formation within the joint region that the reduction in Cu diffusion was not enough to prevent the formation of the intermetallic bridges. The use of Ni diffusion barrier layers was not studied for the eutectic In-Sn-Bi joints. However, most of these joints were already below the target bonding temperature so the Ni layer is not as crucial in optimizing these TLP joints.

In studying the use of the Ni layer in the In-Sn-Cu TLP system, the effect of the Ni layer on the *growth rate*, in addition to the instantaneous thickness, of the joints was analyzed. There was no clear effect of the Ni layer on the resulting thickness or growth rate of the In-Sn-0Cu or In-Sn-2.5Cu joints, as these joints were relatively thin in the beginning. The Ni layer was only found to have a significant effect on the growth rate of the In-Sn-5Cu joints. Prior to plating, the In-Sn-5Cu joints were observed to grow very rapidly (thicknesses in excess of 150 μm) with time due to the presence of Cu-rich intermetallics, such as Cu_6In_5 and $Cu_{11}In_9$, which provided a large source of In and Sn atoms from which the η phase could form. By plating the Cu substrate for 2 to 3 min (2.2 μm – 3.1 μm Ni layer), the growth rate was reduced enough so that the joint thickness remained below 100 μm after a 4 hr dwell time. Despite the use of Ni plating, the only

joints in the In-Sn-Cu system that were able to achieve thicknesses near the target were those made with the In-Sn-2.5 interlayer.

ii) Microstructure of TLP Joints

As mentioned in the Section 4.4.2, accurate measurements of the reflow temperatures of the TLP joints were unable to be obtained in this work. Based on microstructural analysis, it was evident that none of the joints studied in this work completely solidified to reach a state of complete homogenization. That is, all of the joints still had some fraction of unreacted TLP remaining in the joint after bonding which did not experience a raise in melting temperature. The high temperature stabilities of the joints, therefore, were based on the fraction of low melting (Cu-poor) versus high melting (Cu-rich) phases present in the joint. This was determined through both phase analysis and composition profiles.

Based on a microstructural analysis, it was found that the eutectic In-Sn-Bi joint had the largest fraction of low melting phases, and therefore was expected to be the least stable at elevated temperatures (i.e. have a low reflow temperature). These joints contained a large fraction of In-Bi IPs (T_m = 90 – 110 °C) which were observed to be segregated from the η phases. Also, the joints based on the low-Bi interlayer were found to have a larger fraction of low melting InSn(β) and InSn(γ) phases compared to the joints based on the In-Sn interlayer. In addition, the low-Bi TLP joints consisted of the In_2Bi phase. The microstructural differences between the joints made in the different TLP systems is due to the tendency of Bi to form intermetallics with In which reduces the amount of In available to form the η phase though subsequent reactions with Cu. This, in turn, reduces the amount of Sn which can be dissolved into the η phase which leads to an overall increase in the fraction of low melting phases left remaining in the interconnect zone.

A significant microstructural difference was observed between joints bonded within the In-Sn-Cu system. According to measured composition profiles, it was found that the In-Sn-2.5 Cu joint contained a higher average Cu composition (≈ 40 at%) than either the In-Sn-0Cu and In-Sn-5Cu joints. This composition was reached in very short dwell times of around 0.5 hr – 1.0 hr. Furthermore, the microstructure of the In-Sn-2.5Cu joints was observed to be more homogenous than the other joints produced within the same TLP system.

The diffusion barrier layer was found to have a negative effect on the abilities of the TLP joints to obtain a high temperature stable microstructure due to the prevention of η formation into the joint region. However, increasing the nominal Cu concentration of the interlayer alloy, which enhanced the growth of Cu-rich intermetallics upon dissolution of the Ni layer, greatly reduced the negative effects of the Ni layer on achieving the desired microstructure. This observation had the greatest implications for the In-Sn-5Cu joint, where it was found that the Ni layer could successfully reduce the growth rate of the joint without sacrificing its high temperature stability.

iii) Mechanical Behavior of TLP Joints

The room temperature shear strengths of the TLP joints were found to depend primarily on the properties of the η phase which formed at the substrate/joint interface. There was very little dependency of the room temperature shear strengths on the joint thickness or Ni plating time. For the TLP joints made in the In-Sn-Bi-Cu system, there was also no observed influence of the interlayer's nominal Cu content on the room temperature mechanical properties. Both the low-Bi and eutectic based joints had average strengths which fell mostly within the 13,000 – 17,000 psi (≈ 90 – 120 MPa) range, regardless of Cu composition. Within the In-Sn-Cu system, there was an improvement seen in mechanical response of the joints upon increasing Cu

additions to the interlayer alloy. The eutectic In-Sn joint had room temperature shear strengths comparable that to those joint made in the In-Sn-Bi-Cu system. However, the In-Sn-2.5 and In-Sn-5Cu joints had strengths measured to be in the 20,000 – 25,000 psi (≈ 140 – 170 MPa) range. Based on the microstructural analysis, it is thought that the improved room temperature mechanical response of these joints is the result of a microstructural change in the duplex microstructure of the interfacial η phase. More specifically, the Cu additions may reduce the size difference between the sublayers of coarse η grains (which grow into the liquid) and fine η grains (which grow into the solid) at the S/L interface, which was found to be a crucial location for rupture in similar TLP systems [48]. As a reference, the Pb-Sn solder joint had a room temperature shear strength measured to be 30,410 psi (≈ 210 MPa).

At the operating temperature, the shear strengths of the In-Sn-Bi-Cu joints were found to decrease two orders of magnitude from their measured values at room temperature. In fact, the TLP joints made with the eutectic In-Sn-Bi interlayer were unable to sustain any load at the elevated temperature (100 °C). The use of a Ni layer was found to decrease the operating temperature shear strength of the low-Bi joint by more than 50 %, but it did not have an effect on either the In-Sn-Bi-5Cu or In-Sn-Bi-10Cu joints. The extremely poor mechanical response of the joints made within this TLP system was due to the presence of the low melting In-Bi IPs in the interconnection region.

The TLP joints made within the In-Sn-Cu system were found to have shear strengths which were an order of magnitude greater than those made in the In-Sn-Bi system. The eutectic In-Sn joints without any Cu additions were found to have strengths mainly between 4,000 – 5,500 psi (≈ 30 – 40 MPa). Further improvements in the high temperature mechanical response was observed for increasing Cu additions to the interlayer alloy. Average shear strength ranges

were measured to be 6,000 – 7,500 psi (≈ 40 – 50 MPa) and 7,500 – 9,500 psi (≈ 50 -65 MPa) for the In-Sn-2.5Cu and In-Sn-5Cu joints, respectively. Several shear strengths measurements made for these joints were greater than 10,000 psi (≈ 70 MPa) and were found to approach the strength measured for the Pb-Sn solder joint (15, 140 psi ≈ 100 MPa) at the same temperature.

Unlike the room temperature shear strengths, the strengths measured at the operating temperature were found to depend on joint thickness. This was most prominently observed for the non-plated In-Sn-5Cu joint which was found to have a sharp decrease in operating temperature shear strength over the 4 hr dwell time. However, this effect was eliminated through application of the Ni layer. It is interesting to note that the In-Sn-5Cu joints were the only specimens for which increases in the Ni layer thickness actually improved the mechanical response of the joints at elevated temperatures. In most cases, the Ni layer was found either to have a negligible effect or even a negative effect on the operating shear strengths of the joints due to the lack of Cu diffusion into the reaction zone. This signifies that there is some point (based on the level of Cu addition) at which the growth rate becomes a more crucial parameter in controlling the high temperature mechanical properties of the joint than compared to the amount of the Cu diffusion allowed into the joint.

Failure analysis of the In-Sn-XCu joints tested at operating temperature revealed a fracture surface containing two different regions: one referring to the η phase and the other referring to the InSn(γ) and InSn(β) phases. The majority of the fracture took place through the InSn(γ) and InSn(β) phase, signifying that these low melting phases are those which governed the mechanical response of the TLP joints at elevated temperatures. Thus, unlike the room temperature properties, the high temperature mechanical properties were much more dependent on the processing parameters. This makes sense since the fraction and morphology of the low

melting phases present in the joint was found to vary much more with the TLP processing than the fraction and morphology of the interfacial η intermetallic grains.

iv) Final Recommendations

In this work, a fluxless, lead-free LTTLP bonding process was successfully used to create Cu/Cu joints at both 125° C and 75 °C within the defined processing limits. However, the ability to produce a joint which optimized all the desired joint characteristics (i.e joint thickness, high reflow temperature, and robust room/operating mechanical properties) was found to be a difficult task in that the properties of the interlayer alloys which promote smaller joints (high Bi content and low nominal Cu composition) also tend to promote the formation of microstructures which have poor thermal and mechanical stability at high temperatures. The most promising joints studied in this work, were those made with the In-Sn-2.5Cu interlayer alloy. The TLP joints made with this interlayer resulted in thicknesses mostly ranging from 20 – 45 μm, which is near the desired joint thickness of 25 μm. Furthermore, these thicknesses could be obtained without the need for the Ni layer, which makes the TLP process faster and less expensive. In terms of reflow temperature, these joints produced high temperature stable microstructures in short dwell times (0.5 hr – 1hr) and displayed good mechanical properties under service-life conditions. Also, because these joints did not rapidly grow with increased dwell time, their operating temperature shear strength was not observed to significantly degrade with longer bonding times. However, even with the use of this interlayer alloy, further optimization of the TLP process still needs to be done in order to achieve mechanical properties displayed by conventional Pb-Sn solder joints.

It should be stressed that this assessment was solely based on the target bonding parameters and desired joint characteristics defined by the project goals. Depending on the

specific joining application, other choices for a given TLP process may be more desirable. For instance, if the high temperature mechanical properties of the joint are more crucial than the joint thickness, then the In-Sn-5Cu interlayer (or perhaps an interlayer with even higher Cu additions) may be better suited for the application. Application of the Ni layer in this case would be useful in ensuring the joint remains mechanically stable under service conditions for an extended period of time. On the other hand, if the joint is being used in a very thin device, but in a low stress environment, then an interlayer from within the In-Sn-Bi-Cu system may be used successfully for the application. Regardless of the specific application, the computational and experimental data presented in this work provide a good starting point from which an optimal LTTLP bonding procedure can be designed for a given industrial process.

5.2 Future Work

Much of the microstructural analysis presented in this work was based on qualitative and semi-quantative experimental methods, such as SEM and EDS. It is recommended that a more quantitative method, such as XRD, be performed in order to verify the phase characterizations presented in this work. Also, as was mentioned in Section 4, more mechanical tests should be done to more accurately define the mechanical strengths of the joints presented in this work. Other types of mechanical testing, such as creep tests, should also be performed in order to assess the long term reliability of the joints under service conditions.

The TLP joints studied in the work by no means define a complete set of possible lead free systems from which to develop new, low temperature joining technologies. This work, which focused on only a small subset of joints within the In-Sn-Cu and In-Sn-Bi-Cu systems, also provided a broad, yet thorough, description of how to employ some novel approaches (i.e. base material additions and use of a diffusion barrier layer) to the LTTLP bonding process in

order to optimize the resulting joint properties. The methodologies employed in this research may be useful in other joining processes and other materials systems.

Beyond the scope of this work, a field of interest that was observed during research was that of compositional wetting. During the processing of the TLP joints, it was empirically observed that higher additions of Cu to the interlayer alloy enhanced its spreading characteristics. This was most noticeably prominent in the production of the eutectic In-Sn-Bi-XCu joints as illustrated in Fig. 5.1. Even at the low processing temperature of 75 °C, a significant difference in the spreading characteristics of the alloy was observed with 5 wt% Cu additions. Enhanced wettability of the alloy with Cu additions is thought to be related to the observed Cu-Bi segregation shown in Section 4.4.2 (i). It is envisioned that the Cu promotes the breakdown of stable bismuth oxides on the surface of the Cu substrate which prevent good spreading of the alloy. More detailed computational and experimental studies of the interfacial kinetics must be performed in order to fully comprehend the reactions which govern wetting. The ability to control spreading characteristics through manipulation of the alloy composition will ultimately aid in the development of new fluxless joining technologies.

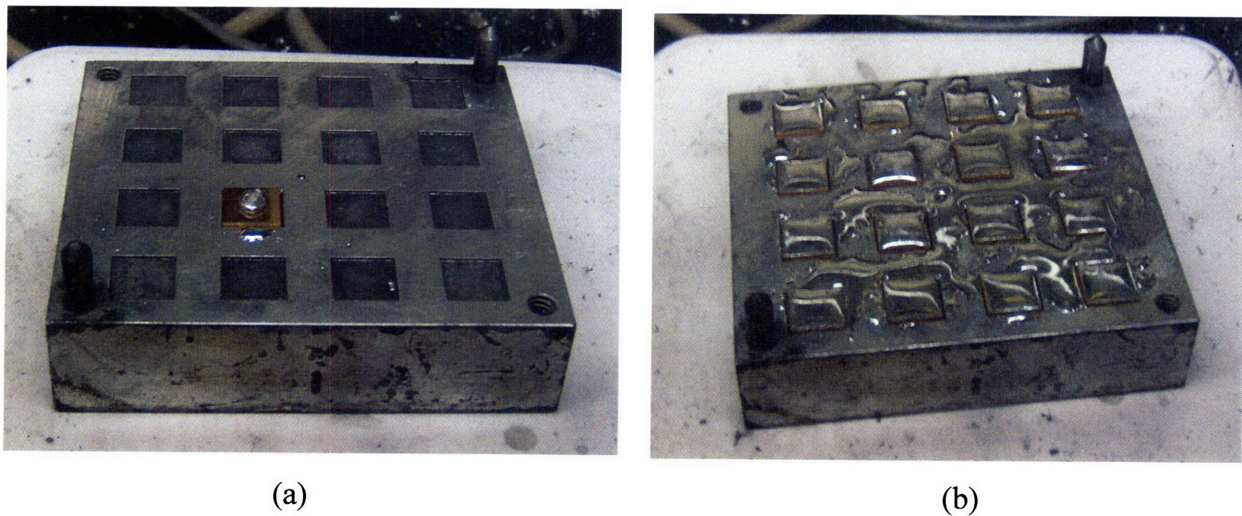

(a) (b)

Figure 5.1: Spreading behavior observed for eutectic In-Sn-Bi alloy on Cu substrate having (a) no Cu additions; and (b) 5 wt% Cu additions. Increasing the Cu content of the interlayer alloy made it much easier to wet the Cu substrate during processing of the TLP joints.

Appendix A: Calculated Equilibrium Solidification Paths

The figures in this appendix are the thermodynamic models used in this work which were calculated by Dr. Raymundo Arroyave using Thermo-Calc®. The first two sets of figures are equilibrium solidification paths which demonstrate the effect of Cu additions on the melting behavior of the 50In-43.6Sn-6.4 Bi (referred to as the low-Bi alloy in the text) and eutectic 50.9In-49.1Sn alloys. The last two figures illustrate the expected phases present in the alloys (at various temperatures) based on the Cu composition. These diagrams are meant to aid in the visualization of the microstructural evolution of joints during the LTTLP bonding process, where high Cu compositions refer to regions near the Cu substrate and low Cu compositions refer to regions towards the central regions on the interconnect zone.

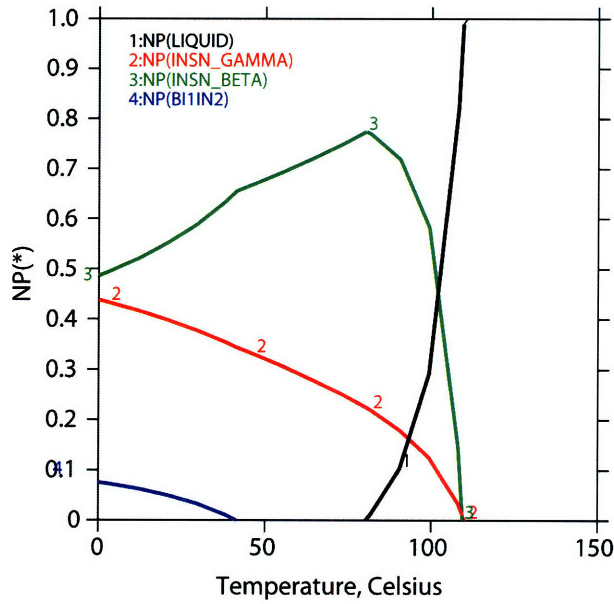

(a)

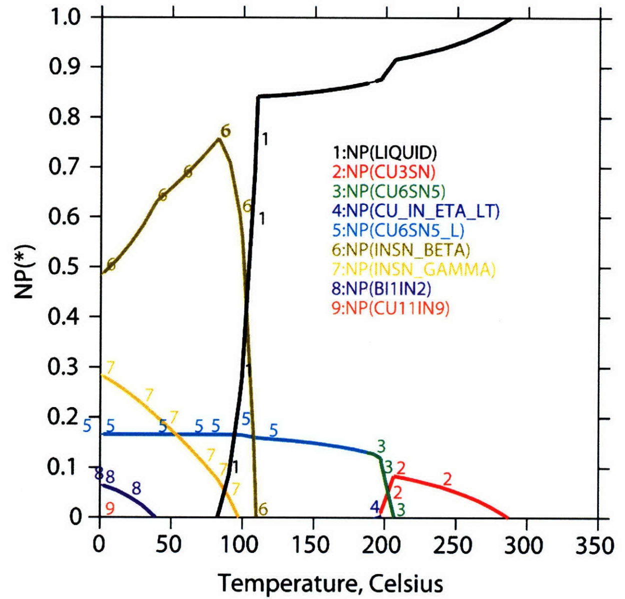

(b)

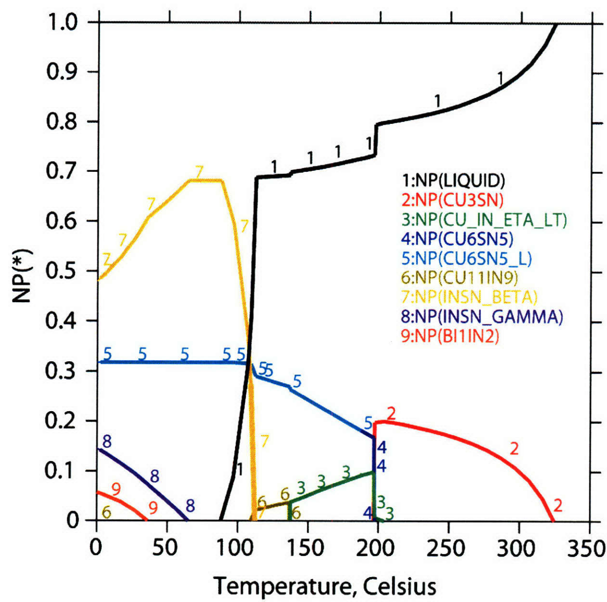

(c)

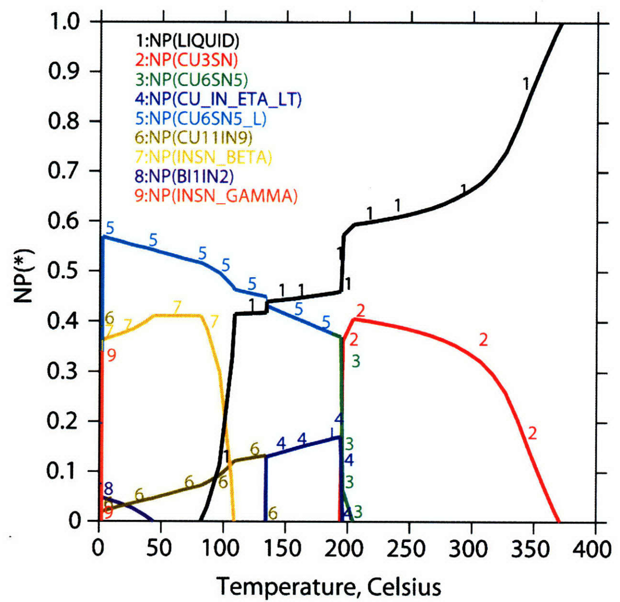

(d)

Figure A.1: Equilibrium solidification paths calculated for the 50In-43.6Sn-6.4 Bi (low-Bi) alloy with (a) no Cu additions; (b) 5 wt% Cu additions; (c) 10 wt% Cu additions; and (d) 20 wt% Cu additions

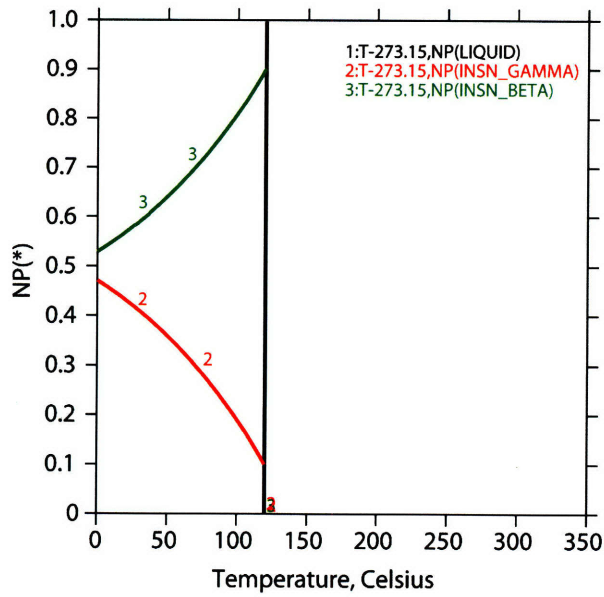

(a)

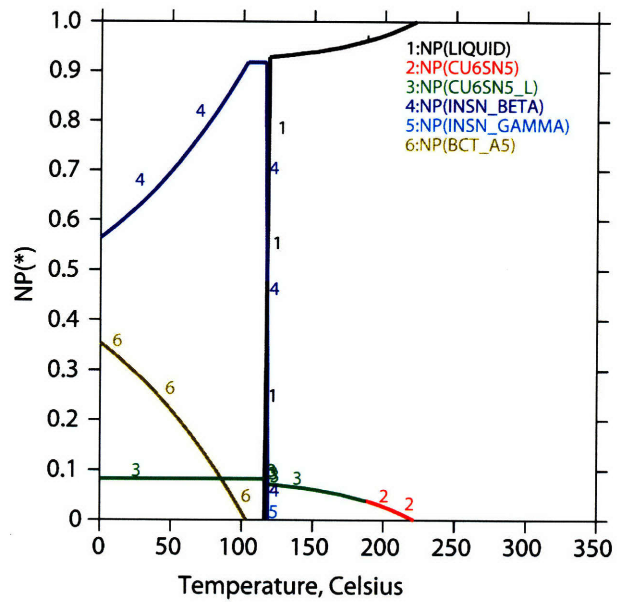

(b)

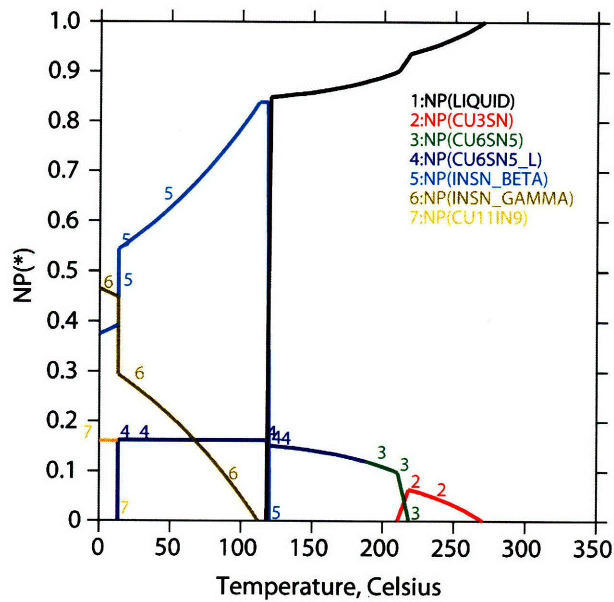

(c)

Figure A.2: Equilibrium solidification paths calculated for the eutectic 50.9In-49.1Sn-6.4 alloy with (a) no Cu additions; (b) 2.5 wt% Cu additions; and (c) 5 wt% Cu additions.

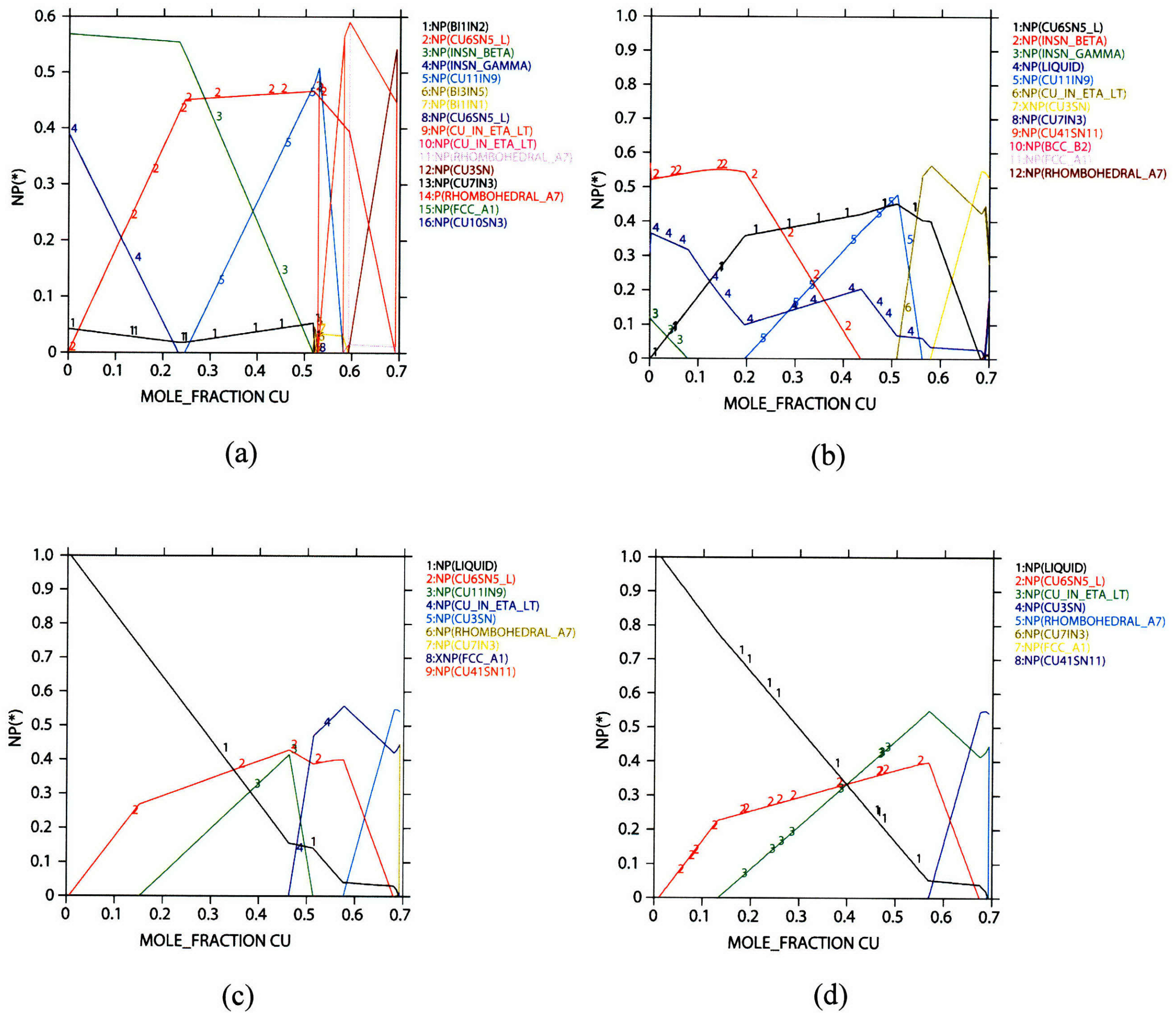

Figure A.3: Prediction of phase fractions in TLP joints made with the low-Bi based In-Sn-Bi-XCu interlayer at (a) room temperature; (b) 100 °C; (c) 125 °C; and (d) 150 °C. Equilibrium conditions are assumed.

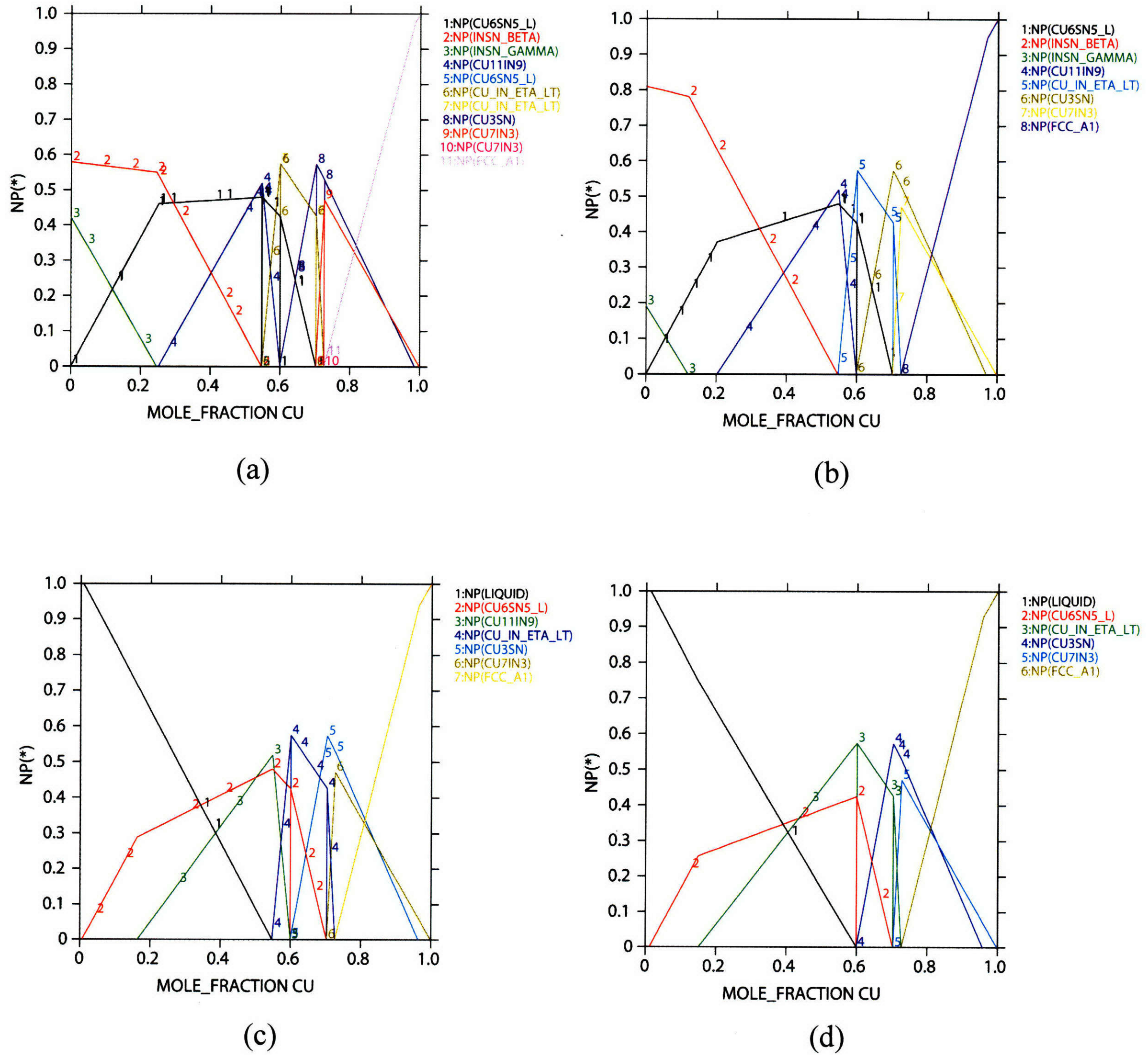

Figure A.4: Prediction of phase fractions in TLP joints made with eutectic based In-Sn-XCu interlayers at (a) room temperature; (b) 100 °C; (c) 125 °C; and (d) 150 °C. Equilibrium conditions are assumed.

References

1. D. R. Frear, J. W. Jang, J. K. Lin and C. Zhang, *JOM,* **53** (2001) 28-32.
2. K. N. Tu, A. M. Gusak and M. Li, *Journal of Applied Physics,* **93** (2003) 1335-1353.
3. M. Hou and T. W. Eagar, *Journal of Electronic Packaging,* **114** (1992) 443-447.
4. K. Bobzin, E. Lugscheider, H. Zhuang, F. Ernst, N. Bagcivan, M. Maes, J. Rosing, S. Ferrara, A. Erdle and A. Kramer, *Microsystem Technologies-Micro-and Nanosystems-Information Storage and Processing Systems,* **12** (2006) 620-625.
5. C. S. Smith, *A search for structure : selected essays on science, art, and history*, MIT Press, Cambridge, Mass., (1981).
6. J. C. Williams and Massachusetts Institute of Technology. Dept. of Materials Science and Engineering., Thesis S.M. --Massachusetts Institute of Technology Dept. of Materials Science and Engineering 2005., (2005).
7. J. F. Lynch, L. Feinstein and R. A. Huggins, *Welding Journal* **61** (1959) 85-89.
8. D. S. Duvall, Owczarsk.Wa and D. F. Paulonis, *Welding Journal,* **53** (1974) 203-214.
9. H. Duan, M. Kocak, K. H. Bohm and V. Ventzke, *Science and Technology of Welding and Joining,* **9** (2004) 525-531.
10. H. P. Duan, K. H. Bohm, V. Ventzke and M. Kocak, *Transactions of Nonferrous Metals Society of China,* **15** (2005) 375-378.
11. H. P. Duan, J. Luo, K. H. Bohm and M. Kocak, *Journal of University of Science and Technology Beijing,* **12** (2005) 431-435.
12. K. Nishimoto, K. Saida, D. Kim and Y. Nakao, *Isij International,* **35** (1995) 1298-1306.
13. N. P. Wikstrom, O. A. Ojo and M. C. Chaturvedi, *Materials Science and Engineering a-Structural Materials Properties Microstructure and Processing,* **417** (2006) 299-306.
14. G. Humpston and D. M. Jacobson, in *Principles of Soldering and Brazing* M. T. Haddad, Ed. (ASM International, Materials Park, 2001) pp. 128-132.
15. Y. Nakao, K. Nishimoto, K. Shinozaki and C. Kang, 'Proceedings Superalloys 1989', Warrendale, PA (1989), pp. 775-783.
16. I. Tuah-Poku, M. Dollar and T. B. Massalski, *Metallurgical and Materials Transactions a-Physical Metallurgy and Materials Science,* **19A** (1988) 675-686.
17. W. F. Gale and D. A. Butts, *Science and Technology of Welding and Joining,* **9** (2004) 283-300.
18. W. D. MacDonald and T. W. Eagar, *Metallurgical and Materials Transactions a-Physical Metallurgy and Materials Science,* **29** (1998) 315-325.
19. D. Shangguan, in *Lead-Free Solder Interconnect Reliability* D. Shangguan, Ed. (ASM International Materials Park, OH 2005) pp. 1-21.
20. T. Yamamoto and K. I. Tsubone, *Fujitsu Scientific & Technical Journal,* **43** (2007) 50-58.
21. Y. Sogo, R. Miwa, A. Hirose and K. F. Kobayashi, *Journal of the Japan Institute of Metals,* **69** (2005) 139-146.
22. A. Winiowski and W. Gawrysiuk, *Archives of Metallurgy and Materials,* **51** (2006) 399-405.
23. M. H. Braga, L. F. Malheiros, D. Soares, J. Ferreira and F. Castro, *Advanced Materials Forum Iii, Pts 1 and 2,* **514-516** (2006) 1682-1686.
24. S. W. Chen, C. H. Wang, S. K. Lin and C. N. Chiu, *Journal of Materials Science-Materials in Electronics,* **18** (2007) 19-37.

25. Y. Cui, X. J. Liu, I. Ohnuma, R. Kainuma, H. Ohtani and K. Ishida, *Journal of Alloys and Compounds,* **320** (2001) 234-241.
26. K. Doi, H. Ohtani and M. Hasebe, *Materials Transactions,* **45** (2004) 380-383.
27. H. Ipser, H. Flandorfer, C. Luef, C. Schmetterer and U. Saeed, *Journal of Materials Science-Materials in Electronics,* **18** (2007) 3-17.
28. B. J. Lee, C. S. Oh and J. H. Shim, *Journal of Electronic Materials,* **25** (1996) 983-991.
29. N. Moelans, K. C. Hari Kumar and P. Wollants, *Journal of Alloys and Compounds,* **360** (2003) 98-106.
30. K. W. Moon and W. J. Boettinger, *Jom,* **56** (2004) 22-27.
31. N. Dariavach, P. Callahan, J. Liang and R. Fournelle, *Journal of Electronic Materials,* **35** (2006) 1581-1592.
32. K. S. Kim, K. Suganuma, J. M. Kim and C. W. Hwang, *Jom,* **56** (2004) 39-43.
33. A. Sharif and Y. C. Chan, *Journal of Electronic Materials,* **34** (2005) 46-52.
34. S. J. Wang and C. Y. Liu, *Journal of Electronic Materials,* **32** (2003) 1303-1309.
35. C. Y. Liu, C. H. Lai, M. C. Wang and M. H. Hon, *Journal of Crystal Growth,* **290** (2006) 103-110.
36. A. Yamaguchi, Y. Yamashita, A. Furusawa, K. Nishida, T. Hojo, Y. Sogo, A. Miwa, A. Hirose and K. F. Kobayashi, *Materials Transactions,* **45** (2004) 1282-1289.
37. I. E. Anderson, B. A. Cook, J. L. Harringa and R. L. Terpstra, *Jom-Journal of the Minerals Metals & Materials Society,* **54** (2002) 26-29.
38. A. Hirose, H. Yanagawa, E. Ide and K. F. Kobayashi, *Science and Technology of Advanced Materials,* **5** (2004) 267-276.
39. R. Kisiel, W. Gasior, Z. Moser, J. Pstrus, K. Bukat and J. Sitek, *Archives of Metallurgy and Materials,* **50** (2005) 1065-1071.
40. W. D. Macdonald and T. W. Eagar, *Annual Review of Materials Science,* **22** (1992) 23-46.
41. G. Humpston and D. M. Jacobson, in *Principles of Soldering* (ASM International Materials Park, OH 2004) pp. 189-242.
42. S. Sommadossi, W. Gust and E. J. Mittemeijer, *Materials Chemistry and Physics,* **77** (2002) 924-929.
43. G. Humpston and D. M. Jacobson, in *Principles of Soldering* (ASM International Materials Park, 2004) pp. 1-47.
44. C. B. Lee, S. B. Jung, Y. E. Shin and C. C. Shur, *Materials Transactions,* **42** (2001) 751-755.
45. Y. Kariya, Y. Hirata and M. Otsuka, *Journal of Electronic Materials,* **28** (1999) 1263-1269.
46. Y. Kariya and M. Otsuka, *Journal of Electronic Materials,* **27** (1998) 866-870.
47. N. S. Bosco and F. W. Zok, *Acta Materialia,* **52** (2004) 2965-2972.
48. S. Sommadossi, J. Huici, P. K. Khanna, W. Gust and E. J. Mittemeijer, *Zeitschrift Fur Metallkunde,* **93** (2002) 496-501.
49. D. A. Porter and K. E. Easterling, *Phase transformations in metals and alloys*, Chapman & Hall, London ; New York, ed. 2nd, (1992).
50. W. Koster, T. Godecke and D. Heine, *Zeitschrift Fur Metallkunde,* **63** (1972) 802-807.

About the Author

David Fischer graduated with his B.S. in Materials Science and Engineering from Lehigh University in 2005. While at Lehigh, David made the Dean's List every semester and received the 2003 Tarby Award and 2005 John Osborne Award for having the highest cumulative GPA in his major. He was also a member of the Tau Beta Pi Engineering Honor Socitey, Phi Eta Sigma National Honor Society, and Alpha Sigma Mu Honor Society. Upon arriving at MIT in the Fall of 2005, David has been a member of Prof. Thomas Eagar's Welding and Joining Research Group. He has also been a teaching assistant for MIT's undergraduate course in the mechanical behavior of materials.